Stony Brook University

The Murine Hepatic and Splenic Response to *Francisella tularensis*

A Dissertation Presented

by

John Wilson Rasmussen

to

The Graduate School

In Partial Fulfillment of the

Requirements

for the Degree of

Doctor of Philosophy

in

Molecular and Cellular Biology

(Immunology and Pathology)

Stony Brook University

December 2008

Stony Brook University

The Graduate School

John Wilson Rasmussen

We, the dissertation committee for the above candidate for the Doctor of Philosophy degree, hereby recommend acceptance of this dissertation.

Jorge L. Benach, Ph.D. – Dissertation Advisor
Professor and Chairman,
Department of Molecular Genetics and Microbiology
Director, Center for Infectious Diseases

David G. Thanassi, Ph.D. – Chairperson of Defense
Associate Professor,
Department of Molecular Genetics and Microbiology

Howard B. Fleit, Ph.D.
Associate Professor, Department of Pathology

Martha B. Furie, Ph.D.
Professor, Department of Pathology

Marc G. Golightly, Ph.D. SI (ASCP)
Professor, Department of Pathology
Director of Clinical Immunology Laboratories

This dissertation is accepted by the Graduate School.

Lawrence Martin
Dean of the Graduate School

Abstract of the Dissertation

The Murine Hepatic and Splenic Response to *Francisella tularensis*

by

John Wilson Rasmussen

Doctor in Philosophy

in

Molecular and Cellular Biology

(Immunology and Pathology)

Stony Brook University

2008

The spleen and liver are target organs of one of the most pathogenic bacteria known to man: *Francisella tularensis*, the causative agent of tularemia. The focus of this dissertation was to identify and characterize the immune cells that become activated during tularemia infection, as these could have an important role in the severity of the infection. Mice were infected with sublethal doses of *F. tularensis* live vaccine strain, and cells from various organs were analyzed by histology, flow cytometry and immunofluorescent microscopy. An immature myeloid cellular population rapidly accumulated in the liver, spleen and bone marrow during the acute tularemia infection. This population was characterized by co-expression of Gr-1 and CD11b markers and had the greatest increases of all cellular phenotypes compared to uninfected mice.

Cells expressing Gr-1 and CD11b, also known as myeloid derived suppressor cells (MDSCs), have been associated with immune suppression in both infectious and non-infectious conditions but their role in *F. tularensis* infection had never been determined. MDSCs were purified by live cell sorting to follow ex vivo cellular differentiation. In the presence of granulocyte macrophage colony-stimulating factor, the cells differentiated into dendritic cells and mature macrophages. Purified MDSCs were adoptively transferred into mice infected with sublethal doses of *F. tularensis*. The passively transferred cells did not lead to increased mortality or severity of infection. Additionally, B cells appear to have a regulatory role in MDSC accumulation. Mice deficient in B cells had delayed bacterial clearance and increased pathology in the liver and spleen, associated with sustained accumulation of Gr-1$^+$ CD11b$^+$ cells when compared to wild type mice. In tularemia, an accumulation of MDSC appears to regulate the infection in its early stages and may provide a threshold for survival.

Table of Contents

List of Abbreviations

ALT – alanine transferase

APC – allophycocyanin

BSA – bovine serum albumin

CFSE - carboxylfluorescein diacetate succinimidyl ester

CFU – colony-forming unit

DAPI – 4',6-diamidino-2-phenylindole

DC – dendritic cell

DMEM – Dulbecco's Modified Eagle Medium

DPI – day post-inoculation

ELISA – enzyme-linked immunosorbent assay

FACS – fluorescence-activated cell sorter

FITC – fluorescein isothiocyanate

FO B – follicular B

GM-CSF – granulocyte macrophage colony-stimulating factor

HBSS – Hanks' Balanced Salt Solution

ID – intradermal

IFA – immunofluorescence antibody assay

IFN - interferon

Ig – immunoglobulin

IP – intraperitoneal

IV – intravenous

kDa - kilodalton

LD_{50} – median lethal dose

LDH – lactate dehydrogenase

LPS – lipopolysaccharide

LVS – live vaccine strain

MOI – multiplicity of infection

PAMP – pathogen associated molecular pattern

PBS – phospate-buffered saline

PE – R-phycoerythrin

PerCP – peridinin chlorophyll protein

PGE_2 – prostaglandin E_2

MDSC – myeloid derived suppressor cell

MH – Mueller-Hinton

MZ B – marginal zone B

NK – natural killer

RT – room temperature

SD – standard deviation

SDS-PAGE – sodium dodecyl sulfate polyacrylamide gel electrophoresis

TLR – toll-like receptor

TNF – tumor necrosis factor

TUNEL – terminal deoxynucleotidyl transferase-mediated dUTP-X nick end labeling

WT – wild type

List of Tables

List of Figures

Acknowledgements

This dissertation would not be possible without the support and assistance I have received during my five and half years at Stony Brook University. First of all I would like to thank my advisor, mentor and friend, Jorge Benach. I have always felt fortunate to be a member of Jorge's laboratory and have the opportunity to learn from and lean on such a talented and seasoned scientist. I will miss our discussions of science, but also those of politics, family and life in general. I would like to thank my dissertation committee for their invaluable advice and direction for my progression in graduate school. I would like to thank the members of the Benach laboratory for their counsel and help in experimentation and having a good laugh along the way. Likewise, many thanks to all those individuals at the Center for Infectious Diseases, which provides a most pleasant and stimulating learning environment. I thank my parents, Paul and Diana Rasmussen, who have always been positive influences and encouraged me to obtain as much education as possible. Finally, to Jane, for her unconditional love and support, who unselfishly moved her life from Salt Lake City to Stony Brook and became the mother of the two greatest joys of our lives, Emma and Lucy.

Chapter I

Introduction

A. Tularemia

Francisella tularensis, one of the most infectious bacteria known, causes the zoonotic disease tularemia. Pneumonic forms of the disease can be fatal, but more commonly acquired cutaneous forms of tularemia are contracted from close contact with infected animals and by the bite of arthropod vectors (72). In its natural setting, tularemia is the third most common tick-borne disease and also the second most common laboratory-associated infection in the United States (91, 163). Tularemia has declined steadily in the United States from thousands of cases in the 1950's to fewer than 200 cases per year today (22, 34). Current interest in *Francisella* continues as a model of study for intracellular bacteria but also for its potential as an agent of bioterrorism (56, 149).

The reasons for the high morbidity and mortality of clinical tularemia are not understood. As with other infections, the resulting disease is the outcome of the interplay among the infecting agents and the various host responses. Although a significant amount of work has been done on the pathogenesis of tularemia in recent years, there is still a gap in the understanding of possible virulence factors of the bacterium and of the host defense against this infection. This dissertation was prepared to fill

aspects of this gap on the host immune response to *F. tularensis*, specifically in the liver and spleen.

Causative Agent. In 1911, the bacterium to be known as *Francisella tularensis* was first isolated in Tulare County in central California from squirrels infected with a plague-like illness (142). Some eight years later, Edward Francis, for whom the bacterium is named, isolated the bacteria from human blood and proposed the term 'tularemia' to describe the disease caused by *F. tularensis* (151, 180). *F. tularensis* is a small, gram-negative coccobacillus that has a wide geographical and zoonotic distribution. Since 1911, natural infections of *F. tularensis* have been reported in North America, Europe, Asia and Australia, and the bacterium has been isolated from over 250 species of animals. In the United States, most tularemia cases occur in the rural south-central and western states, but all 50 states, except Hawaii, have reported past cases (56).

The natural reservoir of *F. tularensis* is unknown, but arthropod vectors, such as ticks, flies and mosquitoes, may carry the bacteria and subsequently transmit it to mammals (167). Rabbits, hares and rodents are typical sources of human disease due to increased exposure by hunters or farmers who come in contact with these infected animals. Tularemia is also commonly known as 'rabbit fever', 'meat-cutter's disease' or 'deer-fly fever' depending on its mode of transmission (72,

151). Human infection can follow ingestion of contaminated food or water, contact of open skin wounds with infected animal carcasses, bites from various blood-sucking arthropods, or inhalation of aerosolized bacteria (5, 72, 73).

There are various forms of tularemia in humans that reflect the route of exposure. The most common form is ulceroglandular tularemia, which occurs at the site of the cutaneous infection and usually arises by contact with an infected animal or bite of an arthropod. Other described forms include: oculoglandular tularemia, usually due to eye contact with infected fingers; oropharyngeal tularemia, which results from ingestion of contaminated food or water; and pneumonic tularemia, the most severe form of the disease, which typically occurs by inhalation of the bacteria (56, 72, 180). Typically, symptoms will be seen 3-6 days after exposure but may take up to three weeks to develop (73, 180). The onset of tularemia is usually abrupt, with flu-like symptoms and fevers, chills, malaise and headaches. A dry cough and sore throat may also develop. If untreated, symptoms may last from several weeks to months. Before antibiotics it has been estimated that fatality rates reached as high as 60% for pneumonic tularemia, but treatment has lowered fatalities to less than 2% (56, 72, 149).

Bioterrorism. *F. tularensis* is recognized as a potential biological weapon due to its high infectivity, ease of dissemination and a high fatality

rate (56). It was studied by Japanese germ warfare research units between 1932 and 1945, and in the United States it was stockpiled by the military. Moreover, the former Soviet Union reportedly developed strains of *F. tularensis* in the 1990's that were resistant to antibiotics or that would cause illness in vaccinated individuals (56, 149). The Centers for Disease Control and Prevention has classified *F. tularensis* as a Category A agent, along with other diseases of notoriety, such as anthrax, plague and smallpox. Since terrorist events in 2001, there has been renewed interest in tularemia, and this has resulted in increased research to develop vaccines, identify virulence factors and improve diagnostics (151).

Subspecies. *F. tularensis* is classified into four subspecies, *tularensis, holarctica, mediasiatica* and *novicida,* based on geographic location and clinical symptoms (Table 1.1). Subspecies *tularensis* and *holarctica* are the main causes of human disease and are known as Type A and Type B, respectively (151). Type A strains are found exclusively in North America, are the most virulent, and cause the most severe form of tularemia (149). Moreover, Type A strains are estimated to have a median lethal does (LD_{50}) dose in humans of fewer than 10 colony forming units (CFU) (72). The virulent Schu4 strain is the Type A prototype. Type B is found in Eurasia and North America but is rarely fatal and is more commonly acquired as a cutaneous infection (167). Due to the highly infectious nature of *F. tularensis*, a Russian Type B strain was attenuated

Subspecies	Primary geographic location	LD_{50} dose in humans	LD_{50} dose in mice
tularensis	North America	<10 CFU	<1 CFU
holarctica	Europe, Siberia, Far East, Kazakhstan and North America	$<10^3$ CFU	<1 CFU
mediasiatica	Central Asia and parts of former Soviet Union	ND	ND
novicida	North America and Australia	$>10^3$ CFU	$<10^3$ CFU

Table 1.1. *Francisella tularensis* subspecies geographic distribution and median lethal dose (LD_{50}) from subcutaneous inoculation in humans and mice. CFU, colony-forming unit. ND, not determined. Adapted from references (96, 149).

to be administered as a live vaccine strain (LVS) for at-risk personnel. LVS attenuation was achieved by multiple passages on agar, followed by intraperitoneal (IP) inoculations into animals and then harvesting as an attenuated strain as animals became moribund (64, 82). Many questions still exist about the basis of attenuation of *F. tularensis* LVS, and concerns about its potential reversion to greater virulence have resulted in its current unavailability for use as a vaccine. However, the LVS is considered the standard for tularemia research, and the majority of *F. tularensis* research has been performed using the LVS. Therefore, *F. tularensis* LVS was used exclusively for all experiments throughout this dissertation. *F. tularensis* subspecies *mediasiatica* and subspecies *novicida* are not clinically important for either humans or animals.

Bacteriology. Although *F. tularensis* is one of the most virulent bacteria known to man, little is understood about the molecular mechanisms responsible for causing disease in the host. *F. tularensis* has a capsule that mediates protection from serum-mediated lysis (157). Also, a *Francisella* pathogenicity island has been found in both Type A and Type B strains that encodes genes necessary for intramacrophage growth (146). Genes coding for a type IV pilus system are found in both Type A and Type B strains (89), and deletions of these genes resulted in an absence of pili and subsequent attenuation in LVS-infected mice (35). Moreover, deletion of genes responsible for type I secretion in *F.*

tularensis LVS also caused attenuated virulence in LVS-infected mice (90). Recently, homologs of genes involved in type VI secretion in other pathogens have been found within the *Francisella* pathogenicity island, but the relevance and function of type VI secretion is still unclear (12). These studies provide the beginning of understanding the complexities of virulence factors responsible for causing disease in tularemia. Collectively, however, they have not provided an explanation for the in vivo virulence of this organism. Thus, it is likely that these features of the bacterium are enhanced by the response of the host in the development of clinical severity.

Animal Model. The most common animal model for tularemia research has been the mouse. The use of LVS in mice is convenient as the LVS maintains virulence in mice while remaining attenuated in human disease. This allows both in vitro and in vivo studies of tularemia to be done at bio-safety level-2. C57BL/6, BALB/c and C3H/HeN are the three most common inbred mouse strains used in experimental LVS animal infections. Virulence is dependent upon route of challenge. C3H/HeN and BALB/c mice inoculated IP with the LVS need <10 CFU to succumb to the infection, thus mimicking the high infectivity of virulent Type A strains in man. C57BL/6 mice are slightly more resistant to the LVS by IP inoculation (82). Mice infected intradermally (ID) need considerably more bacteria to elicit a lethal response, but dissemination is similar in terms of

organs affected and numbers of bacteria when compared to other routes of inoculation. The more susceptible C3H/HeN mice have a LD_{50} of ~10^6 CFUs when challenged ID, while BALB/c and C57BL/6 mice are more resistant (39, 82). However, a primary sublethal LVS inoculation will give protective immunity to secondary virulent Type A infections (71, 179). In fact, in both mice and humans, resolution of a primary *F. tularensis* infection will confer long-lasting immunity to reinfection (179). The murine system has served as an animal model that exhibits remarkable similarities to human disease and pathology (67, 79). This dissertation has focused on using sublethal ID inoculations in mice, which more closely correlate with the natural route of exposure, including cutaneous tularemia by an arthropod vector and exposure through skin from other infected sources.

Pathogenesis. After cutaneous inoculation, *F. tularensis* disseminates throughout the body to organs of the reticuloendothelial system, specifically the liver, spleen, lungs and lymph nodes (68, 120, 180). This phase includes an extracellular bacteremia (78). Tissue colonization of bacteria activates a robust inflammatory response, initially from neutrophils and followed by a large accumulation of mononuclear cells, including macrophages and lymphocytes. In the liver, this influx of cells will develop into a granuloma. In Type A infections, rapidly developing necrosis may not allow granuloma formation, whereas

granulomas in Type B and sublethal infections are predominant because infections of these strains are generally milder. Host survival is contingent upon activation of the immune system to limit the bacterial burden in infected organs (180).

Gross changes in the liver and spleen are not seen until about 4 days post-inoculation (DPI). At this time, the liver turns a pale yellow color and becomes increasingly fragile and flaccid. Type A infections of the spleen cause atrophy with multiple white-gray foci on the surface with hemorrhagic infarcts. No remarkable gross changes are seen in the lung by 5 DPI (42). In an ID challenge, the lung becomes infected, but with lower bacterial numbers and less obvious changes in pathology, as opposed to an aerosolized infection (82).

Histopathologic changes in the liver from a Type A infection can be seen by 1 DPI, as small foci of inflammatory infiltrates with slight increases in neutrophils. Occasionally necrotic hepatocytes can be found near the inflammatory foci. By 2 DPI, some portal areas are infiltrated with macrophages and lymphocytes with overall increases of Kupffer cells in the liver. By 5 DPI, a robust infiltration of mononuclear cells develops within granulomatous areas with multiple areas of hepatic necrosis and vacuolar degeneration of hepatocytes. Furthermore, hepatocytes became a site of infection and replication as they become filled with bacteria. Type B infections elicit similar changes in the liver, but generally with milder

manifestations (42, 67).

Similar to the liver, many histopathologic changes are seen in the spleen during the course of a *F. tularensis* infection. In a Type A infection, changes are first noted by 2 DPI, with an expansion of the red pulp and accumulation of macrophages and neutrophils. By 4 DPI, the red pulp becomes moderately congested, with multifocal infiltrations of neutrophils and many necrotic lymphoid cells in the red pulp and the periphery of the white pulp. By 5 DPI, there is a complete loss of lymphoid follicles, as the white pulp becomes filled with basophilic granules and necrotic cellular debris. Changes are more severe in the red pulp and near central arterioles with occasional thrombosis, hemorrhage and presence of numerous bacteria. Splenic changes in Type B infections are similar but not as severe as seen in a Type A infection (42). Mice challenged intradermally with LVS exhibit a loss of splenic architecture in the red and white pulp. By 5 DPI, necrosis of lymphocytes and cellular infiltrates are seen in the white pulp with severe destruction of lymphoid follicles. Also noted is increased inflammation with a moderate granulomatous response and mild periarteriolar lymphoid sheath hyperplasia (67).

Involvement of the liver and spleen in both clinical and experimental tularemia has been known for a long time regardless of portal of entry or host species (14, 73, 176, 190). These drastic changes in the liver and spleen mark the activation of a robust immune response to combat the

infection. This dissertation is focused on the responses of the liver and spleen during a *F. tularensis* LVS infection in mice challenged intradermally. Specifically, studying the hepatic and splenic infiltrates that develop in response to an infection, using specific cellular markers, and determining what role they play in the innate and adaptive immune responses is the general aim of this dissertation.

B. Innate Immune Response

It has been documented that an early murine infection of *F. tularensis* LVS is controlled by the innate immune system, while long-lived protection and immunity is due to the adaptive immune response (67, 68). The innate host response provides a first line of defense against microbial pathogens in a non-specific manner, which exists before pathogen exposure and is largely associated with cytokines, neutrophils and mononuclear phagocytes. B and T cells mediate the adaptive response and become activated against a specific antigen of the pathogen to promote immunity (67, 72). The importance of the innate immune system has been documented in tularemia, as *scid* mice (deficient in B and T lymphocytes and lacking an adaptive immune response) or even mice deficient in T cells (α/β and γ/δ knockouts) will survive a sublethal tularemia infection for 3-4 weeks before succumbing to death (71, 199), demonstrating that innate immune responses can provide initial control of the infection but cannot inhibit the dissemination of bacteria throughout the

host (67). Important features of the innate immune system and their involvement with *F. tularensis* will be discussed below.

Cytokines. Much of this initial control appears dependent upon pro-inflammatory cytokine production, specifically interferon-γ (IFN-γ) and tumor necrosis factor-α (TNF-α) (7, 70). Mice that received neutralizing antibodies to IFN-γ or TNF-α at the time of *F. tularensis* inoculation succumbed to normally sublethal infections (123). High levels of circulating IFN-γ are found in mice infected with *F. tularensis* (93) and, for survival, IFN-γ is required for the first 2 DPI (123). Moreover, mice genetically deficient in IFN-γ are very susceptible to tularemia (38, 41, 71). Another cytokine, interleukin-12 (IL-12) is also required for protection against *F. tularensis*, as mice deficient in IL-12 will succumb to a sublethal infection (60). IL-12 is an important co-activating signal of IFN-γ, and exogenous addition of IL-12 synergistically increases the amount of IFN-γ produced in mice infected with *F. tularensis* (191). T cells are known to secrete IFN-γ during tularemia (170), but do not appear to be the major contributor in the early infection. Secretion of IFN-γ in the early infection is now largely considered to be natural killer (NK) cell-dependent (128).

Toll-Like Receptors. The host immune system uses pattern recognition receptors to signal cells to initiate protective inflammatory responses to a pathogen. Toll-like receptors (TLRs) are a family of receptors that recognize conserved properties of microorganisms known

as pathogen associated molecular patterns (PAMPs). Expression of TLRs can be found on macrophages, dendritic cells (DCs) and B lymphocytes (189). Two TLRs, TLR2 and TLR4, are potentially important in tularemia as they recognize PAMPs of gram-negative bacteria. TLR2 recognizes many bacterial products, including peptidoglycan and lipoproteins, while TLR4 recognizes the prototypical PAMP, lipopolysaccharide (LPS) (178).

The LPS of *F. tularensis* lacks the robust proinflammatory cytokine response and endotoxicity of the LPS of *Escherichia coli* and other pathogens (77, 158, 186). Mice deficient in TLR4 (C3H/HeJ), thus unable to recognize LPS, are able to clear a sublethal tularemia infection equally as well as WT mice. TLR4 may be important in initiating immune responses, but it appears that this pathway provides minimal activation of the immune response to *F. tularensis* (37). When challenged intradermally, TLR2-deficient mice are no more susceptible to *F. tularensis* LVS than WT mice (41), but when challenged intranasally TLR2-deficient mice have higher bacterial burdens in their tissues compared to WT mice (133), suggesting that TLR2 involvement may be dependent on the route of exposure. Moreover, recent reports suggest that activation of *F. tularensis* infected macrophages and DCs is dependent upon TLR2 (106, 124, 133) and that that IFN-γ production in the liver is controlled by TLR2 (99). Most TLRs, including TLR2 and TLR4, mediate intracellular signaling through the adaptor protein MyD88 (107). Mice deficient in

MyD88 rapidly succumb to a sublethal ID infection within a week of inoculation and have reduced production of IFN-γ and IL-12 (41). This dramatic increase in death would indicate an essential role of TLRs in tularemia, but, to date, the literature has not defined an overpowering phenotype for the TLRs.

Neutrophils. Neutrophils also play an important role during acute infection by phagocytosis of infected cells. Activation of neutrophils occurs in the presence of either live or killed *F. tularensis* LVS (77). In addition, it has been reported that neutrophil chemoattractants and chemokines are upregulated in presence of *F. tularensis* (40). However, during a pulmonary infection the role of neutrophils as primary defenders is greatly reduced compared to a cutaneous infection (43). It has been reported that *F. tularensis* can avoid killing by the neutrophil, by escaping from the phagosome and inhibiting the respiratory burst (141). The importance of neutrophils in tularemia has also been described by use of a monoclonal antibody Gr-1 (clone RB6-8C5) to deplete neutrophils in mice, resulting in sublethal infections rapidly becoming lethal (168). However, by depleting all cells expressing Gr-1, contributions by other cells that express Gr-1 is neglected, including monocyte and DC populations (63). This subject is important to this dissertation, as there is a significant Gr-1^+ cellular population that rapidly accumulates in mice in the early infection (154).

This accumulation will be discussed in much greater detail in the following chapters.

Macrophages. Although *F. tularensis* can be grown in the laboratory on enriched culture media, it is thought that in natural infections, the bacterium replicates within host cells (126). The macrophage has been the model phagocytic cell to study *F. tularensis* infection. However, increasing evidence suggests that other cellular types such as hepatocytes, DCs, B cells and type II lung epithelial cells are also sites of bacterial infection and replication (15, 44, 97, 110, 154). Also, endothelial cells have been shown to undergo proinflammatory changes in the presence of *F. tularensis* (77).

Early studies using infected guinea pigs (49) and chick embryos (30) documented extensive infections of mononuclear phagocytes. An immunofluorescence histopathologic study of monkeys infected with Schu4 demonstrated that the bacterium is present within macrophages of respiratory bronchioles (190). Mononuclear phagocytes are important both as a site of bacterial replication and as effectors of host defense against tularemia. Thus, it is generally agreed that *F. tularensis* readily infects macrophages both in vivo and in vitro and that these cells appear to be a major site of replication for the bacterium in the host (44, 81).

A number of studies have shown that macrophages are also a vital cell in limiting infection. Macrophages control *F. tularensis* infections by

several mechanisms that include production of reactive nitric oxide and superoxide, after exposure to IFN-γ and TNF-α (38, 71, 81, 152). Depletion of macrophages before infection significantly decreases survival time, and activating macrophages in the lungs before infection may help control pulmonary *F. tularensis* infection (20). However, LVS infections in murine and human macrophages indicated that the human cells secrete significantly higher levels of certain proinflammatory cytokines (18).

In turn, *F tularensis* has developed several mechanisms to escape the early protective responses of the host. For example, *F. tularensis* avoids degradation by macrophages through escape from the phagosome within the first few hours of infection (149). The ability of *F. tularensis* to suppress macrophage function has been reported previously (181). *F. tularensis* transiently resides in a nonacidified phagosome with abundant staining for lysosome-associated membrane glycoproteins but with little or no staining for cathepsin D. The phagosomal membranes acquire a densely staining fibrillar coating on their cytoplasmic aspect and subsequently undergo budding, vesiculation, and morphological disruption, giving the bacteria free access to the cytoplasm (20). Recently, it has been shown that *F. tularensis* can suppress the host IFN-γ response in macrophages, thus increasing bacterial survival (150). Moreover it been shown that murine macrophage infection with *F. tularensis* induces apoptosis (116, 123, 135).

Dendritic Cells. Like macrophages, DCs present antigen to T cells, but DCs are the most potent of all antigen presenting cells, largely due to constitutive expression of co-stimulatory markers. DCs are the first cells to engulf and come into contact with a pathogen and are central to link the innate and adaptive immune responses (125). Interactions between DCs and *F. tularensis* have only recently begun to be characterized. Bone marrow derived DCs rapidly increase the expression of cell surface markers (MHC class II and CD86) important to mount an adaptive immune response in the presence of *F. tularensis* LVS (20). Another study found that TNF-α and IL-12 are readily produced from murine DCs infected with *F. tularensis* (124). Interestingly, murine DCs infected with the Type A strain, Schu4, do not show increased expression of MHC class II and CD86, possibly contributing to the greater virulence seen in Type A strains (19). Furthermore, human DCs are more highly activated in the presence of LVS than murine DCs, allowing human cells to control more readily a LVS infection as opposed to its virulence in mice (15).

Natural Killer Cells. NK cells have two important roles in the innate immune response. They can recognize and destroy infected cells by cell-mediated lysis, and they are an important source of IFN-γ. Large populations of NK cells have been shown to control a *F. tularensis* infection in *scid* mice (deficient in B and T lymphocytes) for the first 20 DPI

(71). However, NK cell depletion studies in tularemia do not indicate that NK cells are necessary to recover from infection. Mice that were depleted of NK cells by use of NK1.1 or LGL1 antibodies did not have any significant differences in controlling the early infection when compared to WT mice (123). Another study using NK cell-deficient beige mice did not observe significant changes in bacterial control when compared to WT mice in *F. tularensis* infections, suggesting that NK cell mediated-lysis is not required in tularemia (60). However, NK cells appear very important for the production of IFN-γ in the early infection, as the majority of cells secreting IFN-γ are NK cells (128). Also, NK cells found in the liver secrete large amounts of IFN-γ in response to *F. tularensis* infection (191).

C. Adaptive Immune Response

As stated earlier, the innate immune response will provide initial protection of the host from *F. tularensis* LVS infection, but immunity is dependent upon the adaptive immune response. In tularemia, like other diseases caused by intracellular pathogens, the adaptive immune response is largely based upon a robust T lymphocyte response, while potential contributions from B lymphocytes have not been completely characterized. Both the B cell and T cell roles in tularemia will be described below.

B Lymphocytes. The role of B cells in the adaptive immune response is typically thought of as the ability to produce specific antibody

against a pathogen. However, since *Francisella* is a facultative intracellular pathogen, the requirement of B cells and antibody production in the immune adaptive response has been debated. Nevertheless, recent evidence indicates that during *F. tularensis* infection, mice develop a bacteremia that is largely extracellular (78). This result increases the importance of B cells and antibody in tularemia, as B cells, particularly those in the spleen, are known to have a major role in clearance of blood-borne pathogens (1, 33, 139).

Of late, B cells and antibody production have received greater interest in other infections with intracellular bacteria and appear to optimize the clearance of such bacteria. During a *Chlamydia* infection, B cells have been shown to be important to prime T cells for activation (198). In *Salmonella*, protective immunity is strongly, but not exclusively, dependent on B cells (145). Furthermore, *scid* mice (deficient in B and T lymphocytes) infected with virulent *Listeria* and treated with a monoclonal antibody show significant reduction in bacterial burden during the first hours to days post-inoculation, demonstrating the importance of antibody, independent of B and T cells (62). Also, in *Ehrlichia,* an obligate intracellular bacterium, passive immunity experiments demonstrated that there is a significant role for antibody, although cellular immunity is required for complete clearance of the bacteria (192).

In tularemia, there is recent evidence to believe B lymphocytes are contributing to the development of immunity much more so than previously thought. Mice infected with *F. tularensis* LVS develop a rapid IgM response by 5 DPI and IgG is detected by 10 DPI. Both IgM and IgG can be detected for 4 months post-inoculation (59, 155). This antibody production has been used experimentally as immune serum that is transferred passively to mice prior to bacterial inoculation. Contribution of antibody in tularemia has been reported to be minimal, as mice that receive immune serum are not protected from lethal infections (53, 66, 155). However, Stenmark et al. (174) demonstrated that when B cell deficient mice are administered whole immune serum prior to inoculation, they survive a lethal challenge of *F. tularensis* LVS or a fully virulent Type B strain, thus indicating a role for antibody. Moreover, increased levels of proinflammatory cytokines, TNF-α and IL-12, are seen in mice that receive immune serum (175). Nevertheless, antibody may only provide protection against *F. tularensis* strains of lesser virulence, as mice administered immune serum prior to a Type A infection are not protected (3, 182).

Much of the antibody produced in a primary *F. tularensis* infection is specific for the LPS. Indeed, a rapid antibody response is produced in mice immunized with only the LPS of *F. tularensis* LVS (85). LPS can stimulate protective immunity against low virulence strains, but not Type A strains. Mice immunized with *F. tularensis* LPS were challenged eight

weeks later, intraperitoneally, with a lethal dose of LVS or Schu4 and monitored for survival. Only mice challenged with LVS were protected (85). Furthermore, vaccination with the O-antigen of *F. tularensis* LPS provides some protection against low virulence strains, but not to Type A strains (46). However, mice immunized with a *F. tularensis* mutant of the O-antigen of the LPS survived lethal ID challenges, indicating antigens other than the O-antigen can elicit a protective immune response (160).

Production of antibody by B cells may be beneficial in a primary *F. tularensis* infection, but it does not appear necessary for the development of immunity. Genetically altered CD4 knockout mice vaccinated with *F. tularensis* LVS secrete only small amounts of IgM and no IgG, and when challenged with a lethal secondary LVS dose, these mice exhibit strong protection (199). This result implies that antibody is not necessary to provide protection and immunity. Evidence suggests that B cells have properties other than antibody production that may prove beneficial to link the innate and adaptive immune responses. These properties include antigen presentation, 'natural' antibody production, TLR expression and production of inflammatory cytokines (184).

B lymphocytes appear to confer early protective immunity in tularemia without a robust antibody response, suggesting that there is an increased role in cytokine production. Mice challenged with sublethal doses of *F. tularensis* survive a lethal secondary dose given 2-3 days after

the first inoculation (69). This protection is attributed to B cells as athymic (T cell deficient) mice also survive in an antibody-independent fashion (70). Furthermore, B cell deficient mice subjected to this same experiment do not survive a lethal infection (53). One recent study demonstrates that *F. tularensis* has an unique ability to invade B cells and cause intracellular signaling to induce apoptosis (110).

B cells appear to optimize the clearance of *F. tularensis*. B cell deficient mice inoculated with LVS are only marginally compromised to control a primary infection, but 100-fold less well protected against a secondary challenge. Absence of B cells results in a significant delay of bacterial clearance from liver and spleen and a more prominent and long-lasting granuloma formation in the liver (66). However, B cell deficient mice can compensate for this defect in a secondary infection if reconstituted with either naïve or immune B cells (66). This inability to control a secondary infection in mice has been attributed to a lack of regulation of neutrophils found in B cell deficient mice (21). The role of B cells in tularemia is only beginning to be defined, but B cells have many functions, other than antibody secretion, that appear to be beneficial to the host immune response.

One of the goals of this dissertation was to determine what role B cells and antibody production play in tularemia. The spleen, being one of the first organs to initiate contact with both extracellular and intracellular

bacteria, was used to investigate B cells. The spleen contains three populations of mature B cells: follicular B (FO B) cells, marginal zone B (MZ B) cells and activated plasma cells. These populations can be separated according to cell surface marker expression and were investigated by flow cytometry during the acute phase of a murine tularemia infection. Chapter IV of this dissertation discusses the importance and involvement of B cells in tularemia infected mice and the interplay of these cells with the immature myeloid populations.

T Lymphocytes. After initial presentation of an antigen, T cells expand into large effector cell populations expressing both CD4 and CD8. These T cells work together to control the spread of a pathogen. CD8 T cells can have an effector role in killing bacteria-infected cells, while CD4 T cells provide cytokine secretion for immune response activation. Once the infection is cleared, some effector cells will develop into memory cells, which can rapidly respond to a secondary infection of the pathogen (92).

While the role B cells play in tularemia is unclear, the T cell response is critical for protective immunity and memory. As discussed previously, mice deficient in T cells (α/β knockouts) will survive a sublethal ID challenge with *F. tularensis* for 3-4 weeks before succumbing to death (71, 199). Resolution of the infection is dependent upon T cells. Mice infected with a low dose of a Type A *F. tularensis* undergo severe thymic atrophy and marked depletion of CD4 and CD8 T cells, suggesting

increased virulence of Type A strains may be partially due to targeted T cell destruction (36).

In mice there are three α/β T cell populations, $CD4^+$, $CD8^+$ and $CD4^-$ $CD8^-$ $NK1.1^-$ (double negative), which have effector functions and promote memory to *F. tularensis* LVS infections. All three populations inhibit *Francisella* growth in macrophages, produce IFN-γ and TNF-α cytokines and can facilitate survival in mice (50, 51). To characterize these T cell populations, mice genetically deficient in either CD4 or CD8 were infected with sublethal doses of *F. tularensis*. CD4 or CD8 deficient mice were able to control and clear a primary infection. Interestingly, mice deficient in both CD4 and CD8, thus leaving only double negative α/β T cells, are unable to resolve the infection, indicating that either CD4 T cells or CD8 T cells are absolutely required to control and clear a primary sublethal *F. tularensis* LVS infection. Double negative T cells may contribute to control the infection, but are seemingly not required (47, 199). In mice, contribution of γ/δ T cells is minimal as mice deficient in γ/δ T cells are able to control a *F. tularensis* infection as well as WT mice (199).

The actual effector mechanisms that T cells use to control and clear a *F. tularensis* infection are unclear. Secretion of IFN-γ is an important feature of T cells and critical in the acute tularemia infection. However, the initial production of IFN-γ is not dependent on T cells as NK cells are more

likely the source. Also, IFN-γ contribution in a secondary infection does not appear to be essential to clear the bacteria (68). Mice that recover from a sublethal primary infection and are depleted of IFN-γ prior to a lethal ID secondary challenge do not differ in survival from control mice (171). Conversely, mice depleted of IFN-γ prior to a secondary aerosol challenge succumbed to death (45), indicating that IFN-γ effectiveness may be related to the route of exposure. Other cytokines, such as TNF-α, have been associated with T cell function in the absence of IFN-γ (50). T cells also have to ability to activate the microbial-killing machinery of macrophages. Indeed, when *F. tularensis*-infected macrophages and immune T cells are incubated together, intramacrophage bacterial control is partially dependent upon inducible nitric oxide synthase and nitric oxide (68).

Recently, *F. tularensis* has been reported to modulate the host immune response. Infected macrophages block T cell proliferation and promote production of anti-inflammatory cytokines by release of a soluble mediator, prostaglandin E_2 (PGE_2), thereby suppressing the adaptive immune system and allowing for increased viability of the bacteria (195). Furthermore, intranasally infected mice are seen to induce PGE_2 with lower numbers of IFN-γ producing T cells when compared to ID inoculated mice. Inhibition of PGE_2 in intranasally infected mice results in increased amounts of IFN-γ secreting cells and lower bacterial burden in the lungs

(194). Induction of PGE_2 secretion is advantageous for the bacteria and demonstrates the ability of *F. tularensis* to suppress the host immune response. Overall, the T lymphocyte response to *F. tularensis* infection is mandatory to develop protective immunity, but effector mechanisms of T cells are only beginning to be understood.

D. Aims of the Research

There is conflicting literature regarding the specific contributions of the innate and adaptive immune responses in tularemia. The general objective of this dissertation was to clarify the role of the immune response to tularemia using in vivo experimentation in mice. During an ID murine infection, the liver and spleen are the first organs to come in contact with blood-borne *F. tularensis*. Both of these organs experience dramatic changes in cellular architecture during an early infection, as many cells of the innate immune response rapidly respond and infiltrate these tissues. Investigation of the cellular makeup of this large influx of cells has led to an increased understanding of how the immune system reacts to *F. tularensis* infection. Up until this dissertation, the cellular response to *F. tularensis* in the liver and spleen had not been characterized with specific markers. A list of cell surface markers used throughout this dissertation can be found in Table 1.2.

Research from this dissertation has identified a large accumulation of Gr-1^+ $CD11b^+$ expressing cells in the liver, spleen and bone marrow of

mice infected with *F. tularensis*. Cells expressing Gr-1 and CD11b are indicative of an immature myeloid cell phenotype that can differentiate into mature neutrophils, macrophages or DCs. Moreover, Gr-1^+ $CD11b^+$ cells have immunosuppressive behavior in cancer, traumatic stress, or in fungal, parasitic and bacterial infections (2, 86, 94, 132, 143, 148, 172, 204). This cell phenotype is now defined as a heterogeneous cell population termed myeloid-derived suppressor cells (MDSCs) (83). The large accumulation of MDSCs in mice infected with *F. tularensis* may contribute to suppressing the immune system.

However, MDSCs have also been reported to activate the T cell response in the presence of proinflammatory cytokines. When cultured with IFN-γ and TNF-α, Gr-1^+ $CD11b^+$ cells will differentiate into mature antigen presenting cells (26). Another recent study demonstrated that MDSCs from tumor-bearing mice activate NK cells to produce high levels of IFN-γ (147). In *T. gondii* infection, Gr-1^+ monocytes are required for an effective host response against the parasite, indicating a role in host defense (61). Moreover, it has been documented that upon ex vivo incubation with GM-CSF, MDSCs increase expression of antigen presenting cell markers (55, 197). These studies reveal, that in some conditions, MDSCs do not always suppress and may indeed increase the activation of the immune system.

Surface Marker	Cell Expression	Function
CD3	Mature T	T cell receptor, signal transduction
CD4	MHC class II-restricted T	T cell coreceptor for MHC class II-restricted T cells, signal transduction
CD8	MHC class I-restricted T	Coreceptor for MHC class I-restricted T cells, signal transduction
CD11b (Mac-1)	Granulocytes, monocytes, dendritic, NK, subsets of T and B	Adhesion, chemotaxis, apoptosis
CD11c	Dendritic, macrophages, granulocytes, NK	Adhesion
CD19	B, dendritic	B cell receptor, signal transduction, differentiation
CD21	Mature B	Signal transduction
CD23	Mature B	Low affinity receptor for IgE
CD45 (B220)	Hematopoietic, pan B	Differentiation, activation
CD49b (DX5)	NK	Adhesion
CD138	Activated B	Differentiation
F4/80	Mature macrophages, Kupffer, dendritic	Differentiation
Gr-1 (Ly6C/Ly6G)	Granulocytes, myeloid cells	Differentiation
IgM	Mature B	Differentiation, activation
MHC II (I-A/I-E)	Macrophages, dendritic, B	Antigen presentation
NK1.1 (CD161)	NK, NK T	NK cell-mediated cytotoxicity

Table 1.2. Cell surface marker expression and function for cellular populations described in this dissertation. Adapted from references (92, 115).

The following three chapters of this dissertation are focused on understanding how this virulent bacterium interacts with the immune system, specifically within the liver and spleen of mice infected with *F. tularensis*. Outlined below are the aims of each chapter:

Chapter II Aim. To characterize the cellular makeup of granulomatous lesions found in the liver and identify the large accumulation of CD11b$^+$ cells during an acute murine infection.

Five days after *F. tularensis* inoculation, the livers of mice develop granulomas that are filled with two main subpopulations expressing CD11b. One subpopulation, Gr-1$^+$ CD11b$^+$ cells, was identified as MDSCs, which may contribute to the severity of tularemia by suppressing the immune response. The other subpopulation, MHC II$^+$ CD11b$^+$ cells, is consistent with a mature antigen presenting cell phenotype. Accumulation of one of these subpopulations may imply how the host will ultimately deal with the infection. MDSC accumulation may result in increased pathology, while MHC II$^+$ CD11b$^+$ cell accumulation results in bacterial clearance. This work has been published in Infection and Immunity, Volume 74, Issue 12, pages 6590-6598 (154).

Chapter III Aim. To characterize cellular populations that develop in the spleen during a murine infection and to define a role for the MDSCs in tularemia.

Large accumulations of MDSCs are seen in the spleen and bone marrow of infected mice ten days after inoculation with *F. tularensis*. Splenic MDSCs were purified and monitored in ex vivo culture for cell differentiation, both with and without *F. tularensis*. Moreover, MDSCs were prepared for passive transfer in mice with tularemia and monitored for morbidity, mortality and pathological changes.

Chapter IV Aim. To clarify the contribution of B lymphocytes and antibody production to a *F. tularensis* infection in mice and to document possible interplay with MDSCs.

B cells, whose contribution to the host response in tularemia is not clear, may play a major role in linking the innate and adaptive immune responses. To define a role for B lymphocytes, specific markers were used to identify murine B cell changes by flow cytometry analysis. Also, B cell deficient mice were inoculated with *F. tularensis* and monitored over the course of an infection. With conflicting literature about the benefit of antibody against *F. tularensis*, antibody production from B cells was examined in the early infection. Furthermore, accumulation of MDSCs in *F. tularensis* infected B cell deficient mice was also assessed.

Chapter II

Murine Hepatic Response to *Francisella tularensis*

A. Introduction

As discussed above, there are two subspecies of *F. tularensis,* subspecies *tularensis* (Type A) and subspecies *holarctica* (Type B) that are highly infectious for humans. Type B strains cause only moderate illness and are usually non-fatal. Meanwhile Type A strains cause potentially lethal infections in humans, particularly following exposure to aerosolized organisms. For this reason, Type A *F. tularensis* is considered a potential biological warfare agent (56) and has been classified as a Category A agent of bioterrorism by the Centers for Disease Control and Prevention. An attenuated live vaccine strain (LVS), derived from a Type B *F. tularensis*, does not cause illness in humans but causes a disease in mice that resembles human tularemia (8, 82). Therefore, the LVS strain has been used extensively for experimental studies on the pathogenesis of tularemia. The involvement of the liver and development of granulomas in both clinical and experimental tularemia have been known for a long time regardless of portal of entry or host species (14, 73, 176, 190).

Granuloma formation is a common feature found in infections with intracellular pathogens, such as *Mycobacterium tuberculosis, Listeria monocytogenes, Histoplasma capsulatum* and *Schistosoma mansoni* (65,

84, 98, 103, 104, 183). It is typically thought that granuloma formation occurs to separate the pathogen from the host tissue. This wall can prevent dissemination, protect surrounding healthy tissue, isolate inflammation and control the growth of the bacteria. However, granuloma formation may also act as a reservoir for surviving bacteria, as is the case in tuberculosis, or become a focus of production of inflammatory mediators that ultimately leads to additional damage.

In murine tularemia, single or multiple, randomly-distributed irregular microabscesses of mononuclear cells and a few neutrophils in the hepatic parenchyma have been noted as early as 1 DPI (42). These microabscesses grow into well-circumscribed granulomas composed of mostly macrophages by 4-5 DPI. Hepatocytes can be infected by *F. tularensis*, and these cells can harbor large numbers of bacteria (38, 39, 42, 44, 121, 202). With time, the developing granulomas become prominent in the entire liver, and the cytoplasm of many hepatocytes becomes completely filled with bacteria (44). Liver infection from LVS has also been used to study protective immunity and mouse strain susceptibility (39). Livers from LVS-immunized C57BL/6 mice contain small-to medium-sized areas of focal inflammatory necrosis with both necrotic and apoptotic hepatocytes, while the liver pathology of LVS-immunized BALB/c mice is milder. This mouse strain is more resistant to ID and aerosol inoculation (39). Thus, in murine tularemia, pathogen

virulence, genetic background of the host, and route of inoculation all play a role in pathogenesis, specifically in the liver.

While liver pathology of tularemia is well recognized in a number of experimental models, characterization of the infiltrating cells of the lesions had not been done with specific markers. Nor, for that matter, had the process of cell death in liver infection been documented specifically. In this chapter, experimental sublethal tularemia infection of C3H/HeN mice was used to characterize the liver infiltrates and other signs of hepatic dysfunction. It was found that subpopulations of cells expressing CD11b associate with *F. tularensis* during an early development of hepatic lesions.

B. Materials and Methods

Bacteria: *F. tularensis* LVS (American Type Culture Collection 29684, Manassas, VA) was cultured in Mueller-Hinton (MH) broth (BD Biosciences, Sparks, MD) supplemented with 2% IsoVitaleX Enrichment (BD Biosciences), 5.6 mM D-glucose, 625 μM $CaCl_2$, 530 μM $MgCl_2 \bullet 6H_2O$, and 335 μM ferric pyrophosphate, and incubated at 37°C and 5% CO_2. Mid-log phase bacteria were frozen in 1 ml aliquots at -80°C (77, 89). Bacteria from frozen aliquots were grown on Chocolate II agar (BD Biosciences) at 37°C and 5% CO_2. Single colonies were inoculated into pre-warmed (37°C) MH broth, grown for 16-18 hours, and serially

diluted in MH broth to 10^6 CFU/ml determined by an optical density reading at 600 nm and verified by growth on Chocolate II agar.

Mice*:* Female C3H/HeN mice were purchased from Charles River Laboratories (Wilmington, MA) and used from 6 to 10 weeks of age. All mice were housed in microisolator cages with free access to food and water. Mice received ID injections of 10^6 CFU of *F. tularensis* LVS. At various time points post-inoculation, mice were euthanized, immediately followed by blood and organ collection. The institutional review board approved all animal procedures. Streaking on Chocolate II agar plates and counting the numbers of colonies determined the number of viable bacteria in blood.

White blood cell counts and enzymes*:* Total white blood cell counts were done manually in Petroff-Hausser chambers. Differentials were determined by enumeration from Giemsa-stained peripheral blood smears. The Research Animal Diagnostic Laboratory, Columbia, MO, did serum clinical chemistries for liver and kidney function. The tests included determinations for alanine transferase (ALT), alkaline phosphatase, direct and total bilirubin, lactate dehydrogenase (LDH), creatinine, and blood urea nitrogen.

Cell isolation: Following euthanization of mice, livers were perfused with large volumes of Hanks' Balanced Salt Solution (HBSS) (Invitrogen, Grand Island, NY) until the organ was blanched. Once

removed, livers were minced and incubated in digestive medium [0.05% collagenase A (Roche, Indianapolis, IN) and 0.002% DNase I (Sigma, St. Louis, MO) in HBSS] at 37°C at 80 rpm for 30 min to provide a single cell suspension of tissue. Cells were collected and centrifuged for 10 min at 400 × g followed by suspension on a Percoll gradient (GE Healthcare, Piscataway, NJ) and centrifugation for 30 min at room temperature (RT) at 400 × g in a swing-out rotor. Mononuclear cells were enumerated in Petroff-Hausser chambers prior to antibody staining for flow cytometry.

Flow cytometry: Mononuclear cells (10^6) were resuspended in fluorescence-activated cell sorter (FACS) buffer [0.2% bovine serum albumin (BSA) (Sigma), 0.09% NaN_3 (Sigma) in phosphate buffered saline (PBS) (Invitrogen)] and incubated with anti-FcγR antibody (clone 2.4G2) (BD Pharmingen, San Diego, CA) before appropriate amounts of conjugated antibodies or isotype controls were added and incubated for 30 min at 4°C (see below). Cells were washed twice with FACS buffer and centrifuged for 5 min at 400 × g at 4°C before being fixed in 500 μl of 1% formalin in PBS. At least 10,000 viable cells were acquired on the basis of forward light and side light scattering and then quantified by a BD FACS Calibur instrument and analyzed with WinList software (Verity Software House, Topsham, ME). Two-tailed *P*-values were calculated using an unpaired t-test with InStat software (GraphPad, San Diego, CA).

Antibodies for flow cytometry and immunofluorescence: The following antibodies were used for flow cytometry and confocal microscopy: fluorescein isothiocyanate (FITC) anti-mouse CD45R/B220 (clone RA3-6B2), FITC anti-mouse CD11c (clone HL3), FITC anti-mouse CD49b/Pan NK cells (clone DX5), R-phycoerythrin (PE) anti-mouse CD3 (clone 17A2), PE anti-mouse CD45R/B220 (clone RA3-6B2), PE anti-mouse CD11c (clone HL3), PE anti-mouse I-A/I-E (MHC II) (clone M5/114.15.2), PE anti-mouse Ly-6G and Ly-6C (Gr-1) (clone RB6-8C5), peridinin chlorophyll-a protein (PerCP) anti-mouse CD4 (clone RM4-5), PerCP-Cy5.5 anti-mouse CD11b (also known as Mac-1) (clone M1/70), allophycocyanin (APC) anti-mouse NK1.1 (clone PK136), APC anti-mouse CD8 (clone 53-6.7) from BD Pharmingen; Alexa Fluor 488 anti-mouse CD4 (clone GK1.5), Alexa Fluor 647 anti-mouse CD8a (clone 53-6.7), Alexa Fluor 647 anti-mouse CD11b (Mac-1) (clone M1/70) from Biolegend (San Diego, CA); and Alexa Fluor 488 anti-mouse F4/80 (clone CI:A3-1) from Serotec (Raleigh, NC). Isotype-matched antibodies (all from BD Pharmingen) were used as a control for non-specific binding. Polyclonal rabbit anti-*F. tularensis* LVS was harvested after four injections of heat-killed organisms. FITC anti-rabbit IgG from Chemicon Int. (Temecula, CA) or Alexa Fluor 555 anti-rabbit IgG from Molecular Probes (Eugene, OR) were used as secondary antibodies to *F. tularensis* antisera.

Hematoxylin and eosin staining and immunohistology on tissue sections: Livers were aseptically removed and immediately fixed in 10% neutral buffered formalin, embedded in Blue Ribbon paraffin (Surgipath, Richmond, IL), sectioned at 5 μm, stained with hematoxylin and eosin, dehydrated in graded alcohols, cleared with xylene and mounted with Acrymount (Statlab Medical Products, Lewisville, TX). Tissue sections were examined by light microscopy.

Detection of caspase-3 was achieved by dewaxing and rehydration of paraffin sections with xylene and graded alcohols, followed by quenching of endogenous peroxidase with methanol and hydrogen peroxide and blocking with Tween-BSA. Rabbit anti-cleaved caspase-3 (Asp175) from Cell Signaling Technology (Danvers, MA) was diluted in blocking solution and added to sections for overnight incubation at RT. Sections were then washed and treated with polyclonal biotinylated anti-goat IgG (Vector Laboratories, Burlingame, CA) for 1 hour at RT. Sections were washed, and avidin biotinylated enzyme complex reagent (Vector Laboratories) was added for 45 minutes at RT, followed by five washes and incubation with diaminobenzidine (Sigma-Aldrich Corporation, St. Louis, MO) for 10 minutes. Sections were rinsed in water, counterstained with hematoxylin and dehydrated in graded alcohols, and cleared with xylene.

Terminal deoxynucleotidyl transferase-mediated dUTP-X nick end labeling (TUNEL) assays were performed according to the manufacturer's protocol using an in situ cell death detection kit with tetramethylrhodamine red (Roche Applied Science, Indianapolis, IN).

For detection of bacteria in the liver, paraffin sections were treated for 30 min with rabbit anti-*F. tularensis* LVS IgG, after dewaxing and rehydration of the sections. A secondary alkaline phosphatase-labeled goat anti-rabbit IgG from Zymed (South San Francisco, CA) was added for 30 minutes at RT, and then Vulcan Fast Red Chromogen (Biocarta, San Diego, CA) was used to visualize the bacteria.

Immunofluorescent staining of frozen tissue sections: Tissues removed from mice were immediately placed in freshly made 1% formalin in PBS and gently shaken for 1 hour at 4°C. The tissues were removed, blotted dry, placed in freshly made 30% sucrose in PBS at 4°C, and left overnight. The tissues were removed, blotted dry, placed in Neg -50 freezing compound (Richard-Allan Scientific, Kalamazoo, MI), rapidly frozen in isopentane that had been cooled with liquid nitrogen, and stored at -80°C. For some experiments, organs were immersed in Optimal Cutting Temperature Compound (Sakura Finetek, Torrance, CA), then frozen and stored as above.

Frozen tissue sections were cut at 5 µm in the cryostat at -25°C, air dried, and fixed in acetone for 30 seconds. Twenty µl of the various

antibodies (see above), diluted in 0.01 M PBS (pH 7.4), were applied to sections and incubated in the dark for 25 minutes. Slides were washed three times in PBS and, when appropriate, secondary antibodies were added for 25 minutes in the dark. Mouse spleens, treated in the same manner, were used as positive controls for the antibodies used in this study. After washing, slides were mounted in Opti-Mount (Richard-Allan Scientific, Kalamazoo, MI). The slides were examined by phase-contrast and epifluorescence microscopy using a Nikon eclipse E600 microscope, and images were captured using a Spot camera (Diagnostic Instruments, Inc.). Slides for confocal microscopy were analyzed using a Leica DM IRE2 confocal microscope. Images of the red, green and blue emission signals were captured separately with Leica's LCS software package. Images were processed with Adobe Photoshop.

C. Results and Discussion

The pathology of liver involvement in experimental tularemia has been studied with standard histopathological procedures, and the existence of granulomatous-looking, necrotic lesions has been observed in several studies (17, 38, 42, 44, 120). However, the infiltrating cells of the hepatic lesions have not been characterized with respect to specific markers, and the nature and extent of cell death has not been examined with specific markers.

Intradermal inoculation of C3H/HeN mice with *F. tularensis* LVS led to a detectable bacteremia for the first week post-inoculation. The peak of this infection was between days three and six of the infection (Figure 2.1). In the periphery, this bacteremia was accompanied by leukocytosis with an initial reversal in the ratio of lymphocytes to neutrophils in the differential, as well as a modest increase in the percentage of circulating monocytes by 4 DPI (Table 2.1). A similar pattern of leukocytosis and reversal of the differential has been demonstrated for experimental infections of other strains of mice (42). There were marked increases in serum levels of ALT (Figure 2.2A) and LDH (Figure 2.2B). This pattern is consistent with early inflammation in the liver without reducing the ability of the liver to conjugate and secrete bilirubin, as evidenced by the normal values obtained for direct and indirect bilirubin and alkaline phosphatase. Kidney function was within normal limits. Moreover, increases of liver to mouse weight are seen during the course of infection (Figure 2.3). These findings indicate that tularemia causes an infectious hepatitis.

The liver increases in size during the course of infection as many immune cells are recruited to contain the infection. Early foci characterized by infiltration of a large number of mononuclear cells morphologically consistent with macrophages and a few neutrophils were noted in infected livers (Figure 2.4B) (39, 42). These lesions had a focus of mononuclear infiltration. As these lesions matured, necrotic

hepatocytes with pyknotic nuclei were common within the inflammatory foci (Figures 2.4C and 2.4D). The evolution of the granulomatous response is typical, where neutrophils with a short half-life appear early and mononuclear cells persist. Neutrophils are known to be important for defense in a primary tularemia infection (43, 169). The perivascular location of many of the granulomas (Figure 2.4C) suggests that the infiltrate derives from circulating cells from the blood as opposed to an expansion of the resident cells.

Bacteria invade the liver parenchyma early in randomly distributed locations (Figure 2.5B). Some bacteria appear to be associated with Kupffer cells based on the location of these cells on the sinusoids, but others are within hepatocytes (Figure 2.5B and 2.5C). Figure 2.5C contains a hepatocyte swollen with bacteria, similar to what has been observed by others (44). These heavily infected hepatocytes could become focal points for the development of the granulomas. In the hepatic lesion of 5 DPI, it is difficult to determine whether the bacteria are extracellular or associated with hepatocytes, macrophages or both (Figure 2.5D). Nonetheless, there is severe damage to hepatocytes, and numerous bacterial colonies are present in the lesions. These results indicated that hepatic dysfunction in tularemia is likely to be a contributor to the morbidity and mortality of this infection, although liver disease in some instances can be reversible.

To characterize the cells in the lesions observed in the livers of infected mice, immunofluorescence microscopy on frozen liver sections was performed using specific cell surface markers for macrophages, lymphocytes and *F. tularensis* antibody. Infection of the liver parenchyma was already present on the first day after inoculation (Figure 2.6). In later stages, the vast majority of the mononuclear cells within the granulomas were $F4/80^{-}$ $CD11b^{+}$ (Figure 2.7). A few $F4/80^{+}$ $CD11b^{-}$ cells were found in the borders of the lesion; these may represent a population of Kupffer cells (101). The $F4/80^{-}$ $CD11b^{+}$ cells may represent monocyte/macrophages recruited from blood to the liver. Cells with this phenotype have been shown to traffic from the peripheral blood to the inflamed retina in a murine model of autoimmune uveoretinitis (196). Blood monocytes can express both F4/80 and CD11b markers (88), so it is possible that the phenotype of the infiltrating mononuclear cells may be derived from blood with a subsequent downregulation of the F4/80 marker. Another possibility is that $F4/80^{-}$ $CD11b^{+}$ cells are a subset of resident macrophages similar to those described in the spleen, optic nerve and the connective tissue of the lung in which expression of F4/80 antigen is downregulated by inflammatory stimuli (23, 25, 74, 193). Regardless of the possible origin of $CD11b^{+}$ $F4/80^{-}$ cells, *F. tularensis* was found associated with these cells, correlating with a $CD11b^{+}$ phenotype that has been shown to be involved in the hepatic killing of other bacteria (24).

CD11b can be expressed on a variety of cells, including granulocytes, T cells, B cells, NK cells, DCs and monocytes. To further characterize the $CD11b^+$ infiltrating mononuclear cells, immunofluorescence microscopy was performed using specific markers for cell types known to express CD11b. Neutrophils were ruled out by morphology as a major cell type contributing to the infiltrate of the granulomas (Figures 2.4C and 2.4D). $CD3^+$, $CD4^+$ and $CD8^+$ T cells and $B220^+$ B cells were not detected in the granulomatous areas of hepatocyte necrosis at 1 and 5 DPI. However, the $CD11b^+$ cells did colocalize with markers specific for myeloid cell populations, which were most consistent with macrophages and DCs. One population expressed both macrophage ($CD11b^+$) and granulocyte ($Gr\text{-}1^+$) markers and was the predominant phenotype in the granuloma (Figure 2.8A). The lesions also contained a significant population that had a MHC II^+ $CD11b^+$ phenotype (Figure 2.8B) and a $CD11c^+$ $CD11b^+$ DC phenotype (Figure 2.8C). NK cells ($NK1.1^+$ and $CD49/DX5^+$) were seen in the liver tissue at 5 DPI but were not associated with the hepatic lesions (Figure 2.8D).

Coexpression of Gr-1 and CD11b is indicative of myeloid derived suppressor cells (MDSCs) that can either differentiate into mature granulocytes, macrophages or DCs (162). Immature myeloid cells ($Gr\text{-}1^+$ $CD11b^+$) do not express MHC class II molecules and exhibit dull F4/80 expression, if at all (102, 136), correlating with the predominant phenotype

($F4/80^{-}$ $CD11b^{+}$) seen at 5 DPI in Figure 2.5. MDSCs accumulate and inhibit the T cell immune response in tumor-bearing mice (86, 148, 173). In addition, they have been found to have immunosuppressive effects in mice infected with various pathogens (2, 10, 94, 143). However, it has been noted that depending on the cytokine milieu that is present, MDSCs can either activate or inactivate the T lymphocyte immune response. Bronte et al. (26) showed that when cultured in vitro with proinflammatory cytokines (IFN-γ and TNF-α), $Gr\text{-}1^{+}$ $CD11b^{+}$ cells differentiate into functional antigen presenting cells. However, when these cells are cultured with an anti-inflammatory cytokine (IL-4), the cells greatly increase T cell suppression. Therefore, the function of MDSCs is dependent upon the inflammatory response of the host initiated by a pathological process.

Chen et al. (38) have reported that mice deficient in IFN-γ and infected with *F. tularensis* have reduced size and number of granuloma formations in the liver during an early infection compared to WT mice. Other cytokines deemed important to evoke the T-cell independent response to *F. tularensis* in the liver are TNF-α and IL-12 (93). Moreover, cells responsible for IFN-γ production in the liver, such as NK cells (17), are resident to the liver and need IL-12 for optimal response and proper granuloma formation in the liver (191). Unable to mount the appropriate cytokine response, the hepatic lesions, which are largely composed of

MDSCs, will not fully form, limiting the host's ability to wall off the dissemination of bacteria by granuloma formulation and allowing increased bacterial burden in the liver (17). During an early *F. tularensis* infection in the liver of normal mice, a rapid accumulation of MDSCs develops in the presence of IFN-γ. The liver responds by forming a granuloma that will limit tissue damage and control bacterial replication.

To further quantify the abundance of cellular populations, flow cytometry analysis was performed on liver tissue from uninfected mice and mice infected with *F. tularensis* LVS at 5 DPI. Markers were used for T cells (CD3), B cells (B220), DCs (CD11c and CD11b), NK cells (DX5 and NK1.1), macrophages (F4/80, MHC class II and CD11b) and MDSCs (Gr-1 and CD11b) (Table 2.2). Results of the quantification of mononuclear cells in the liver by flow cytometry were consistent with the imaging results. Markers for B and T cells were similarly expressed in both uninfected mice and mice inoculated with *F. tularensis* LVS five days earlier. These results confirm the presence of the intrahepatic lymphocyte population. Interestingly, the intrahepatic lymphocyte population did not increase and even decreased in expression by 5 DPI, suggesting a level of inhibition that correlates with an accumulation of MDSCs. A two-fold increase of NK cell marker expression was noted by 5 DPI. This may indicate that NK cells are upregulated to aid the innate response in secretion of cytokines, such as IFN-γ, even though NK cells were not seen

in the granulomas. Total expression of CD11c, which is indicative of DCs, increased 2.5-fold by 5 DPI. Furthermore, the numbers of myeloid DCs ($CD11c^+$ $CD11b^+$) that were found in the lesions also increased, but did not reach statistical significance. The most significant increase of all cellular phenotypes was $CD11b^+$ cells (2.3% uninfected to 21.3% at 5 DPI), which correlates to the majority of cells seen in the hepatic lesions. The bulk of $CD11b^+$ cells were $CD11c^-$, indicating that most $CD11b^+$ cells were not DCs. In addition, $F4/80^+$ $CD11b^+$ cells did not increase significantly, correlating with low levels of this subpopulation in Figure 2.7.

The largest increases in $CD11b^+$ subpopulations observed by flow cytometry analysis were the $Gr\text{-}1^+$ $CD11b^+$ MDSCs and the MHC II^+ $CD11b^+$ $CD11c^-$ macrophages, confirming the immunofluorescence staining of liver tissue. Representative plots from flow cytometry are shown in Figure 2.9A and 2.9B. Correlating to their abundance in the granulomas, $Gr\text{-}1^+$ $CD11b^+$ and MHC II^+ $CD11b^+$ $CD11c^-$ cells are likely major contributors to control of the early *F. tularensis* LVS infection. The $Gr\text{-}1^+$ $CD11b^+$ cells could function as immunosuppressive cells to inhibit the immune response and allow for bacterial survival, or they may serve as a means to wall off the infection until an adaptive response develops. It is tempting to speculate that $Gr\text{-}1^+$ $CD11b^+$ cells differentiate into functional antigen presenting cells largely as MHC II^+ $CD11b^+$ $CD11c^-$

macrophages and to a lesser extent as myeloid DCs ($CD11c^+$ $CD11b^+$) as seen in the hepatic lesions (Figure 2.8).

We have observed and confirmed a necrotic process (39, 42) that is clearly evident at 5 DPI within the liver abscesses (Figure 2.4). Apoptosis of hepatocytes is the hallmark of murine Listeriosis, which is caused by another intracellular organism with a predilection for liver involvement (156). In addition, a number of in vitro studies with murine macrophages have shown that *F. tularensis* infection is able to trigger the apoptotic cascade (100, 117-119). Based on these studies, the extent of apoptosis in the livers of the infected mice was examined. Although apoptotic cells were detected in the livers of mice infected with *F. tularensis* using both caspase-3 and TUNEL markers (Figure 2.10), these levels of apoptosis were qualitatively less than those that have been observed in a sublethal *Listeria* infection (156, 203). Both the necrotic and apoptotic pathways of cell death appear to be important in tularemia, as is also true in some other bacterial infections of the liver. For example, *Listeria* induces apoptosis of hepatocytes (156), but it is also known that murine macrophages succumb to *Listeria* infection in vitro by necrosis (13). Furthermore, apoptotic death of $CD8^+$ T cells has been attributed to a function of Gr-1^+ $CD11b^+$ cells (28). Infection of the liver by microorganisms results in the death of hepatocytes, and myeloid cells could be major contributors to this process.

F. tularensis causes liver damage as evidenced by elevated ALT and LDH serum levels and by the granulomatous-necrotic-apoptotic lesions that appear by 5 DPI. These lesions are mostly composed of $CD11b^+$ cells from two myeloid populations ($Gr\text{-}1^+$ $CD11b^+$ and MHC II^+ $CD11b^+$) that are associated with the bacteria, thus suggesting that these cells are important to control the infection. This is the first time that these cell populations have been associated with a liver infection. These appear to be recruited cells and are accumulated specifically to regulate the infection in its early stage, and therefore it may prove useful in development of vaccines against *F. tularensis* infections to stimulate the activation of these particular cell subsets.

In summary of Chapter II:

- There is a rapid accumulation of $CD11b^+$ cells in hepatic lesions of mice infected with *F. tularensis* LVS.
- $Gr\text{-}1^+$ $CD11b^+$ and MHC II^+ $CD11b^+$ cell subpopulations are the most abundant cell types in the hepatic lesions.
- Expression of markers for NK cells and DCs modestly increased throughout the liver.
- Cell markers for B and T lymphocytes did not increase in liver during acute infection.
- Hepatic cell death in tularemia can be attributed to both necrotic and apoptotic pathways.

D. Tables and Figures

Table 2.1. Total and differential peripheral blood leukocyte counts from mice inoculated with *F. tularensis* LVS.

Days post-inoculation	Mean total cell counts (10^6 cells/ml) ± SD (lymphocyte:neutrophil:monocyte ratio)[a]
0	4.0 ± 0.5 (89:6:5)
1	8.6 ± 2.8 (49:48:3)
2	5.3 ± 2.2 (55:41:4)
3	7.8 ± 4.3 (67:30:3)
4	6.3 ± 1.1 (82:9:9)
5	7.5 ± 2.0 (85:12:3)

[a] Three mice were used at each time point.

Table 2.2. Flow cytometry analysis of cell marker expression of total cell counts from livers of mice inoculated with *F. tularensis* LVS five days earlier compared to that from uninfected livers.

Cell Markers	% Total Cells Uninfected[a]	% Total Cells Five DPI[a]
$CD3^+$	7.6 ± 2.9	6.1 ± 1.4
$B220^+$	3.4 ± 1.3	3.1 ± 1.7
$CD11c^+$	1.1 ± 0.6	2.8 ± 1.8
$CD11c^+$ $CD11b^+$	0.3 ± 0.3	2.1 ± 1.6
$DX5^+$ $NK1.1^+$	2.3 ± 0.6	4.8 ± 0.9[b]
$CD11b^+$	2.3 ± 0.3	21.3 ± 3.1[c]
$F4/80^+$ $CD11b^+$	1.8 ± 1.3	2.8 ± 0.8
MHC II^+ $CD11b^+$ CD11c-	1.2 ± 0.2	10.4 ± 5.2[d]
$Gr\text{-}1^+$ $CD11b^+$	1.5 ± 0.3	13.1 ± 5.3[e]

[a] Results are the means ± standard deviation of three mice.
[b] $P = 0.015$. [c] $P = 0.0005$. [d] $P = 0.039$. [e] $P = 0.020$.

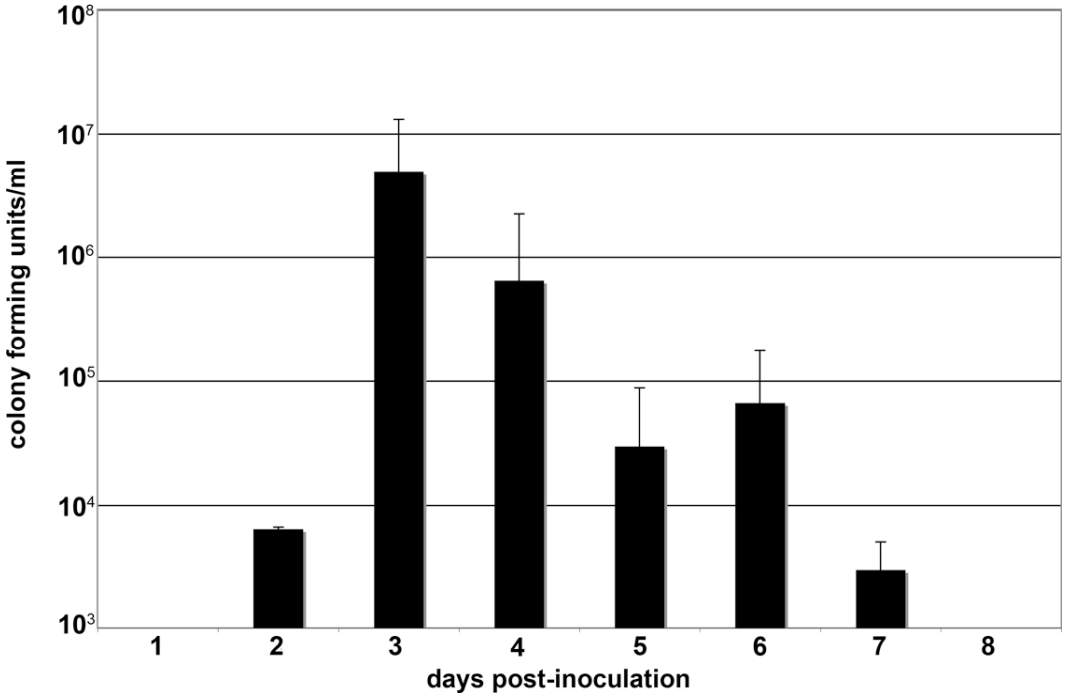

Figure 2.1. Bacteremia in mice infected with *F. tularensis* LVS. Peak of infection in the blood was between 3-6 DPI. Bacteria were enumerated by plating serial dilutions of lysed whole blood on Chocolate II agar, incubated at 37°C and 5% CO_2. Blood was collected by cardiac puncture. Bars represent the means ± SD of three mice per day after inoculation.

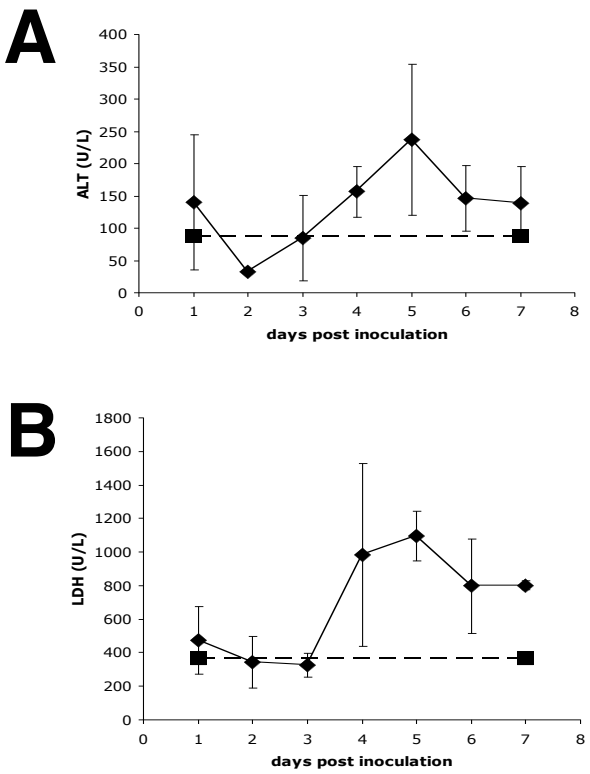

Figure 2.2. Mean levels ± standard deviations of (A) alanine transferase (ALT) and (B) lactate dehydrogenase (LDH) serum levels of mice infected with sublethal doses of LVS. The dashed line represents the upper limit of the normal range for each enzyme. Each diamond represents the mean values ± SD of three mice.

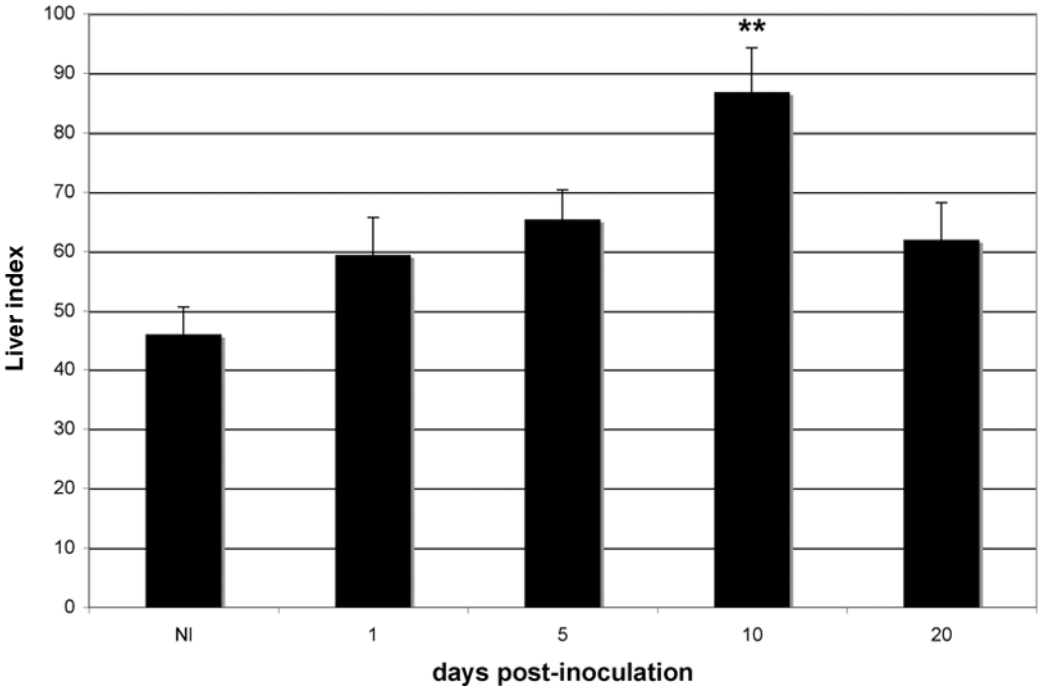

Figure 2.3. Livers of mice infected with *F. tularensis* increase in weight. Mean liver index ± SD of three mice per time point in the infection. Liver index was calculated by using the formula: (liver weight in mg/total body weight in mg) x 1000. Marked increase is due to both an increase in liver weight and a mouse weight loss during infection. ** $P<0.01$ significantly different from normal (NI) control.

Figure 2.4. Hematoxylin and eosin stained sections of livers of mice infected with sublethal doses of LVS. (A) Normal liver. (B) Low power view of hepatic parenchyma showing multiple lesions (arrows) of inflammatory cell infiltrates in the liver of a mouse inoculated with LVS five days earlier. (C) Mononuclear cell inflammatory cell infiltrate of a perivascular focus of inflammation in the liver of a mouse infected with LVS five days earlier. Some neutrophils are evident as indicated by arrows. (D) A five day old lesion within the hepatic parenchyma showing necrotic hepatocytes, pyknotic nuclei and residual mononuclear cell infiltrate. Bars = 150 μm (A-B) and 75 μm (C-D).

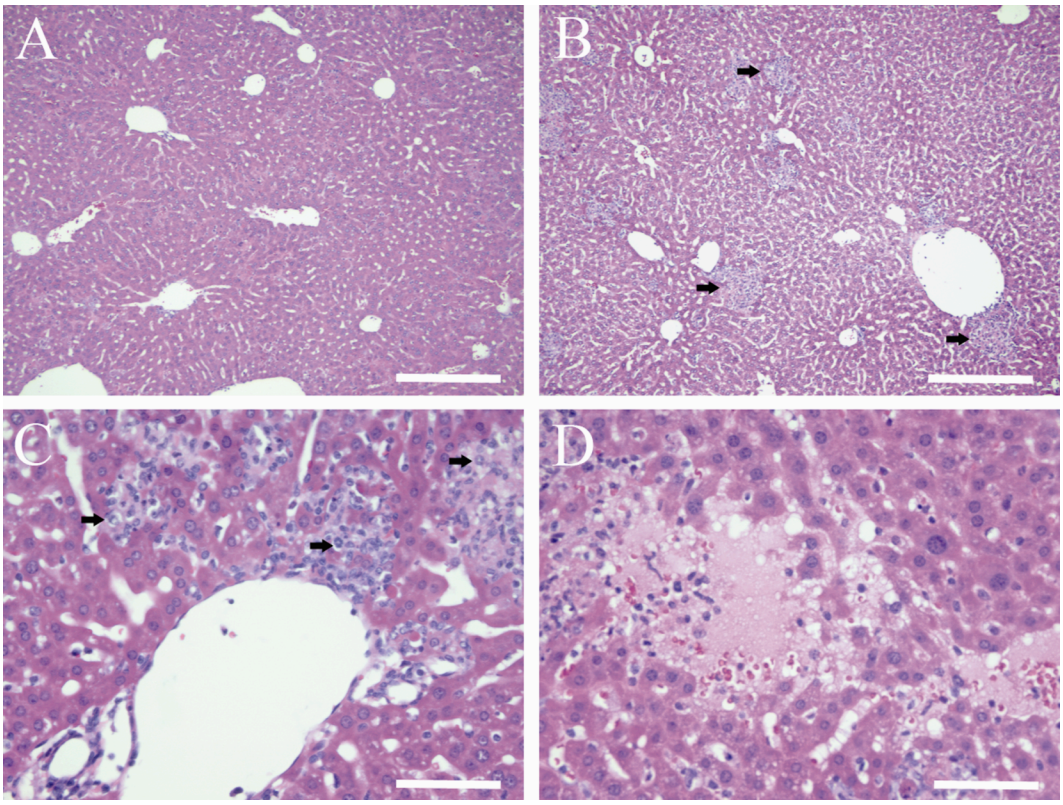
A
B
C
D

Figure 2.5. Detection of bacteria in livers of mice inoculated with sublethal doses of LVS five days earlier. Bacteria (red) were detected with rabbit anti-*F. tularensis* LVS followed by alkaline phosphatase-conjugated anti-rabbit serum. Vulcan Fast Red was used to detect alkaline phosphatase. (A) Normal liver. (B) Low power view of hepatic parenchyma showing multiple sites of bacterial infection. (C) Hepatocytes infected with *F. tularensis*. Some of the hepatocytes are heavily infected and swollen with bacteria. (D) Bacteria concentrated within the granuloma. Bars = 150 μm (A-B) and 50 μm (C-D).

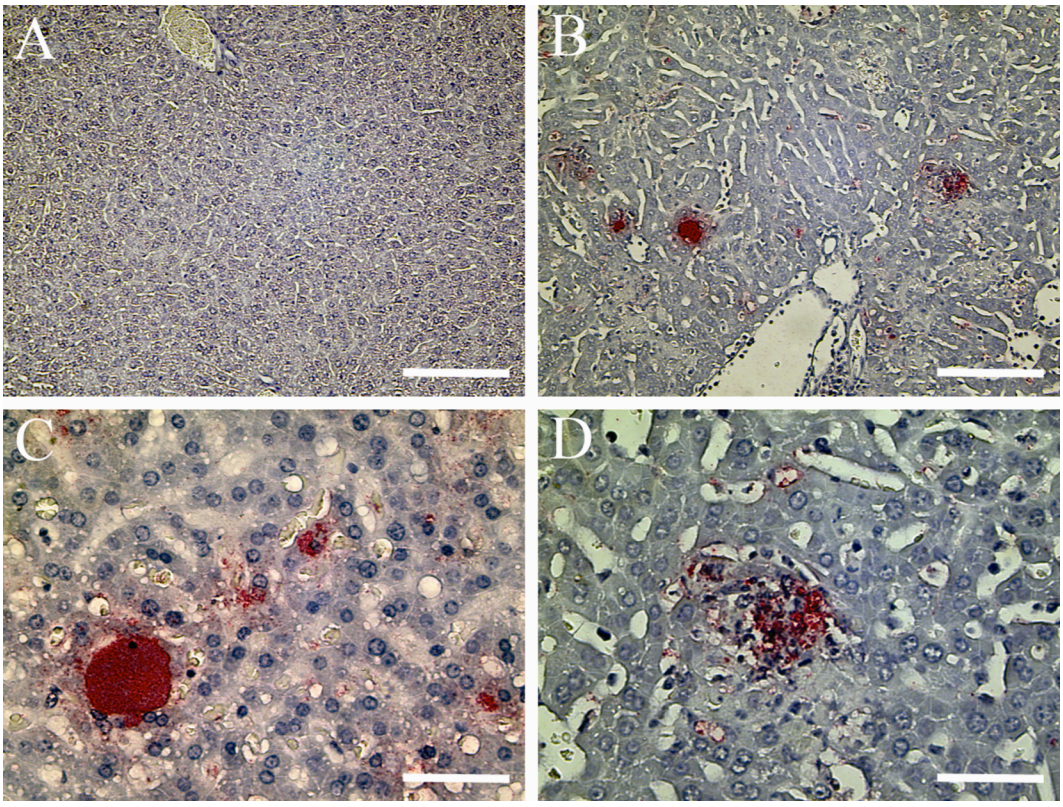
A
B
C
D

Figure 2.6. Immunofluorescent detection of *F. tularensis* and inflammatory cells in the livers of mice inoculated with sublethal doses one day earlier and viewed by confocal microscopy. (A) Merged image, low power view of $CD11b^+$ cells (Alexa Fluor 647, blue), *F. tularensis* (secondary anti-rabbit Ig, Alexa Fluor 555, red) and F4/80 (Alexa Fluor 488, green). (B) Hepatocytes infected with *F. tularensis* (red). (C) Merged image of $CD11b^+$ cell (neutrophil-like, blue) infected with *F. tularensis* (red). Bar lengths indicated in figure.

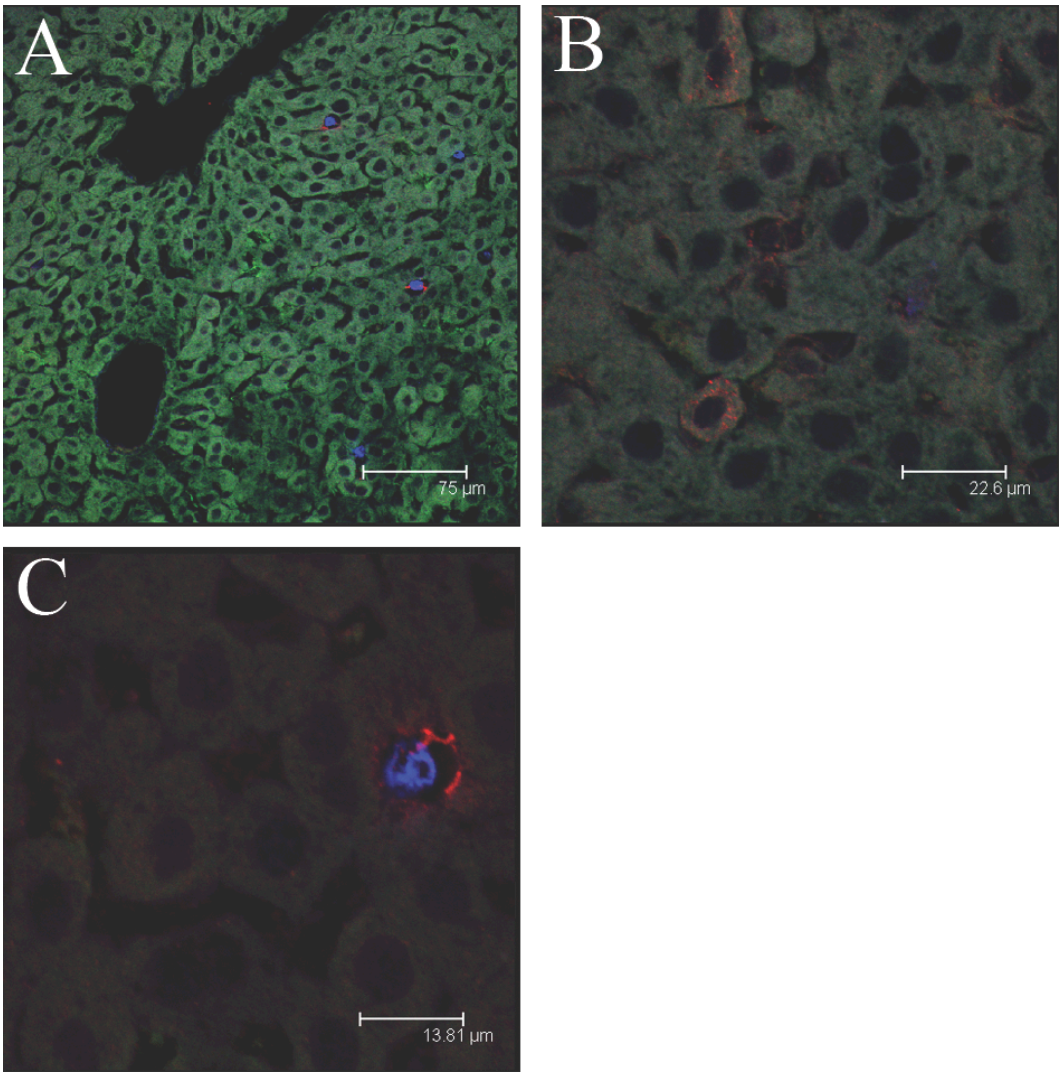
A
75 µm
B
22.6 µm
C
13.81 µm

Figure 2.7. Immunofluorescent detection of *F. tularensis* and inflammatory cells in the livers of mice inoculated with sublethal doses five days earlier viewed by confocal microscopy. (A) F4/80$^+$ cells (Alexa Fluor 488, green). (B) *F. tularensis* (secondary anti-rabbit Ig, Alexa Fluor 555, red) in foci of inflammatory cells. (C) CD11b$^+$ cells (Alexa Fluor 647, blue). (D) Merged image of panels A to C. Note colocalization of CD11b$^+$ cells (blue) and *F. tularensis* (red). Also note the peripheral location of the F4/80$^+$ cells around the foci of infection. Some cells are both F4/80$^+$ and CD11b$^+$ and can be seen in merged images of Panels E and F. Bar lengths indicated in figure.

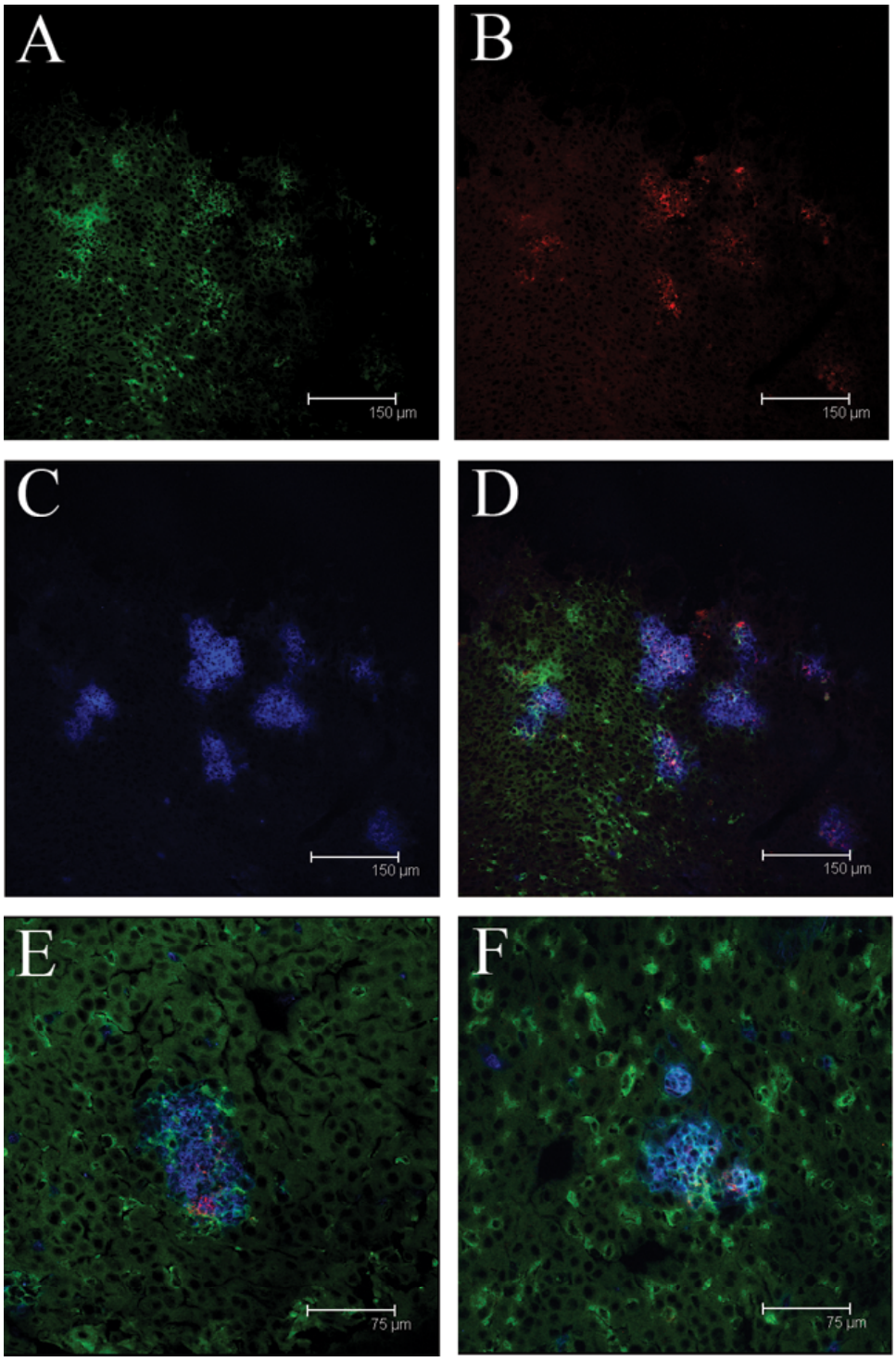
A
150 µm
B
150 µm
C
150 µm
D
150 µm
E
75 µm
F
75 µm

Figure 2.8. Immunofluorescent detection of *F. tularensis* and inflammatory cells in the livers of mice inoculated with sublethal doses five days earlier viewed by confocal microscopy. (A) Merged image of $CD11b^+$ cells (blue), $Gr\text{-}1^+$ cells (red) and *F. tularensis* (green). $Gr\text{-}1^+$ cells colocalize with $CD11b^+$ cells, pink color, and make up the granuloma. (B) Merged image of $CD11b^+$ cells (blue), MHC II^+ cells (red) and *F. tularensis* (green). The granuloma also consists of a cell population MHC II^+ $CD11b^+$ that also associates with the bacteria. (C) Merged image of $CD11b^+$ cells (blue), $CD11c^+$ cells (red) and *F. tularensis* (green). DCs ($CD11c^+$ $CD11b^+$) were found in association with the granuloma. (D) Merged image of $NK1.1^+$ cells (blue), *F. tularensis* (red) and $DX5^+$ (green). NK cells were seen in the tissue but not in association with the bacteria or the hepatic lesions. Bar lengths indicated in figure.

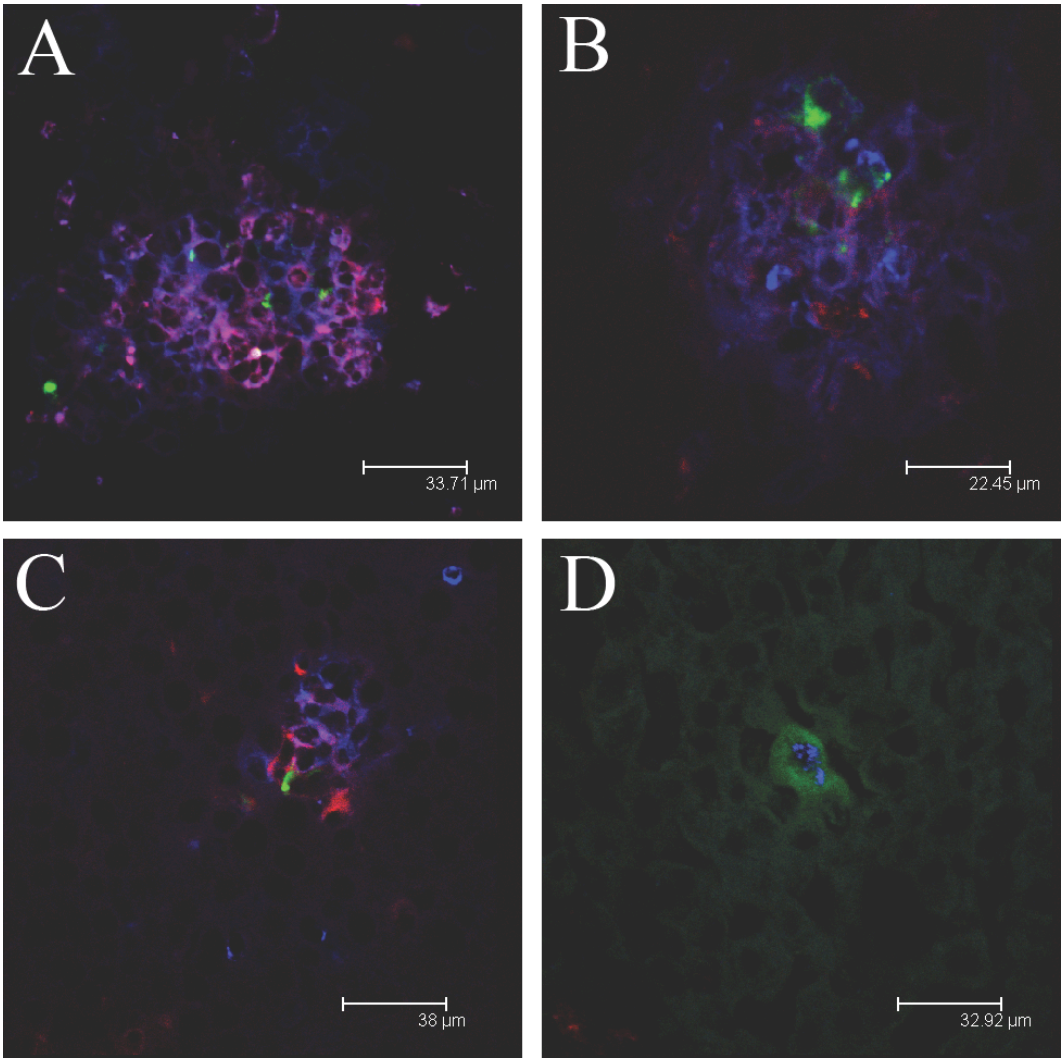
A
33.71 µm
B
22.45 µm
C
38 µm
D
32.92 µm

Figure 2.9. Flow cytometry analysis of predominant cell populations in the liver of *F. tularensis* LVS-infected mice. Accumulation of Gr-1$^+$ CD11b$^+$ immature myeloid cells (A) and MHC II$^+$ CD11b$^+$ cells (B) in a mouse 5 DPI compared to uninfected control. A representative experiment is shown for both (A) and (B).

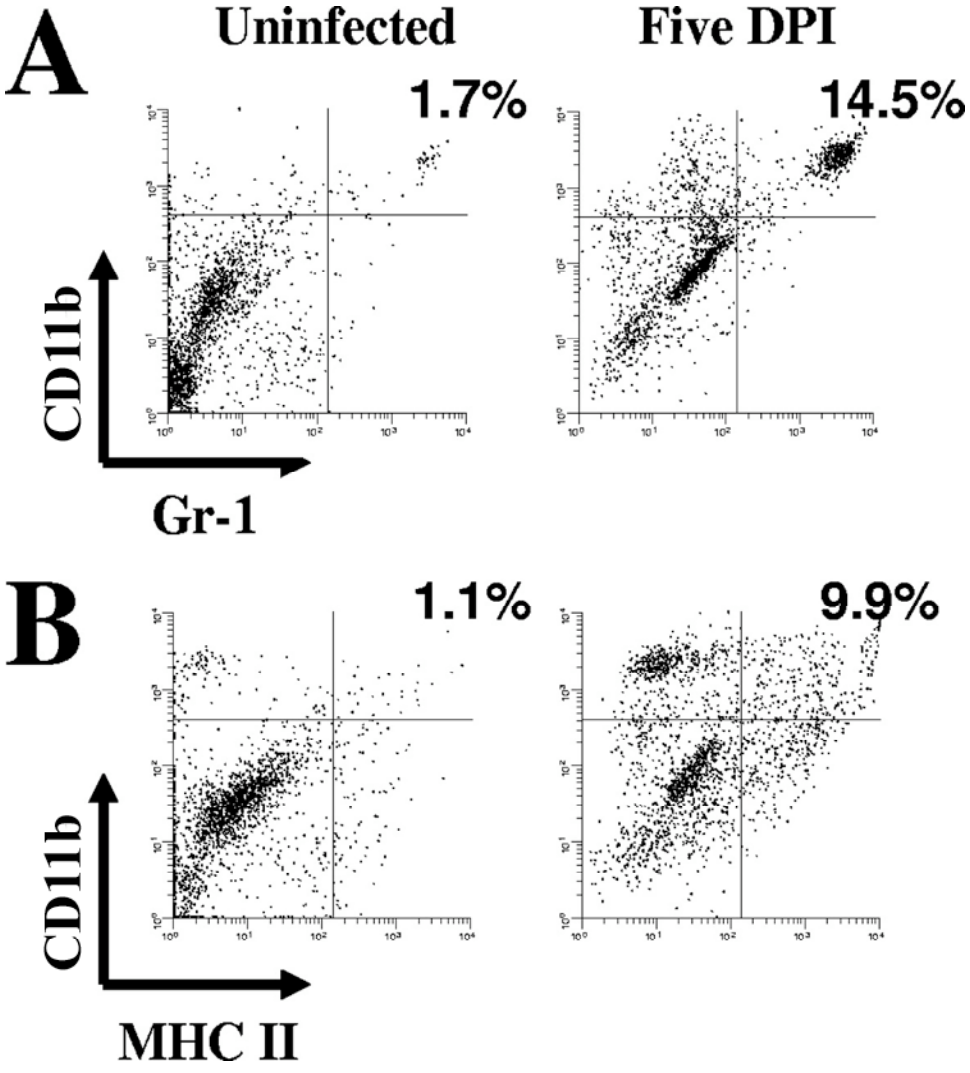
A
Uninfected
Five DPI
1.7%
14.5%
CD11b
Gr-1
B
1.1%
9.9%
CD11b
MHC II

Figure 2.10. Detection of apoptotic cell markers by immunohistochemistry in the livers of mice inoculated with sublethal doses of *F. tularensis* five days earlier. (A) Low power view of anti-cleaved caspase-3 reactivity (brown) within the foci of inflammation and infection. (B and C) High power view of anti-cleaved caspase-3 reactivity (brown) within the foci of inflammation and infection. (D) Low power view of phase contrast of liver parenchyma containing foci of inflammation and infection. (E) TUNEL-positive cells (red), same field as panel D. (F) Merged photograph of panels D and E showing cells with fragmented DNA. Bars = 150 μm (A) and 75 μm (B-G).

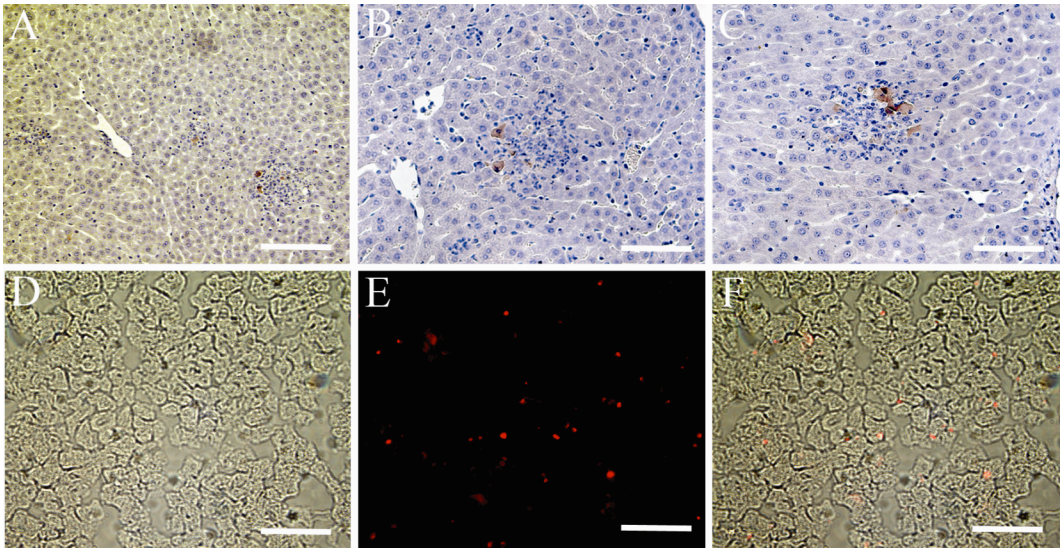
A
B
C
D
E
F

Chapter III

Murine Splenic Response to *Francisella tularensis*

A. Introduction

Francisella tularensis is a facultative intracellular organism that infects hepatocytes and macrophages (6, 9, 18, 44, 52, 79-81, 116, 122). The clinical severity of tularemia, its protean manifestations, and the high death to case ratio (particularly in Type A infections) are the main reasons for the inclusion of *F. tularensis* in the Category A group of agents of bioterrorism. The basis for the virulence and clinical severity of infection with *F. tularensis* is not completely understood. The immune response to this bacterium is being scrutinized closely but there have been no breakthroughs in the understanding of the mechanisms that depress or inhibit the adaptive response (68). Immune suppression during the early infectious process with *F. tularensis* could delay the development of the adaptive response, and this delay could contribute to the high morbidity and mortality of tularemia.

The composition of the cellular immune response in the livers of infected mice has provided a potential clue to immune suppression. The histopathology of hepatic tularemia is characterized by the formation of granulomas (42, 44, 48), and the role of interferon (IFN)-γ in their development has been demonstrated (17, 99, 191). We characterized the cellular composition of infected livers using specific markers. The hepatic

granulomas are composed of several types of cells that express the myeloid cell marker CD11b (also known as Mac-1) (154). The largest subpopulation of cell infiltrating the infected livers expressed Gr-1 and CD11b.

Recent studies have linked the accumulation of the Gr-1$^+$ CD11b$^+$ phenotype with functional immunosuppression in diverse pathological conditions, including bacterial and parasitic infections, acute and chronic inflammation, and cancer, and this recent interest underscores their importance. Much attention has been focused on the role of Gr-1$^+$ CD11b$^+$ myeloid cells in cancer. This cell phenotype is now defined as a heterogeneous cell population termed myeloid-derived suppressor cells (MDSCs) (83). MDSCs accumulate in large numbers in tumors in practically all tested experimental models, as well as in patients with different types of cancer, and cause a global and profound immune suppression (4, 26, 27, 29, 31, 86, 111-114, 162, 164).

In the context of the tularemia infection, studies on the associations of these cells with bacteria are of direct relevance. Although there are some differences among the results and the experiments that have been done in the context of infection, the results are remarkably similar in their demonstration of immunosuppression associated with the Gr-1$^+$ CD11b$^+$ phenotype.

The earliest observations of precursor myeloid cells being involved in immunosuppression were made in a *Salmonella* infection model in 1991. In this study, the appearance of macrophage precursors was shown to play an important regulatory role in the immune response to these bacteria (2). Burns infected with *Pseudomonas aeruginosa* have large populations of Gr-1$^+$ CD11b$^+$ cells. Ex vivo experiments showed that cell-to-cell contact is not required when burn-derived MDSCs inhibit the production of antimicrobial peptides by keratinocytes when both types of cells are cocultured. This study also demonstrated that secreted effector molecules from the MDSC population suppress antimicrobial peptide production through secretion of IL-10 and the chemokine CCL2 (109). A recent study showed that Gr-1$^+$ CD11b$^+$ cells cause a profound immunosuppression in experimental sepsis after passive transfer. Interferon-γ production is reduced in mice that receive the transfer of Gr-1$^+$ cells (55). Gr-1$^+$ CD11b$^+$ cells have also been implicated in immune suppression in fungal and parasitic infections (95, 143). Infection with *Toxoplasma gondii* results in the infiltration of Gr-1$^+$ CD11b$^+$ myeloid cells that have potent nitric oxide-dependent immunoregulatory properties and induce IL-2-reversible anergy of both pulmonary CD8$^+$ and CD4$^+$ lymphocytes (187).

However, recent studies have begun to appreciate that the heterogeneous MDSCs can be further subdivided into functionally and

morphologically distinct subpopulations. Murine monocytes are composed of two distinct subpopulations characterized by expression or lack of Gr-1 (87, 88). Gr-1 is expressed on neutrophils, inflammatory monocytes, and some populations of dendritic cells (177). Monoclonal antibody to Gr-1 (clone RB6-8C5) also binds two loci of lymphocyte antigen complex 6, known as Ly6C and Ly6G (76). Recently, monoclonal antibodies to Ly6C and Ly6G have been used to separate Gr-1 subpopulations into neutrophil-like ($CD11b^+$ $Ly6C^{int}$ $Ly6G^{hi}$) and inflammatory monocytic ($CD11b^+$ $Ly6C^{hi}$ $Ly6G^-$) cells (54, 200). In fact, $Gr\text{-}1^+$ $CD11b^+$ cells form two separate myeloid lineages with apparent opposing functions as a result of infection with Mycobacteria (58). Also, in *T. gondii* infection, the monocytic component of the MDSCs is required for an effective host response against this parasite (61). These results indicate that the heterogeneous MDSCs have more functions in host defense than was previously believed.

Both monocytes and neutrophils are important in innate immunity in *F. tularensis* infection. *F. tularensis* replicates within macrophages and are thus shielded from the humoral immune response (79). Mice that are depleted of neutrophils using antibodies to Gr-1 succumb to otherwise sublethal doses of *F. tularensis* LVS (168). However, this method of depletion affects other cell types as well.

Due to their immunosuppressive nature and their accumulation in large numbers in the liver, spleen and bone marrow of mice infected with *F. tularensis*, we have considered that MDSCs could play a significant role in the severity of the infection leading to greater morbidity and mortality or in the protective immune response. To determine this, we have demonstrated that these cells can be elicited from several organs of mice infected with sublethal doses of *F. tularensis*. These cells were then purified by cell sorting, followed in ex vivo culture for cellular differentiation and prepared for adoptive transfer to determine if there is enhancement of tularemia severity.

B. Materials and Methods

Bacteria. *F. tularensis* LVS (American Type Culture Collection 29684, Manassas, VA) was cultured as previously described (Chapter II).

Mice. Female C3H/HeN, C57BL/6 and BALB/c mice were purchased from Charles River Laboratories (Wilmington, MA) and used from 6 to 10 weeks of age. All mice were housed in microisolator cages with free access to food and water. Mice received ID injections of 10^5 – 10^6 CFU of *F. tularensis* LVS. At various time points post-inoculation, mice were euthanized, and their blood and organs were used for determination of bacterial burdens. Mice were weighed immediately after euthanization to calculate a ratio of spleen to body weight. At least 3-6

mice were used for each time point and for each experiment. All animal procedures were approved by the institutional review board.

Flow cytometry. Excised spleens were gently teased apart to a single cell suspension and collected in Dulbecco's Modified Eagle Medium (DMEM) medium (Invitrogen, Carlsbad, CA). Bone marrow cells were collected from mice by removing the femurs and tibiae of both legs and cutting the epiphysis to expose the marrow. The cavities of the bones were flushed with DMEM medium to collect the bone marrow cells. Both spleen and bone marrow cells were treated with cell lysis buffer (144 mM NH_4Cl and 17 mM tris(hydroxymethyl)aminomethane pH 7.4 in water) before resuspension and stained as previously described (Chapter II).

Antibodies for flow cytometry. The following antibodies were used for flow cytometry and confocal microscopy: fluorescein isothiocyanate (FITC) anti-mouse CD11c (clone HL3), FITC anti-mouse CD49b/Pan NK cells (clone DX5), FITC anti-mouse CD21 (clone 7G6), R-phycoerythrin (PE) anti-mouse CD3 (clone 17A2), PE anti-mouse I-A/I-E (MHC class II) (clone M5/114.15.2), PE anti-mouse Ly-6G and Ly-6C (Gr-1) (clone RB6-8C5), PE anti-mouse CD138 (Syndecan-1) (clone 281-1), peridinin chlorophyll-a protein (PerCP) anti-mouse CD4 (clone RM4-5), PerCP-Cy5.5 anti-mouse CD11b (Mac-1) (clone M1/70), PerCP-Cy5.5 anti-mouse IgM (clone R6-60.2), allophycocyanin (APC) anti-mouse Ly-6G and Ly-6C (Gr-1) (clone RB6-8C5), APC anti-mouse NK1.1 (clone

PK136), APC anti-mouse CD8 (clone 53-6.7) from BD Pharmingen; APC anti-mouse CD23 (clone 2G8) from Southern Biotech (Birmingham, AL); Alexa Fluor 647 anti-mouse CD11b (Mac-1) (clone M1/70) from Biolegend (San Diego, CA); and Alexa Fluor 488 anti-mouse F4/80 (clone CI:A3-1) from Serotec (Raleigh, NC). Isotype-matched antibodies (all from BD Pharmingen) were used as a control for non-specific binding.

Microscopy. Spleens were aseptically removed and immediately fixed in 10% neutral buffered formalin, dehydrated in ethanol, embedded in Blue Ribbon paraffin (Surgipath, Richmond, IL), sectioned at 5 µm, stained with hematoxylin and eosin, and mounted with Acrymount (Statlab Medical Products, Lewisville, TX). For detection of bacteria and cellular markers in the spleen, paraffin sections and frozen tissue sections were stained with antibodies listed above for flow cytometry and treated as previously described (Chapter II). *F. tularensis* was detected with polyclonal rabbit antisera followed by alkaline phosphatase-conjugated anti-rabbit IgG and Vulcan Fast Red Chromogen (Biocarta, San Diego, CA) for paraffin sections. For immunofluorescence assays, secondary FITC anti-rabbit IgG from Chemicon Int. (Temecula, CA) or Alexa Fluor 488 anti-rabbit IgG (Invitrogen) was used to detect *F. tularensis*.

Slides were examined by phase-contrast and epi-fluorescence microscopy using a Nikon Eclipse E600 microscope, and images were captured using a Spot camera (Diagnostic Instruments, Inc., Sterling

Heights, MI). Slides for confocal microscopy were analyzed using a Leica DM IRE2 confocal microscope. Images of the red, green and blue emission signals were captured separately with Leica's LCS software package. Images were then processed with Adobe Photoshop.

MDSC purification. Live cell sorting was performed from both uninfected and infected spleens to collect cells expressing Gr-1$^+$ CD11b$^+$. First, CD11b$^+$ cells were collected in magnetic cell sorting buffer [2 mM ethylenediaminetetraacetic acid (EDTA), 0.5% bovine serum albumin in PBS at pH 7.2] from a suspension of spleen cells by using magnetic beads specific for CD11b according to the protocol of the manufacturer (Miltenyi Biotec, Auburn, CA). Magnetically purified CD11b$^+$ cells were then were stained with APC anti-mouse Ly-6G and Ly-6C (anti-Gr-1) (clone RB6-8C5) and sorted by the FACSAria cell sorting system (BD). Purity of sorted cells was checked by flow cytometry with consistent purity of >98%. Staining of cells with the Annexin V and propidium iodide apoptosis detection kit (BD Pharmingen) was used to quantify cell viability. Single cell suspensions of sorted cells were either fixed in methanol for Giemsa stain or stained with 4´,6-diamidino-2-phenylindole (DAPI) (Invitrogen) and mounted with Vectashield (VectorLabs, Burlingame, CA) for microscopy.

Ex vivo culture and *F. tularensis* infection of MDSCs. Purified cells were cultured ex vivo in RPMI 1640 medium (Invitrogen) supplemented with 10% fetal bovine serum, 2 mM L-glutamine, 200 U/ml

penicillin, and 50 μg/ml streptomycin at 37°C and 5% CO_2 on 24 well cell culture plates (BD) at a density of $3x10^5$ cells/well. For all ex vivo experiments, aliquots of the sorted cells as well as medium were plated and cultured on Chocolate II agar (BD Biosciences, San Jose, CA) for detection of contaminating residual bacteria. Cells were stimulated with 10 ng/ml recombinant mouse granulocyte macrophage colony-stimulating factor (GM-CSF) (R&D Systems, Minneapolis, MN) for 7 days after sorting, detached with porcine pancreatic trypsin 1-300 (MP Biomedicals, Solon, OH) and EDTA and analyzed for cellular differentiation by flow cytometry. For infection studies, MDSCs were grown for 24 hours, washed and placed in medium without antibiotics before addition of *F. tularensis*. A multiplicity of infection (MOI) of 10, 15, or 30 bacteria per MDSC was added to each well. Plates were centrifuged for 4 min at 400 x g and placed in an incubator at 37°C and 5% CO_2. After 2 hours of incubation with bacteria, cells were washed and cultured with 10 μg/ml gentamicin in RPMI medium for 1 hour to kill extracellular bacteria. In order to lyse the cells, 10 mg/ml of saponin (Sigma, St. Louis, MO) in PBS was added after two additional washes. Serial dilutions of lysates were then plated and cultured on Chocolate II agar (BD Biosciences, San Jose, CA) at 37°C and 5% CO_2 to determine bacterial CFUs. Other cells were incubated for an additional 15 hours after the 2 hour infection plus 1 hour of gentamicin treatment before determination of CFUs. Some of the cells were also

used for immunofluorescence assays. Briefly, cells were grown on coverslips, infected with bacteria for 2 or 18 hours and fixed with 2.5% p-formaldehyde, followed by permeabilization with 0.5% Triton X-100. Cover slips were placed in 3% BSA blocking solution for 1 hour before addition of rabbit anti-*F. tularensis* IgG. After 1 hour, cells were washed, and secondary FITC-conjugated anti-rabbit IgG was added for an additional hour. Samples were then counterstained with DAPI to visualize the nuclei. Controls consisted of normal rabbit serum and secondary conjugate alone.

Adoptive Transfer of MDSCs. After purification of MDSCs from spleens of mice that had been infected 10 days earlier, the cells were washed and resuspended in pre-warmed PBS with 0.1% BSA at a concentration of $1x10^7$/ml. MDSCs were then incubated with carboxylfluorescein diacetate succinimidyl ester (CFSE) (Molecular Probes, Carlsbad, CA) diluted in dimethyl sulfoxide to a final concentration of 5 μM for 10 min at 37°C (130, 131). Staining was quenched by adding a 5-fold volume of cold RPMI medium and placing on ice for 5 min. Cell viability was determined using Annexin V and propidium iodide, and the inoculums were adjusted to compensate for the presence of dead cells. Cells were washed and resuspended in RPMI, and $2x10^6$ cells were transferred into the tail vein of naïve mice. Twenty-four hours after transfer, bone marrows and spleens were collected from uninfected

mice and processed for flow cytometry analysis to detect CFSE-labeled cells in the various tissues.

For the actual passive transfer experiment, naïve C3H/HeN mice received $4x10^6$ purified MDSCs or RPMI medium only intravenously, and 16 hours after transfer, mice were inoculated intradermally with sublethal doses of *F. tularensis*. The mice were monitored for 10 days and then euthanized to collect blood, spleen and liver for CFU determinations and for histology.

Statistics. *P*-values were calculated comparing uninfected normal (NL) data to infected data by an unpaired analysis of variance using the Dunnett multiple comparison test to determine significance with InStat software (GraphPad, San Diego, CA).

C. Results

MDSCs make up the prominent expanding cellular phenotype of the spleen in mice infected with *F. tularensis*. The spleen enlarged during acute tularemia as a result of increased cellularity and underwent marked changes in the architecture by lymphoid follicle disintegration and involution with associated expansion of the red pulp (Figure 3.1). Large numbers of bacteria were detected throughout the spleen by 5 DPI, with a preference for the red pulp (Figure 3.2). Spleen weight to mouse weight increased almost five-fold in the first ten days of the experimental infection after ID inoculation of sublethal doses of *F. tularensis* (Figure 3.3). The

composition of the spleen cells for the first 20 days of the infection showed that the largest increase consisted of three subpopulations of $CD11b^+$ cells (Table 3.1). Of these, the $Gr1^+$ $CD11b^+$ cell phenotype accounted for the largest of the subpopulations. Use of triple markers showed two large subpopulations of cells $Gr\text{-}1^+$ $CD11b^+$ MHC II^- and $Gr1^+$ $CD11b^+$ $F4/80^-$ that were characterized as F4/80– and MHC class II– negative and positive for Gr-1 and CD11b. In the absence of expression of the F4/80 and MHC class II monocyte/macrophage markers, these were concluded to be MDSCs, whereas the other subpopulations of $CD11b^+$ cells marked with F4/80 and MHC class II were classified as monocytes/macrophages. Therefore, the MDSC population had the greatest increase of all cellular phenotypes in spleens of infected mice. Their accumulation in the spleen was apparent from the first day after inoculation and progressed rapidly to a peak in numbers by day 10 post-inoculation. After 20 days, the levels of these cells remained elevated relative to an uninfected spleen but were markedly reduced from the levels documented at 10 days after inoculation. The subpopulation of monocyte/macrophages ($F4/80^+$ MHC II^+ $Gr\text{-}1^+$ $CD11b^+$) also increased in the infected spleens by 5-10 DPI but were not major contributors to the overall increase in cellularity (Table 3.1).

Other cell types increased in numbers as well and contributed to the hyper-cellularity of the spleen 10 days after inoculation. CD4 and CD8 T lymphocytes were significantly increased at 10 DPI but maintained the

ratio seen in normal spleens. Significant B cell increases from compared controls at 10 DPI were only seen in plasma cell expression (IgM^+ $CD138^+$) indicating an active antibody response to the infection. Prior to the increases at 10 DPI, numbers of cells expressing markers for MZ and FO B cells were diminished possibly indicating their differentiation into plasma cells. Significant increases in DCs ($CD11c^+$ $CD11b^+$) were also seen by 10 DPI when compared to control levels. NK cells ($DX5^+$ $NK1.1^+$) were detected in the spleen but did not have significant increases (Table 3.1).

The increases in the MDSC population in the spleen over time in C3H/HeN mice are documented in Figure 3.4A. Although the MDSC population of the spleens of C57BL/6 (Figure 3.4B) and BALB/c (Figure 3.4C) grew similarly, the numbers of these cells were reduced compared to the C3H/HeN mice. Increases of Gr-1^+ $CD11b^+$ cells were seen not only in absolute numbers of splenocytes but also by percentages of total splenocytes from C3H/HeN mice. Nearly a quarter of all cells by 10 days post-inoculation expressed Gr-1 and CD11b cell markers (Figure 3.5). For these reasons, we continued our subsequent investigations using C3H/HeN mice. Nonetheless, there are noted differences in the response of different mouse strains to infection with *F. tularensis* (82), and the role of the MDSCs in this differential response may be of importance.

Several markers were used to document the location of *F. tularensis* relative to the MDSCs in the spleen. Because the histological architecture of the spleen changed dramatically in this infection, the MDSCs appeared to be distributed throughout the organ and not specifically associated with either the well-differentiated red or white pulp. The bacteria colocalized with the Gr-1$^+$ CD11b$^+$ cell population of the spleen (Figure 3.6), and the high numbers of both bacteria and cells of this phenotype were evident in spleens of mice infected five days earlier. Bacterial burdens in the spleen decreased thereafter (data not shown). This is a similar observation to that made for the liver granulomas containing large numbers of MDSCs with superimposed *F. tularensis* from Chapter II (Figure 2.8). From the immunohistological sections of frozen spleens, it is not possible to determine whether all the bacteria are internalized within the MDSC, although clearly there are some triply stained cells (Figure 3.6D, arrows) that would suggest intracellular bacteria.

MDSCs increase in the bone marrow of mice infected with *F. tularensis*. Significant increases in the percentages of MDSCs in the bone marrow also occur (Figure 3.7), paralleling the increases in the spleen (Table 3.1, Figure 3.4A), and the liver granulomas (Table 2.2, Figure 2.9). The presence of large numbers of MDSCs in the organs

affected by *F. tularensis* as well as in the bone marrow is indicative of their important role in modulating this infection.

MDSCs are composed of a heterogeneous cell population that can be purified using Gr-1 and CD11b cell surface markers. Using forward and side light scatter and Gr-1 and CD11b cell surface markers, a morphologically heterogeneous population of cells was purified. Giemsa staining of the sorted cells showed a neutrophil-like cell type with a ring nucleus with scant granulation, and a mononuclear cell type, in approximately equal numbers (Figure 3.8). In myelopoiesis of there is an immature neutrophil ring-shaped nucleus that is highly granular, but MDSCs ring-shaped cells only have little granulation indicating these cells are not exactly like neutrophil precursors. The heterogeneous nature of the MDSCs has been documented before in infection (55, 58, 144) and in cancer (4, 27, 200). Forward and side light scatter showed that the sorting process yielded mostly live cells (Figure 3.9A) with 8-10% dead cells (Figure 3.9B). High levels of purity of cells sorted with Gr-1 and CD11b surface markers were consistently reached (Figure 3.9C-E).

MDSCs from both infected and uninfected mouse spleens differentiate into macrophage-like and dendritic cell phenotypes in ex vivo culture. An aliquot of the MDSCs sorted using Gr-1 and CD11b cell markers from uninfected and infected mice (day 10 post-inoculation) were re-analyzed immediately with Gr-1, CD11b, F4/80 and CD11c

markers (D0, Figure 3.10) for baseline comparisons. As expected, these assays reflected the purity levels obtained after sorting the MDSCs using Gr-1 and CD11b markers (Figures 3.9C-E). The numbers of MDSCs expressing F4/80 and CD11c were less than 1% (D0, Figure 3.10). The percentage of cells that expressed these markers was the same in infected and uninfected spleens; however, larger numbers of cells were harvested from the infected organs.

Aliquots of the MDSCs sorted using Gr-1 and CD11b markers from uninfected and infected mice were cultured in RPMI 1640 medium supplemented with 10 ng/ml of GM-CSF for seven days to characterize ex vivo differentiation. To this end, MDSCs incubated for seven days with GM-CSF from both infected (Figure 3.10) and uninfected mice (Figure 3.11) were subjected to FACS analysis for expression of markers associated with monocyte/macrophages ($F4/80^+$ $CD11b^+$) and DCs ($CD11c^+$), as well as for Gr-1. MDSCs from infected organs differentiated into $F4/80^+$ $CD11b^+$ cells and into DCs ($CD11c^+$) and almost totally lost Gr-1 expression after seven days of stimulation with GM-CSF (Figure 3.10). This same differentiation pattern was also seen in MDSCs from uninfected mice was also seen, where monocyte/macrophage and dendritic cell markers were acquired with a concomitant loss of Gr-1 (Figure 3.11). Expression of CD11b was maintained at high levels (95 – 99%) for the seven days of ex-vivo culture with GM-CSF (data not shown).

Thus, splenic Gr-1$^+$ CD11b$^+$ cells from both infected and uninfected mice differentiated into monocyte/macrophages and DCs in the presence of the appropriate growth factor. GM-CSF is essential for ex vivo growth of sorted MDSCs (55). There is a possibility that GM-CSF induced the differentiation of the heterogeneous MDSCs but maintained the survival only of monocyte/macrophages and DCs, resulting in the enrichment of these cells.

MDSCs in ex vivo culture can ingest but do not support growth of intracellular *F. tularensis*. Splenic MDSCs from infected mice were incubated for 24 hours in medium containing GM-CSF. At that time, *F. tularensis* at MOI of 10, 15, and 30 was added to the MDSC cultures for 2 or 18 hours in RPMI 1640 medium supplemented with 10 ng/ml of GM-CSF. One hour prior to harvesting of the cells, 10 μg/ml of gentamicin was added to the cultures. At the end of each time point, the cells were washed extensively, counted and lysed. Cells harboring *F. tularensis* were also enumerated by fluorescence microscopy (Figure 3.12A and 3.12B).

MDSCs ingested *F. tularensis* (Figure 3.12). After the 2 hour period of incubation with *F. tularensis*, about one quarter of the cells had ingested bacteria at MOI of 10 and 15 and about half at a MOI of 30. We were able to grow *F. tularensis* from the cell lysates. The addition of gentamicin to the medium enhanced the likelihood that bacterial cultures were derived

from intracellular organisms, although it is not possible to state categorically at this time that gentamicin is not taken up by these cells. After 18 hours of coincubation, the percentages of infected cells were higher than the percentages at 2 hours, but the CFUs obtained from the bacterial cultures of the cell lysates were reduced by more than 50% indicating that the intracellular bacteria may be unable to grow and survive in MDSCs (Figure 3.12). Reduction of cells from 2 hours to 18 hours was not due to bacterial-induced apoptosis, as uninfected cells also showed similar reductions in total cell counts (data not shown).

At 2 hours of incubation, ingested *F. tularensis* appeared to be evenly distributed between the neutrophil-like (ring nuclei) and mononuclear cells (Figure 3.12A). After 18 hours of coincubation, ingestion of bacteria was predominant in the mononuclear phenotype (Figure 3.12B). This may be a function of the differentiation of these cells in GM-CSF stimulated cultures which, could lead to a reduction of the ring forms. Alternatively, there may be selective mortality of the granulocytic phenotype. Annexin V and propidium iodide assays indicated a 10-15% range of mortality from the 2 hour to the 18 hour time points.

Adoptive transfer of MDSCs into mice does not alter the course of experimental subclinical infection with *F. tularensis*. For eliciting MDSCs for adoptive transfer experiments, C3H/HeN mice were infected intradermally with sublethal doses of *F. tularensis*. On day 10

post-inoculation, splenocytes were harvested, washed and resuspended in buffer with antibiotic to eliminate residual bacteria. Splenocytes were incubated with anti-CD11b magnetic beads and then stained with fluorescently conjugated Gr-1 and sorted by high-speed FACSAria. After sorting, cells were counted and resuspended in medium without antibiotics. Aliquots of the cells in medium were used for plating on Chocolate agar II to determine the presence of residual bacteria in both the medium and the cells; no bacteria were recovered. The remaining sorted cells were incubated with CFSE diluted in dimethyl sulfoxide, as described (Figure 3.13). After centrifugation and resuspension, $2x10^6$ cells (adjusted to compensate for dead cells) were transferred into the tail vein of C3H/HeN mice. Mice were sacrificed 24 hours after the transfer to detect CFSE-labeled Gr-1^+ $CD11b^+$ cells in the target organs. To this end, spleens and bone marrows were harvested for FACS analysis. CFSE-labeled Gr-1^+ $CD11b^+$ cells were detected in both the bone marrows and spleens of the mice receiving the cell transfers (Figure 3.14A-D), indicating that the cells homed to the intended organs.

For the actual adoptive transfer experiments, MDSCs were elicited and processed as above, including determinations of bacterial presence and cell viability, and $4x10^6$ cells were inoculated into the tail vein of mice that were infected intradermally with sublethal doses of *F. tularensis* 16 hours later. The number of cells transferred is consistent with other

adoptive transfer studies with MDSCs (55, 61). Control mice were inoculated with medium. The mice were monitored for 10 days at which time the mice were sacrificed, and spleens and livers were used for both bacterial burden determinations and histopathology.

There were no significant differences in any of the parameters measured between the adoptive transfer and control mice. Parameters included mortality, scored animal appearance, organ bacterial burdens, and numbers of hepatic granulomas (data not shown).

D. Discussion

The splenomegaly of experimental infection with *F. tularensis* was characterized by lymphoid follicle disintegration and involution along with expansion of the red pulp. Expansion of a MDSC ($Gr\text{-}1^+CD11b^+$) population (Table 3.1, Figures 3.4 and 3.5) was the main contributor to splenomegaly. These cells were not at all prominent in normal mice. Most $Gr\text{-}1^+CD11b^+$ cells in the tularemia-infected spleen were negative for expression of MHC class II and F4/80, emphasizing their immature myeloid nature (Table 3.1). Simultaneous analysis of four myeloid markers (F4/80, MHC II, Gr-1, and CD11b,) provided further proof that the majority of these splenocytes had not developed into the monocyte/macrophage lineage. The splenic responses to experimental tularemia centered on the expansion of the MDSCs, and as such paralleled the expansion of these cells in the hepatic granulomas

characteristic of this infection as seen in Chapter II (Figures 2.8 and 2.9). A parallel expansion of the Gr-1$^+$ CD11b$^+$ population in the bone marrow was also noted in our mice (Figure 3.7). This would suggest that medullary proliferation was occurring more or less simultaneously with the accumulation in both the spleen and liver (154). The large numbers of MDSCs in the spleens of tularemia-infected mice suggest the possibility of splenic proliferation, a notion bolstered by the presence of mitotic cells in both spleen and livers (not shown). Although cells of the myeloid lineage are derived from the bone marrow, extramedullary proliferation in the spleen in response to tumor-derived growth factors, proinflammatory proteins and sepsis has been documented (55, 166).

Immature myeloid cells with suppressor functions have been previously observed in the spleens and tumors of mice (26, 29) in models of chronic inflammation (75) and in polymicrobial sepsis (55). Specifically, MDSCs have been shown to inhibit T-cell immune responses (114, 161, 164). We considered the possibility that this could be the case in murine tularemia. In mice infected with *F. tularensis*, there is a modest expansion of T cells in the spleen (Table 3.1) and not at all in the liver (Table 2.2). Ten days after infection, the absolute number of MDSCs in the spleen had increased 15-fold (Figure 3.4). At the same period of time, T lymphocyte populations (CD3, CD4, and CD8) increased two-fold from uninfected numbers while B lymphoctye populations (CD21, CD23, and CD138) did

not significantly increase (Table 3.1). It remains to be seen whether the MDSCs induced in murine tularemia are responsible for T cell inhibition and, if this were to be the case, retard the immune response against this infection.

In this context, while there are absolute increases in the numbers of MDSCs in the spleens of mice from different strains, the percentages of this cell population were not as high in BALB/c and C57BL/6 mice as in C3H/HeN mice. Lethality of *F. tularensis* infection depends on mouse strain, infecting dose, and route of inoculation. Earlier studies have shown that the intraperitoneal and intravenous LD_{50} for C57BL/6 and BALB/c mice are higher than those for C3H/HeN mice (82). In our own comparisons of mouse strain susceptibility, we have also noted that the C3H/HeN mice have a lower LD_{50} for ID infection with *F. tularensis* than C57BL/6 and BALB/c animals, and this increased susceptibility could be related to the larger MDSC response in the former.

Ex vivo differentiation of MDSCs resulted in the development of professional phagocytes, as mature macrophage markers as well as those of DCs were highly expressed by 7 days with GM-CSF. Ex vivo differentiation of tularemia-derived MDSCs into antigen presenting cells correlates with other results in tumor-bearing mice (197) and in polymicrobial sepsis (55). This ex vivo preference appears to be due to

the action of GM-CSF. However, in vivo differentiation of MDSCs may also be dependent upon many other stimulating factors or cytokines.

Recently, it has been demonstrated that *F. tularensis* can inhibit the immune response of the host through various pathways. *F. tularensis* infection inhibits IFN-γ production by inducing expression of a negative IFN-γ regulator, SOCS3, in both murine and human monocytes (150). Also, it has been shown that *F. tularensis* suppresses the adaptive immune response by release of prostaglandin E_2, which induces anti-inflammatory cytokine production and blocks T cell proliferation (195). Interestingly, the release of prostaglandin E_2 in cancer has been shown to induce expression of MDSCs (165). The basis of understanding complex immunosuppressive activity from *Francisella* is only beginning, and contributions toward suppression by MDSCs may be of initial benefit to the bacterium.

On the other hand, the evidence obtained in this study suggests that there are other roles for the MDSCs. There are several lines of evidence that suggest that these cells could be beneficial to a protective host response. The greatest accumulation of these cells in spleen, liver and bone marrow occurs by day 10 post-inoculation, at a time of frank recovery of the mice, and when bacteria in the spleen are either absent or not numerous. Although we cannot be certain that in vivo differentiation of MDSCs into antigen presenting phagocytes occurs in the same manner as

our ex vivo experiments suggest, there are indications that this may be the case (61). The MDSCs ingest and do not support growth of *F. tularensis*, which is certainly in line with a protective role. Lastly, passive transfer of these cells did not lead to increased mortality or morbidity in mice subsequently infected with sublethal doses of *F. tularensis*. Taken together, we suggest that these cells have a complex role in infection with *F. tularensis* that can be related to the actions of specific subsets of cells within the heterogeneous MDSC population or to the different and changing functional state of these cells (200). Rapid accumulation of MDSCs cells in the liver, bone marrow and spleen may allow a niche wherein the bacterium can survive, but allow the host to avoid further dissemination and await the adaptive response and appropriate cytokines that can induce MDSCs to differentiate into mature phagocytes to clear the infection, thus providing a bridge from innate immunity to the adaptive immune response.

In summary of Chapter III:

- MDSCs account for much of the splenomegaly in mice infected with *F. tularensis.*
- MDSCs (Gr-1$^+$ CD11b$^+$) accumulate in spleens and bone marrow of infected mice and are a heterogeneous population.

- C3H/HeN mice are more susceptible to tularemia and contain larger populations of MDSCs than other mouse strains during infection.
- MDSCs from infected and uninfected mice differentiate into mature antigen presenting cells in ex vivo culture in the presence of GM-CSF.
- MDSCs ingest and do not support growth of *F. tularensis* in ex vivo culture.
- Adoptive transfer of MDSCs into mice infected with *F. tularensis* does not lead to increased morbidity or mortality.

E. Tables and Figures

Cell Type	Markers	NL	D1	D5	D10	D20
MDSC	$Gr\text{-}1^+$ $CD11b^+$ $MHC\ II^-$	5.7 ± 0.3	10.5 ± 2.5	16.1 ± 3.3	70.7 ± 9.3**	14.0 ± 2.0
MDSC	$Gr\text{-}1^+$ $CD11b^+$ $F4/80^-$	5.4 ± 0.5	9.9 ± 2.6	18.2 ± 7.2	78.4 ± 10.8**	13.3 ± 1.6
Macrophage	$F4/80^+$ $MHC\ II^+$ $Gr\text{-}1^+$ $CD11b^+$	0.4 ± 0.0	0.7 ± 0.1	8.8 ± 4.4**	7.6 ± 1.0**	1.2 ± 0.3
Pan T	$CD3^+$	27.8 ± 2.5	17.1 ± 3.5	35.6 ± 3.1	40.2 ± 9.0*	33.8 ± 10.2
T helper	$CD3^+$ $CD4^+$	18.2 ± 1.9	11.5 ± 2.6	20.8 ± 1.0	26.1 ± 7.1*	20.1 ± 5.7
T cytotoxic	$CD3^+$ $CD8^+$	7.5 ± 0.8	4.9 ± 0.9	9.0 ± 0.2	14.8 ± 4.2**	11.9 ± 3.1
FO B	IgM^+ $CD21^{+/-}$ $CD23^+$	20.9 ± 3.7	14.6 ± 2.8	10.3 ± 4.4**	23.3 ± 4.6	23.9 ± 6.3
MZ B	IgM^+ $CD21^+$ $CD23^-$	9.6 ± 2.4	7.0 ± 1.3	11.9 ± 3.4	16.5 ± 2.3	13.2 ± 4.4
Plasmablasts	IgM^+ $CD138^+$	3.4 ± 1.6	2.4 ± 0.5	2.9 ± 0.5	7.6 ± 0.8**	3.3 ± 0.4
DC	$CD11c^+$ $CD11b^+$	0.8 ± 0.3	0.6 ± 0.2	1.7 ± 1.1	2.4 ± 0.5*	1.2 ± 0.3
NK	$DX5^+$ $NK1.1^+$	0.6 ± 0.2	0.3 ± 0.1	0.9 ± 0.6	1.3 ± 0.2	0.5 ± 0.2

Table 3.1. Flow cytometry analysis of cell marker expression of splenocytes from normal (NL) mice and mice inoculated with *F. tularensis* at various days post-inoculation. Numbers are mean of splenocytes ($x10^6$) ± standard deviation from three C3H/HeN mice. * $P < 0.05$, ** $P < 0.01$ significantly different from normal (NL) control.

Figure 3.1. Hematoxylin and eosin stained sections of spleens of mice infected with sublethal doses of *F. tularensis*. Spleens were aseptically removed and immediately fixed in 10% neutral buffered formalin, embedded in paraffin, sectioned at 5 μm, stained with hematoxylin and eosin, dehydrated in graded alcohols, cleared with xylene and mounted with Acrymount. Tissue sections were examined by light microscopy. (A) Normal spleen. (B) Low-power view of spleen infected five days earlier showing cellular loss in red pulp and disruption in the white pulp. (C) By seven days post-inoculation, an influx of mononuclear cells in the red and white pulp disrupts normal splenic architecture. (D) Many giant-like cells are seen in spleen at seven days post-inoculation. Bars, 200 μm (A-C) and 50 μm (D).

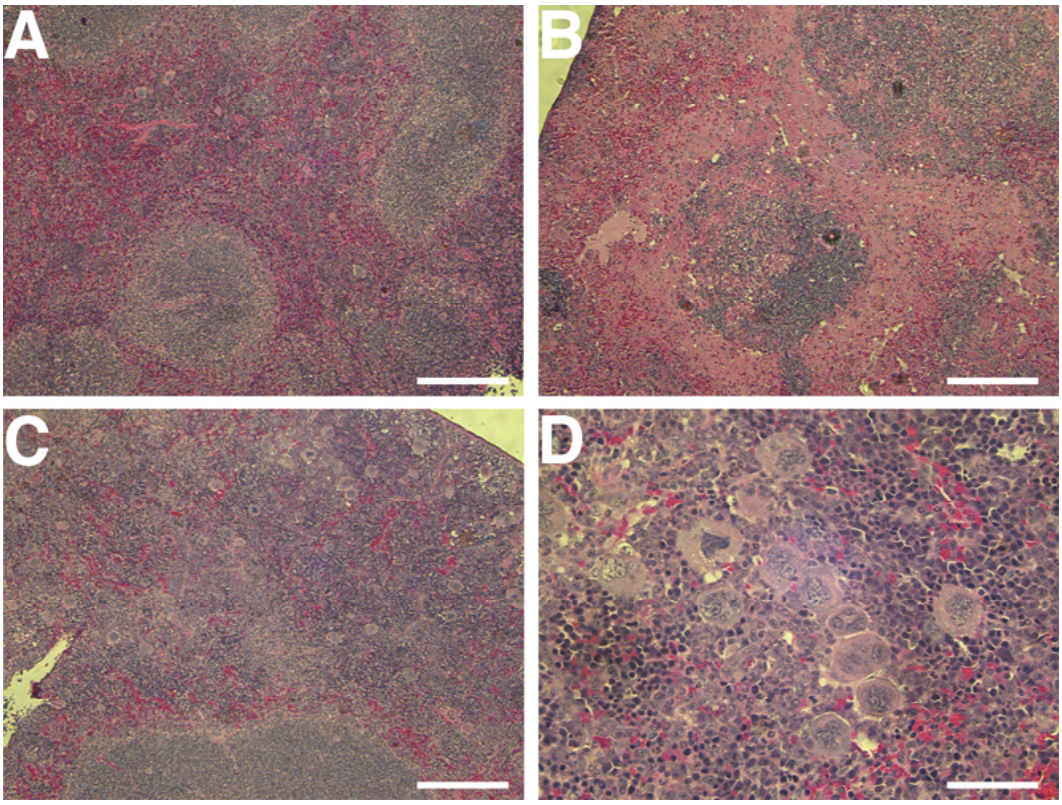
A
B
C
D

Figure 3.2. Detection of bacteria in spleens of mice infected with sublethal doses of LVS five days earlier. After dewaxing and rehydration of paraffin sections, bacteria were detected with a rabbit anti-*F. tularensis* LVS followed by alkaline phosphatase-conjugated anti-rabbit serum. Vulcan Fast Red was used to detect alkaline phosphatase. (A) Uninfected spleen. (B) Low power view of spleen showing vast growth of bacteria by 5 DPI; most bacteria appear in the red pulp of the spleen. (C) High power view showing bacteria infection of mononuclear cells. Bars, 100 μm (A and B) and 50 μm (C).

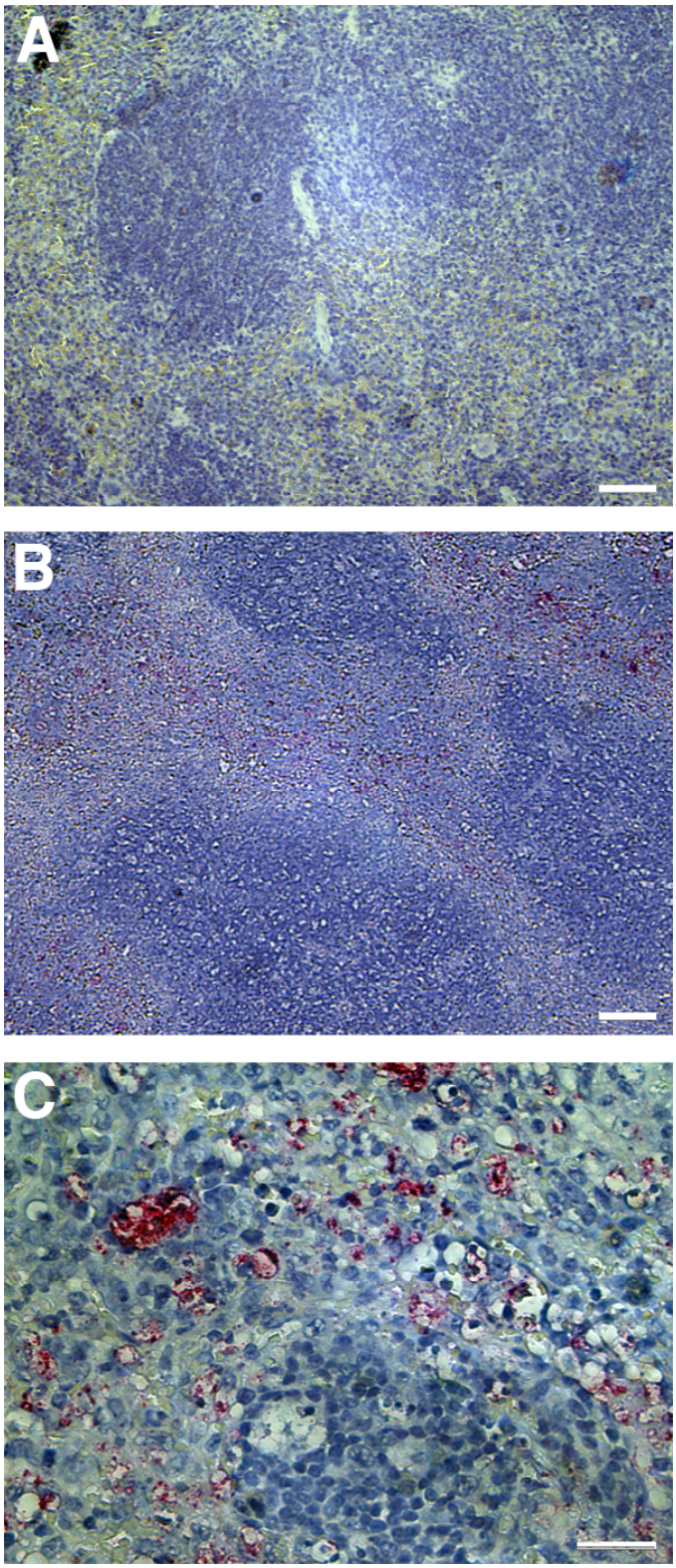
A
B
C

Figure 3.3. Spleens of mice infected with *F. tularensis* greatly increase in size and weight. (A) Mean spleen index ± SD of 3-4 mice per time point during the infection. Spleen index was calculated by using the formula: (spleen weight in mg/total body weight in mg) x 1000. Marked increase is due to both an increase in spleen weight and a mouse weight loss during infection. By 10 DPI, the spleen increases five fold compared to uninfected spleens. This increase is depicted in insert (B) by comparing an uninfected spleen (Nl) and a 10 DPI spleen from age-matched mice. * $P < 0.05$, ** $P < 0.01$, significantly different from normal (Nl) control.

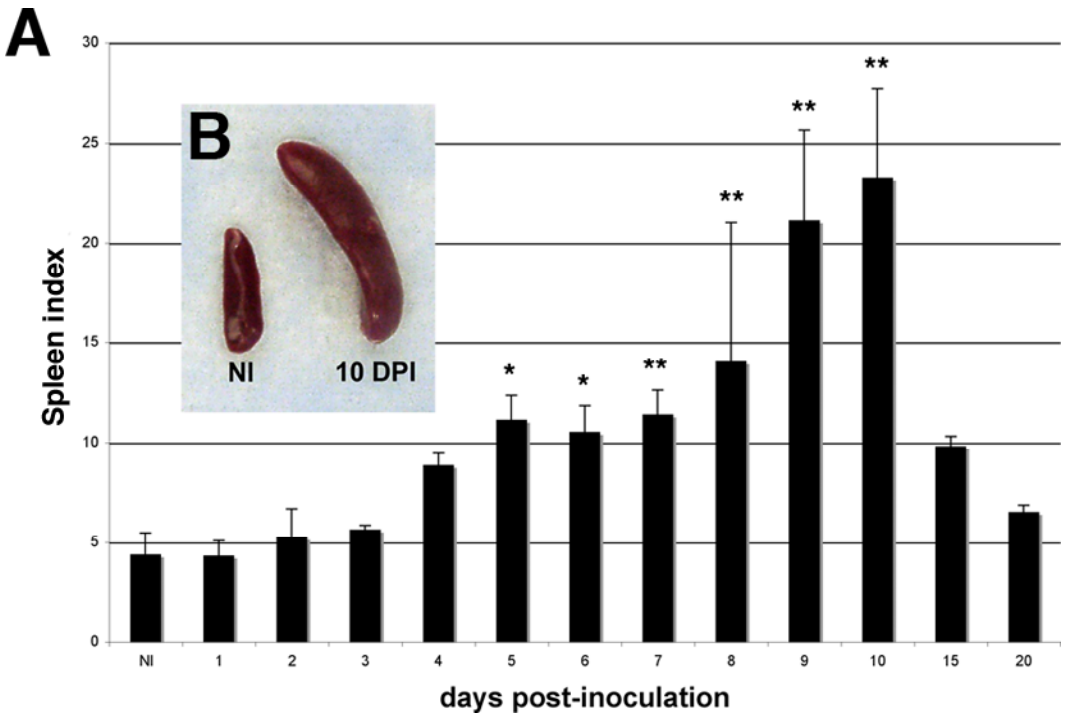
A
B
NI
10 DPI
Spleen index
days post-inoculation
0
5
10
15
20
25
30
NI
1
2
3
4
5
6
7
8
9
10
15
20
*
*
**
**
**
**

Figure 3.4. Accumulation of MDSCs (Gr-1$^+$ CD11b$^+$) in spleens of three strains of mice infected with sublethal doses of *F. tularensis*. Splenocytes were collected, immunofluorescently stained for cell surface markers Gr-1 and CD11b and enumerated by flow cytometry. Spleens were removed on various days post-inoculation from (A) C3H/HeN mice, (B) C57BL/6 mice and (C) BALB/c mice. Each bar represents mean ± SD of three mice. * $P < 0.05$, ** $P < 0.01$ significantly different from normal (Nl) control.

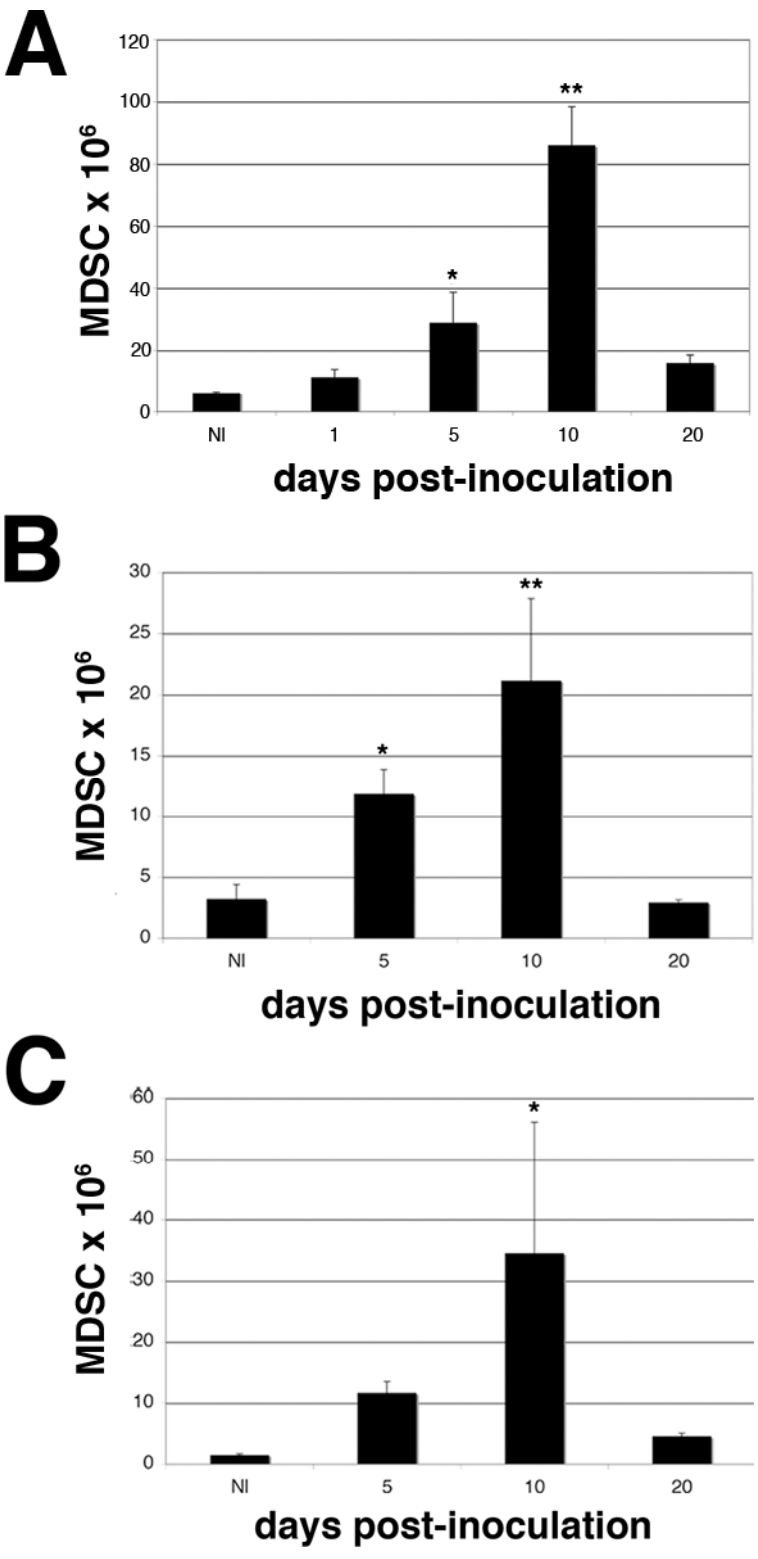
A
MDSC x 10^6
120
100
80
60
40
20
0
*
**
NI
1
5
10
20
days post-inoculation
B
MDSC x 10^6
30
25
20
15
10
5
0
*
**
NI
5
10
20
days post-inoculation
C
MDSC x 10^6
60
50
40
30
20
10
0
*
NI
5
10
20
days post-inoculation

Figure 3.5. Percentage of MDSCs (Gr-1$^+$ CD11b$^+$) in spleens of C3H/HeN mice infected with sublethal doses of *F. tularensis*. Spleens were removed from mice on various days post-inoculation and splenocytes were collected, immunofluorescently stained for cell surface markers Gr-1 and CD11b and enumerated by flow cytometry. Representative histograms of the percentage of cells expressing Gr-1 and CD11b in an uninfected mouse (A) and in a mouse infected with *F. tularensis* 10 days earlier (B). (C) Time course of the accumulation of MDSC as a percentage of total splenocytes. Each bar represents mean ± SD of three mice. ** $P < 0.01$ significantly different from normal (Nl) control.

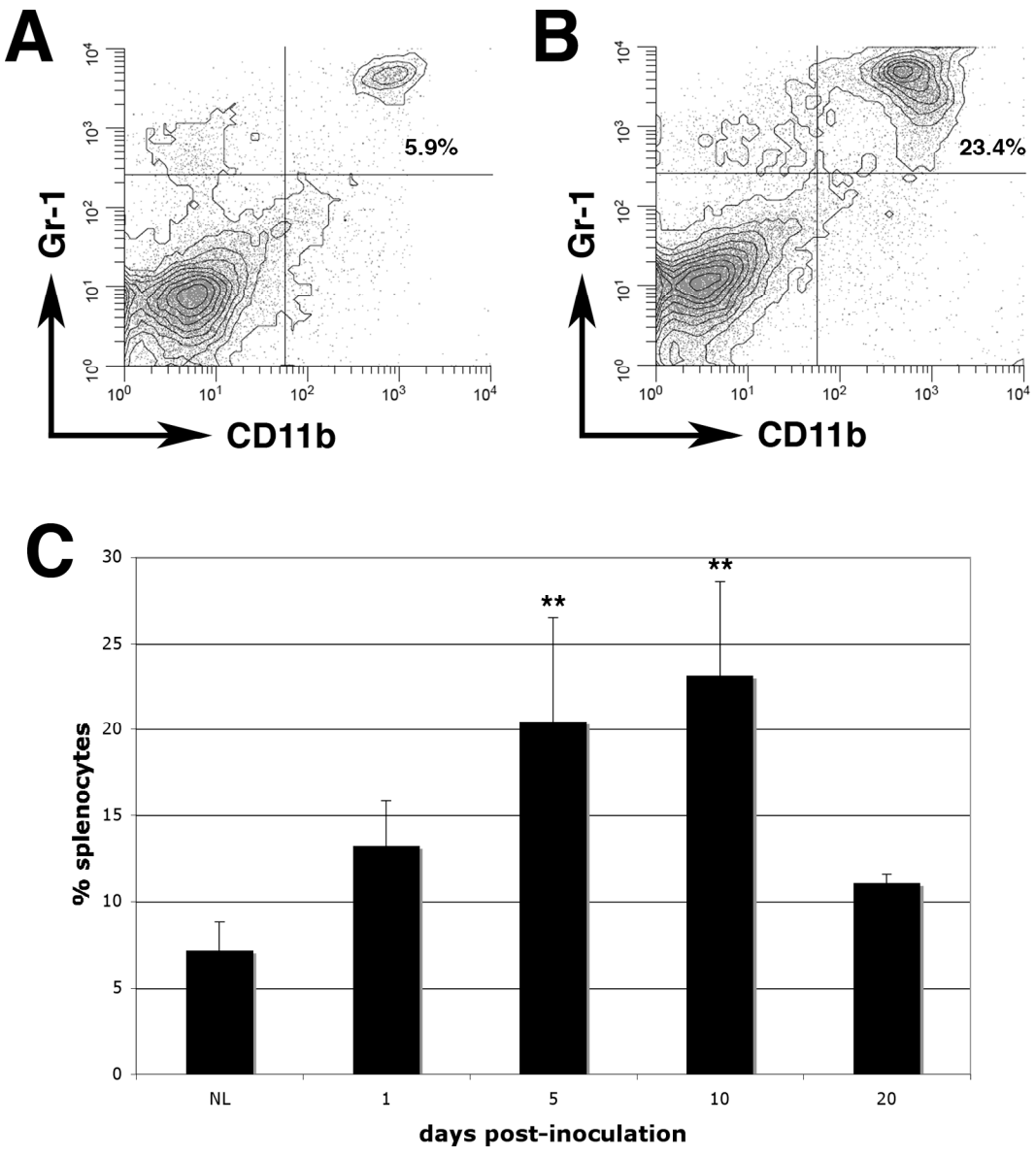
A
5.9%
Gr-1
CD11b
B
23.4%
Gr-1
CD11b
C
% splenocytes
days post-inoculation
NL
1
5
10
20
**
**

Figure 3.6. Immunofluorescent detection of *F. tularensis*, Gr-1 and CD11b cell markers in spleens from mice infected five days earlier. Tissues removed from mice were immediately fixed in 1% formalin for 1 hour and then placed in a 30% sucrose solution overnight. Tissues were then frozen in isopentane cooled with liquid nitrogen. Frozen tissue sections were cut at 5 µm in the cryostat, and stained with appropriate antibodies. (A) *F. tularensis* (secondary anti-rabbit Ig, Alexa Fluor 488, green). (B) Gr-1^+ cells (PE, red). (C) $CD11b^+$ cells (Alexa Fluor 647, blue). (D) Merged image of panels A to C. Note colocalization of Gr-1^+ and $CD11b^+$ cells with *F. tularensis*, white arrows. Bar lengths indicated in figure.

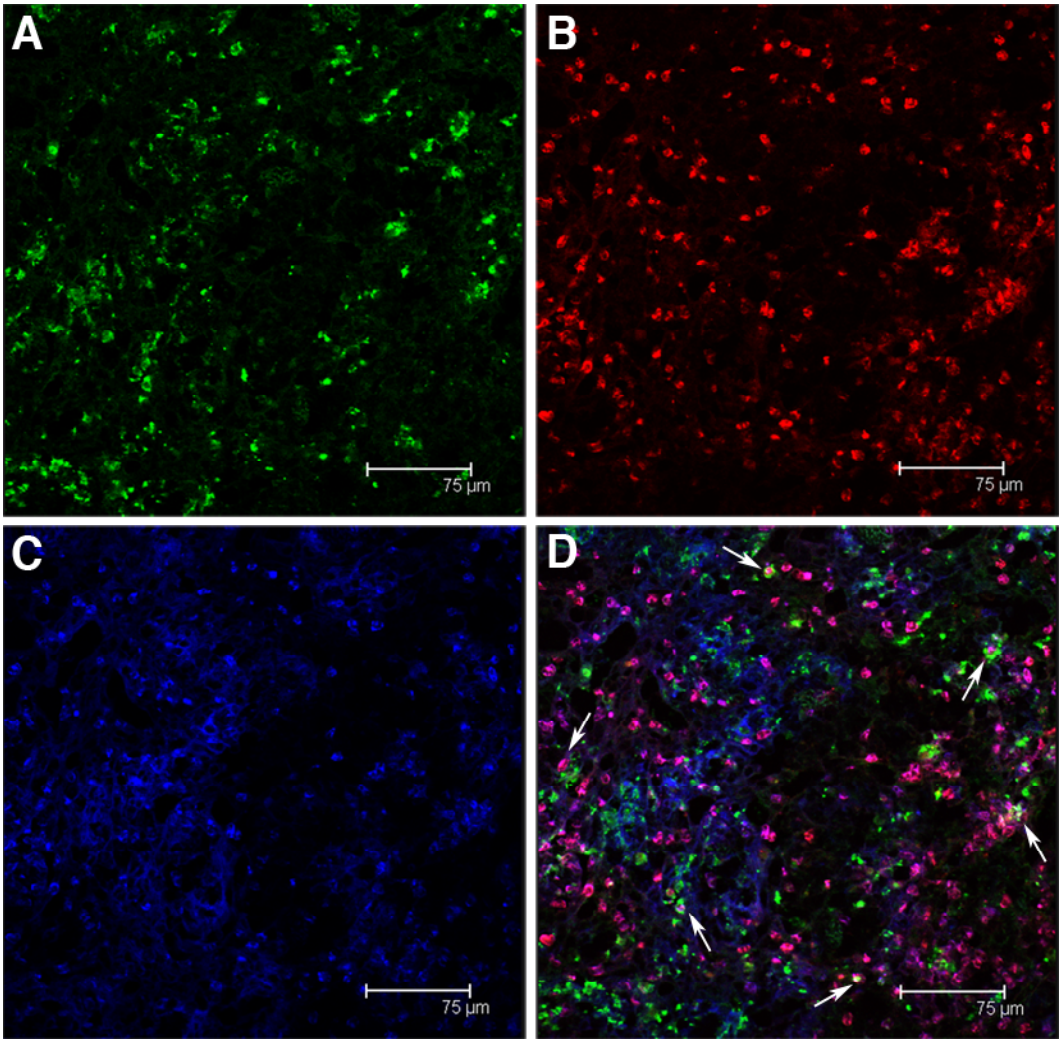
A
75 µm
B
75 µm
C
75 µm
D
75 µm

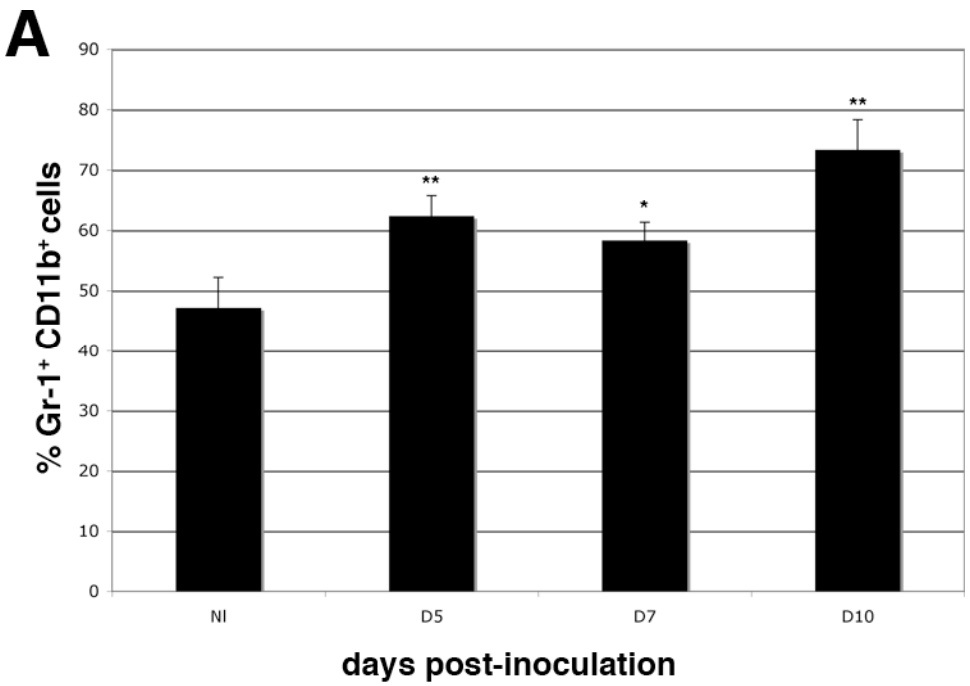

Figure 3.7. Mean and standard deviation of percent of MDSCs in bone marrow of mice infected with sublethal doses of *F. tularensis* at various time points in the infection. Bone marrow from femur and tibia was collected and stained with fluorescent antibodies for Gr-1 and CD11b for flow cytometry analysis. Each bar represents mean ± SD of three mice. * $P < 0.05$, ** $P < 0.01$ significantly different from normal (NI) control.

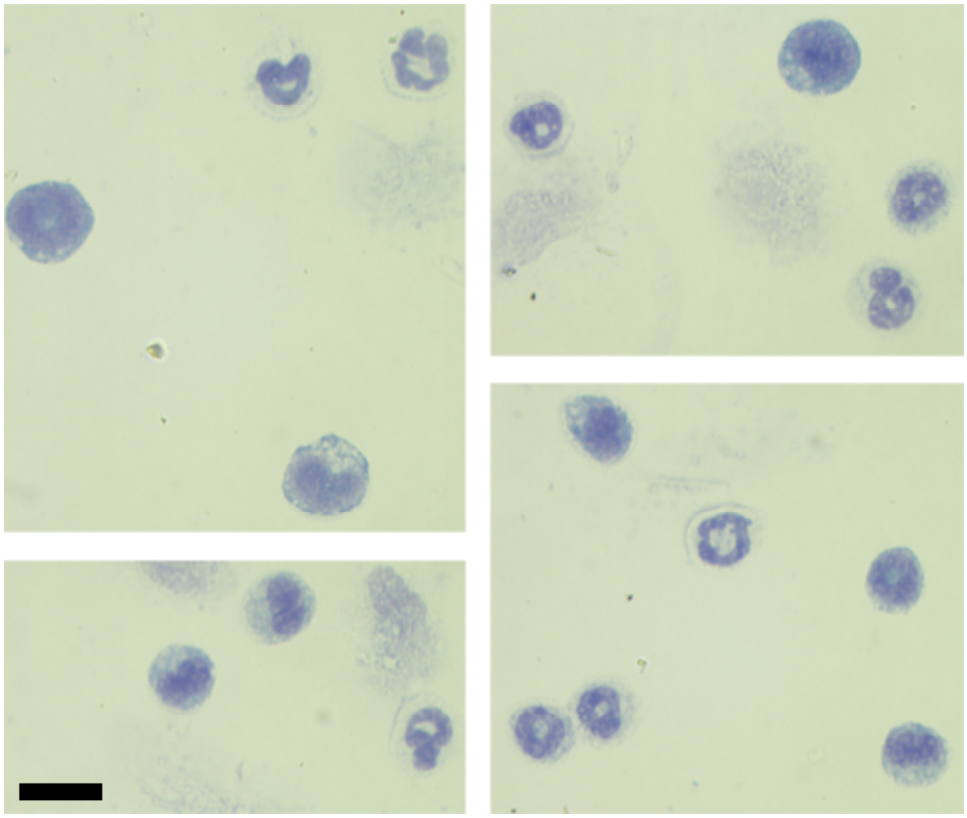

Figure 3.8. Giemsa stained, purified Gr-1$^+$ CD11b$^+$ cells from magnetic and fluorescent sorting show a heterogeneous population of cells with mononuclear and ring-shaped nuclei. Bar, 10 μm.

Figure 3.9. Purification of MDSCs from mice infected with *F. tularensis* ten days earlier. Spleens were removed from mice and incubated with anti-CD11b MicroBeads to collect CD11b cells by magnetic separation. $CD11b^+$ cells were then stained with fluorescent anti-Gr-1 antibody and purified by fluorescent separation using a cell sorter. Forward and side scatter profile (A) and detection of cell death markers (B) of MDSCs by flow cytometry after purification. (C-E) Three separate experiments demonstrate high purity of sorted MDSCs by detection of Gr-1 and CD11b by flow cytometry.

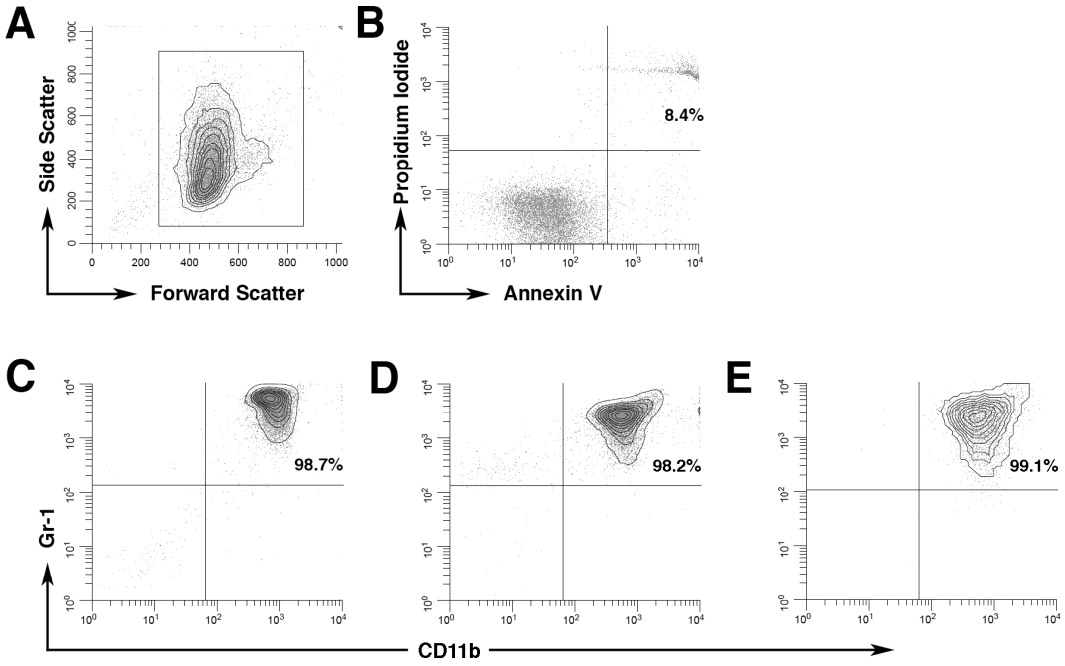
A
Side Scatter
Forward Scatter
B
Propidium Iodide
Annexin V
8.4%
C
98.7%
Gr-1
CD11b
D
98.2%
E
99.1%

Figure 3.10. Ex vivo cellular differentiation of purified MDSCs from mice infected with *F. tularensis* ten days earlier and stimulated with GM-CSF. MDSCs were lifted from wells by trypsin digest, then quantified and stained with fluorescent markers for flow cytometry analysis. (A) Cellular differentiation seen by forward and side scatter of MDSCs. After 7 days of ex vivo culture MDSCs increase in size and granularity. (B) MDSCs differentiate into cells expressing F4/80 and CD11b cell markers and (C) dendritic cell marker CD11c by seven days of ex vivo culture. (D) Expression of Gr-1 decreases by seven days of ex vivo culture with GM-CSF.

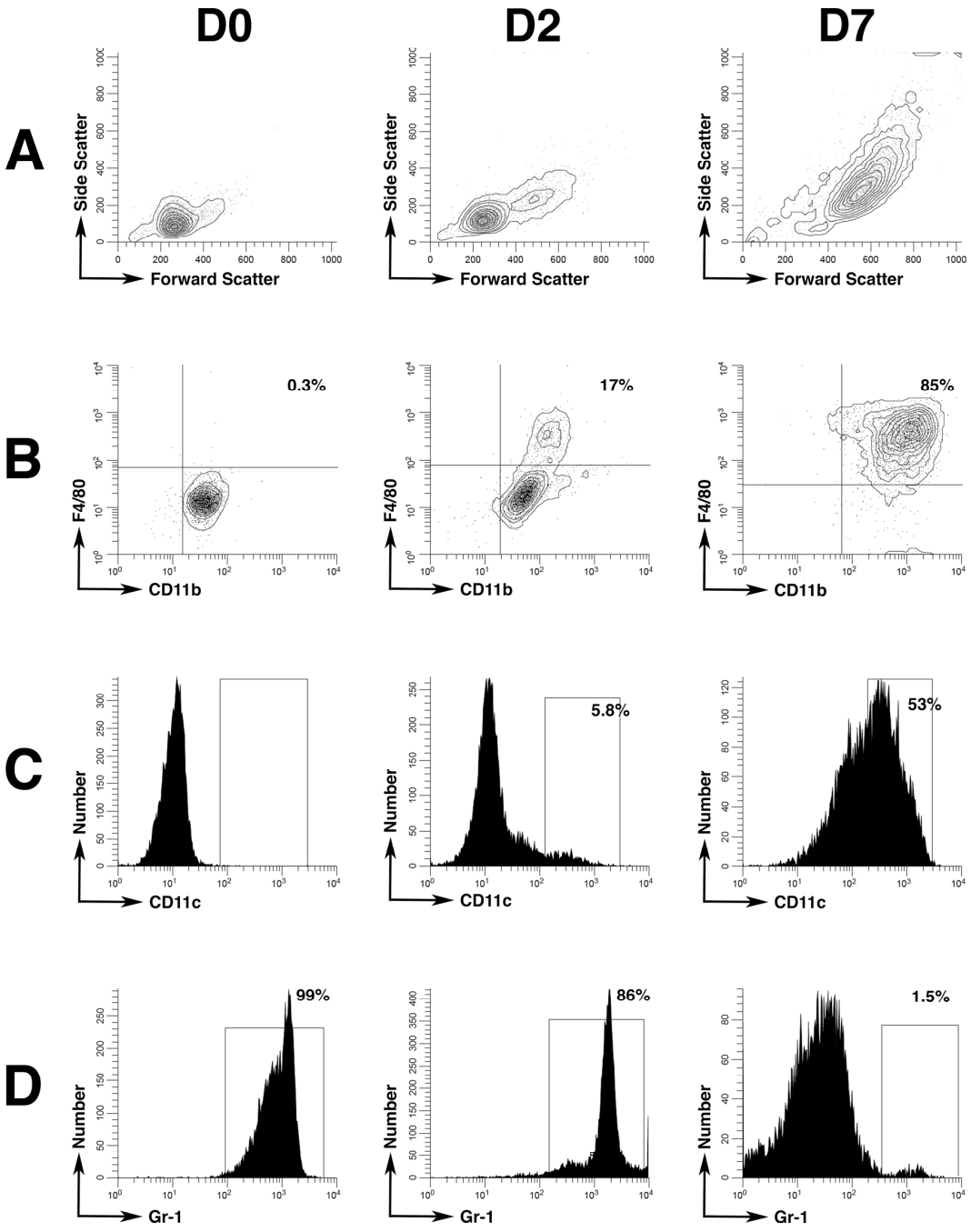
D0
D2
D7
A
B
C
D
Side Scatter
Forward Scatter
F4/80
CD11b
0.3%
17%
85%
Number
CD11c
5.8%
53%
Gr-1
99%
86%
1.5%

Figure 3.11. Ex vivo cellular differentiation of MDSCs purified from uninfected mice and stimulated with GM-CSF. MDSCs were lifted from wells by trypsin digest, then quantified and stained with fluorescent markers for flow cytometry analysis. Similar to MDSCs from infected spleens (Figure 3.8) MDSCs from naïve mice also exhibit cellular differentiation seen by forward and side scatter. (A) Differentiation begins by 2 days of culture and after 7 days of ex vivo culture MDSCs greatly increase in size and granularity. (B) MDSCs differentiate into cells expressing F4/80 and CD11b cell markers and (C) dendritic cell marker CD11c by seven days of ex vivo culture. (D) Expression of Gr-1 decreases by seven days of ex vivo culture with GM-CSF.

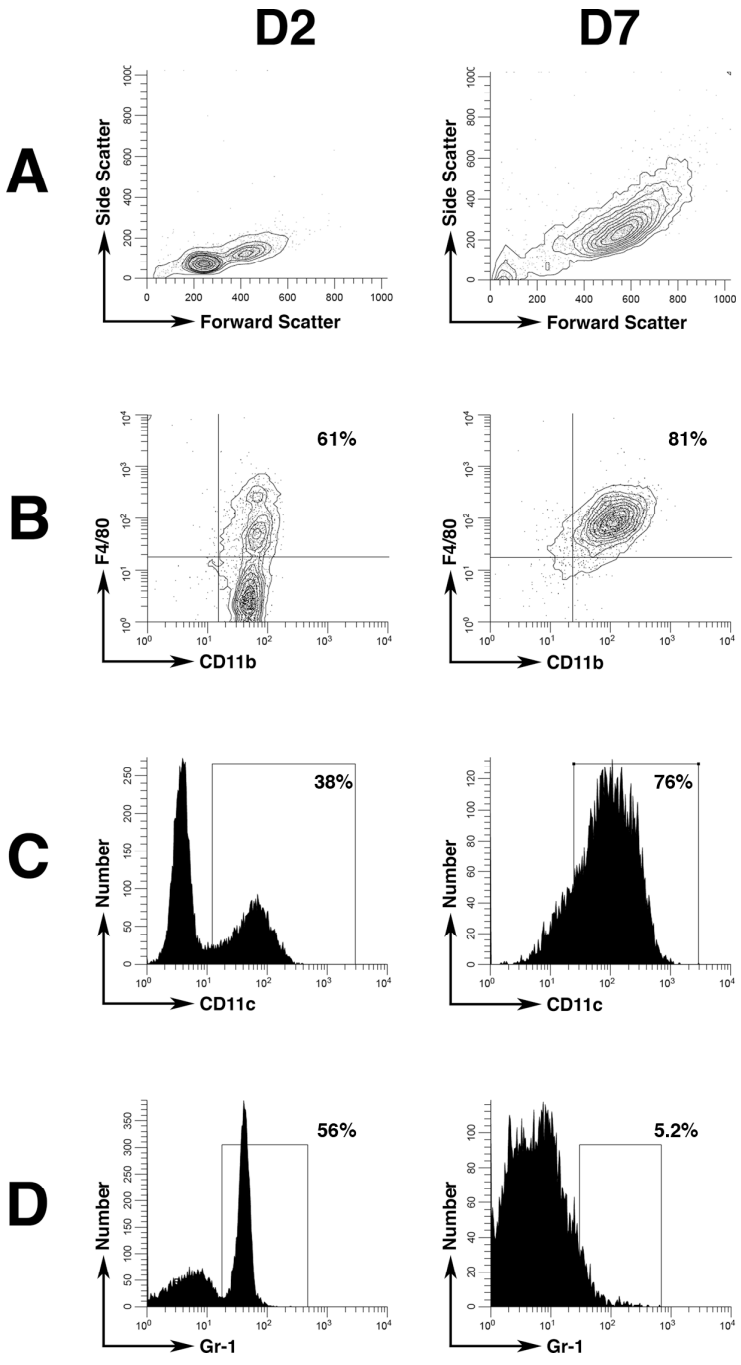
D2
D7
A
Side Scatter
Forward Scatter
B
F4/80
CD11b
61%
81%
C
Number
CD11c
38%
76%
D
Gr-1
56%
5.2%

Figure 3.12. Ex vivo intracellular infection of Gr-1$^+$ CD11b$^+$ sorted MDSCs with *F. tularensis*. Bacteria were cultured with MDSCs on 24 well plates for two hours before addition of gentamicin to kill extracellular bacteria. Three separate experiments are shown with different MOIs, percent infected cells and CFUs recovered. MDSCs recovered after 2 and 18 hours were stained with DAPI and anti-*F. tularensis* IgG in an immunofluorescent antibody assay (IFA). IFA of MDSCs at 2 hours (A) and 18 hours (B) after infection. DAPI (blue) was used to visualize nuclei of cells infected with *F. tularensis* (green). Bars, 10 μm.

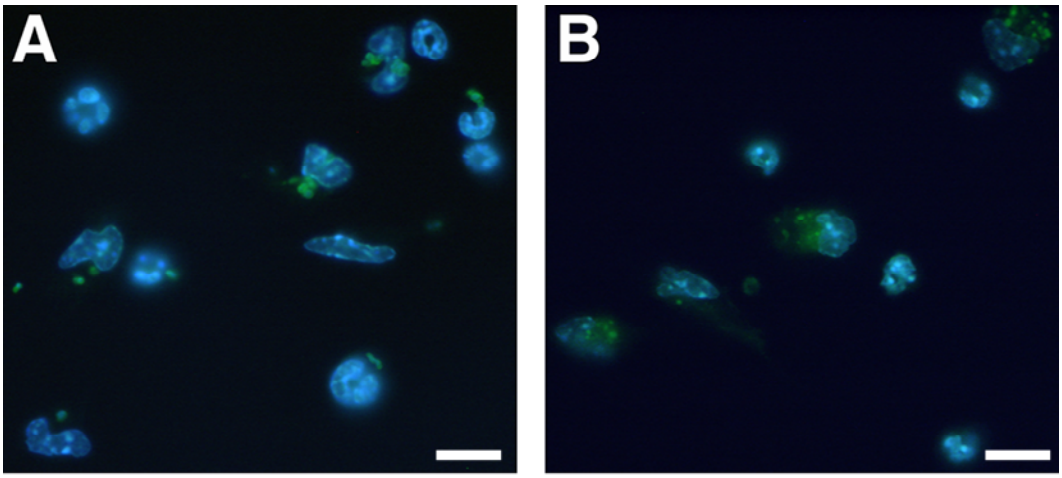

Time	Experiment	~MOI	% Infected cells	CFUs/total cells
2 hrs	Exp 1	10	25.1 ± 3.0	2200/105,000
	Exp 2	15	29.7 ± 2.8	3600/128,000
	Exp 3	30	51.6 ± 3.9	ND
18 hrs	Exp 1	10	29.1 ± 1.9	1100/58,000
	Exp 2	15	38.7 ± 2.7	1200/64,000
	Exp 3	30	69.4 ± 4.0	ND

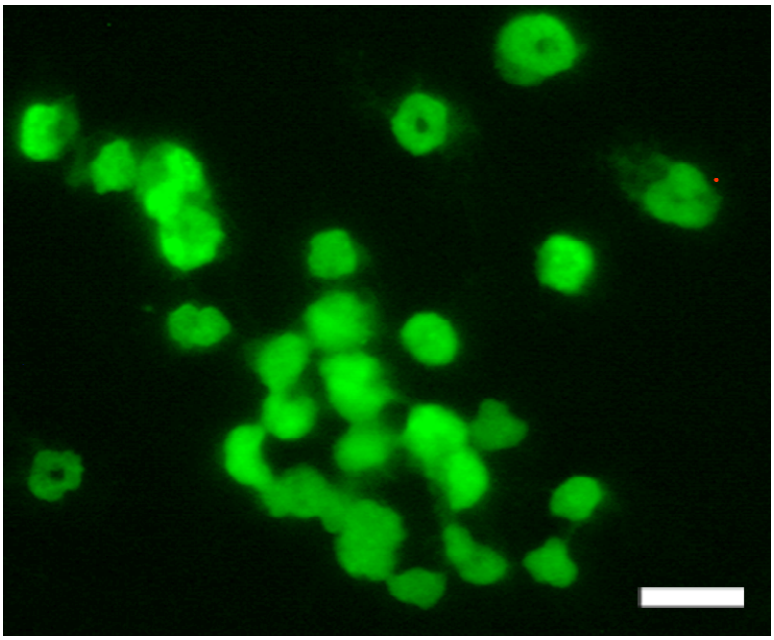

Figure 3.13. Fluorescent image of MDSCs stained with CFSE. MDSCs were incubated with CFSE to verify the homing of these cells to the spleen and bone marrow after an adoptive intravenous transfer. Bar, 10 μm.

Figure 3.14. Recovery of MDSCs from uninfected mice that received intravenous transfer of MDSCs treated with CFSE. MDSCs were traced to the spleen and bone marrow of mice 16 hours post-IV transfer. (A) Gr-1 and CD11b expression of splenocytes from mice with IV transfer. (B) CFSE expression from gated Gr-1^+ $CD11b^+$ splenocytes from panel A. (C) Bone marrow content of Gr-1^+ $CD11b^+$ cells from mice with IV transfer. (D) CFSE expression from gated Gr-1^+ $CD11b^+$ splenocytes from panel C.

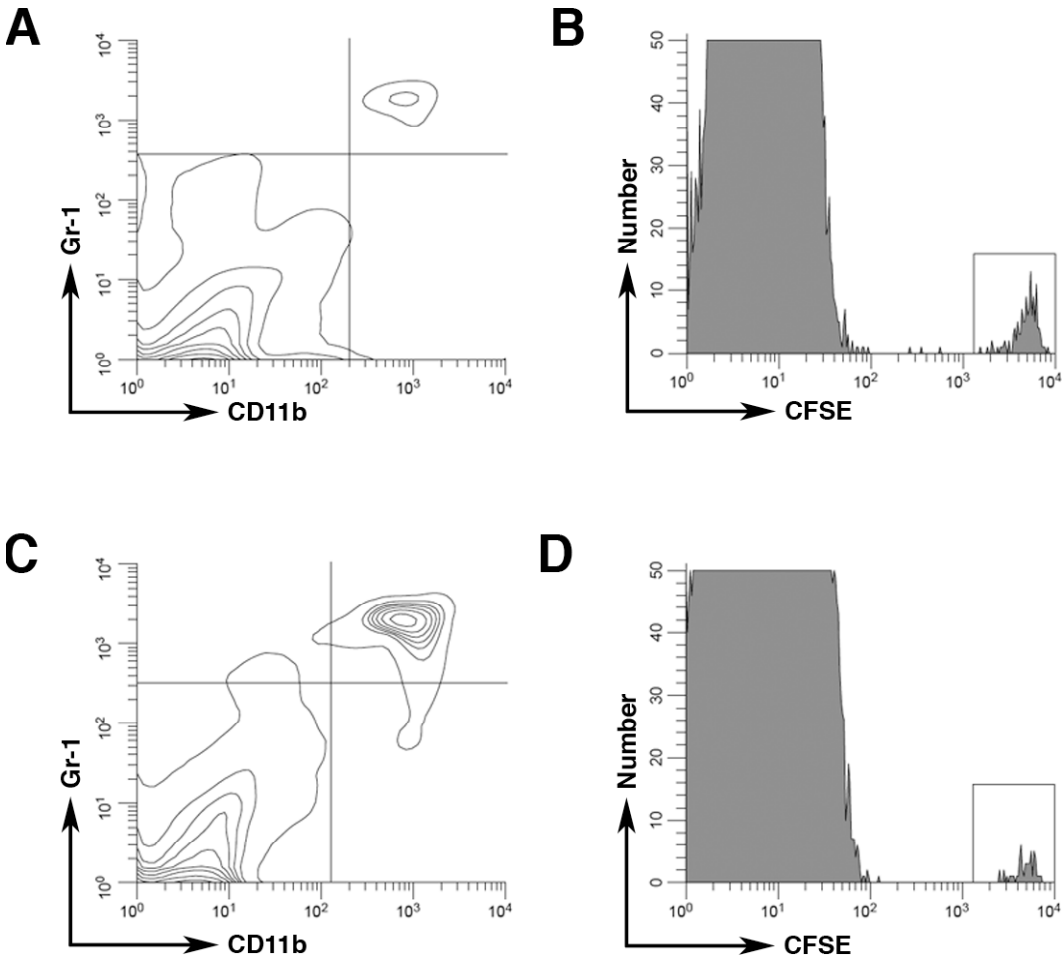
A
Gr-1
CD11b
B
Number
CFSE
C
Gr-1
CD11b
D
Number
CFSE

Chapter IV

B cell Involvement in Experimental Tularemia

A. Introduction

Since *Francisella* is a facultative intracellular pathogen, the importance of B cells in the host's immune response has been debated. Recently, B cells and antibody production have received greater attention as to their contribution in fighting intracellular pathogens. In mice infected with *Chlamydia*, B cells are critical in the early infection for priming and initiation of the T cell response required for immunity (198). For *Salmonella*, protective immunity is strongly, but not exclusively, dependent on B cells (145), and mice without B cells are deficient in producing cytokines necessary for a robust T cell adaptive response (140). Moreover, B cells have been implicated in regulating T cell expansion and differentiation into effector cells in viral infections (16).

Production of antibody is largely regarded as the main effector function for B lymphocytes, especially in infection with extracellular pathogens, where antibody binding will accelerate bacterial clearance through opsonization and Fc receptor mediated phagocytosis. However, in tularemia, contribution of antibodies to the control of the infection has not been fully characterized. Mice that receive immune serum prior to *F. tularensis* LVS inoculation are not protected from lethal infections (53, 66, 155). Conversely, another study demonstrated a protective role of

antibodies; B cell deficient mice administered whole immune serum survive a lethal challenge from Type B strains (174). However, early tularemia research has shown that passive transfer of immune serum will not protect against Type A infections (3, 182). *F. tularensis*, traditionally known as an intracellular pathogen, has a significant extracellular phase in the blood during an early infection (78). An extracellular bacteremia markedly increases the possibility of a decisive role for B cells and specific antibody production in response to *F. tularensis*.

In tularemia, there is recent evidence that B lymphocytes are contributing to the development of immunity much more so than previously thought. T cells are known to be required for long-term protection in a murine ID challenge; however, there is a T cell-independent phase that is important for short-term protection (70). B cells may be directly related to this T cell-independent phase, as B cells provide an early protective immunity that is due to cytokine release rather than specific anti-LVS antibodies (53).

B cell deficient mice have been used in tularemia to further clarify potential benefits of B cells in controlling the infection. When B cell deficient mice are inoculated with LVS, they are only marginally compromised to control a primary infection but 100-fold less well protected against a secondary challenge. Absence of B cells results in a significant delay of bacterial clearance from spleen and liver and a more prominent

and long-lasting granuloma formation in the liver (66). Significance of a larger granuloma in B cell deficient mice is of importance to this dissertation, as granulomas contain large amounts of $CD11b^+$ cells, corresponding to the subpopulations that make up the hepatic lesions in Chapter II (154). Bosio and Elkins demonstrated that cytokine expression is no different between B cell deficient mice and WT mice and that B cells are involved in regulating neutrophil trafficking, as B cell deficient mice exhibit a neutrophilia upon a secondary infection (21).

For this study, the spleen was used to investigate the role of B cells in tularemia. The spleen, a secondary organ of the immune system, filters the blood of the host and consequently becomes one of the first organs to initiate contact with bacteria or infected cells. As discussed in Chapter III, during the acute phase of a murine tularemia infection, the architecture of the spleen changes drastically, with marked changes in myeloid cells and lymphocytes (Table 3.1). The spleen is a front line defender and central in bridging the innate and adaptive immune responses.

There are three main mature B cell subsets in the spleen, MZ B cells, FO B cells and antibody secreting plasma cells (Table 4.1). Blood first arrives in the spleen through the sinuses of the marginal zone, where MZ B cells reside (138). MZ B cells display restricted antigenic specificities and target repetitive epitopes on bacterial polysaccharide (201). MZ B cells can bridge the innate and adaptive immune responses

by rapidly binding antigen to differentiate into antibody producing cells in a T cell-independent manner (127, 137). FO B cells participate in T cell-dependent responses through somatic hypermutation and class switch recombination, thus expanding the diversity of B cell receptors and enabling an antibody response to numerous microbial antigens (153). Plasma cells, develop as B cells become activated and differentiate into antibody secreting cells.

Herein, the role of prominent splenic B cell fractions and antibody produced during the acute infection were investigated in WT and B cell deficient (B6.129S2-Igh-6^{tm1Cgn}/J) mice inoculated with *F. tularensis* LVS. Murine B lymphocytes were monitored by flow cytometry during the course of infection. Antibodies to *F. tularensis* developed as a result of the acute infection. The literature has conflicting evidence on the protective capacity of these antibodies. In an effort to clarify antibody contribution, reactive monoclonal antibodies were purified in preparation for passive transfer into infected mice, as passive immunization is an important approach in the biodefense arsenal (32). The results of this dissertation work indicated that B cell function may be connected with myeloid cell regulation, which can optimize the clearance of bacteria from the host.

B. Materials and Methods

Bacteria: *F. tularensis* LVS (American Type Culture Collection 29684) was cultured as previously described (Chapter II).

Mice: Female C3H/HeN mice were purchased from Charles River Laboratories (Wilmington, MA). Female C57BL/6 and B cell deficient (B6.129S2-Igh-6^{tmlCgn}/J in C57BL/6 background strain) mice were purchased from Jackson Laboratories (Bar Harbor, ME). B6.129S2-Igh-6^{tmlCgn}/J mice are deficient in mature B cells because they lack expression of membrane bound IgM (108). All mice for experimentation were used from 6 to 10 weeks of age. C57BL/6 and B cell deficient mice were housed in maximum isolation to avoid environmental contamination of immunodeficient mice. All mice were housed in microisolator cages with free access to food and water. Mice received ID injections of *F. tularensis* LVS at a range of doses and were monitored or euthanized at various time points post-inoculation, immediately followed by blood and organ collection. At least 3-6 mice were used for each time point. The institutional review board approved all animal procedures.

Splenocyte isolation. Excised spleens were gently teased apart with needles, and all cells were collected in DMEM by gentle massaging. Splenocytes were prepared and stained with various fluorescent antibodies to detect cellular populations, as previously described (Chapters II and III).

Lipopolysaccharide purification. *F. tularensis* lipopolysaccharide (LPS) was purified by phenol extraction from bacterial colonies grown on Chocolate II agar (BD Biosciences). Briefly, bacteria were placed in

centrifuge tubes with pure phenol, vigorously mixed with a pipette, centrifuged and boiled, before addition of Proteinase K (Roche Applied Science, Indianapolis, IN) and overnight shaking at 37°C. The next day a 0.3 M sodium acetate (Fisher Scientific, Pittsburg, PA) and ethanol (Pharmco-AAPER, Brookfield, CT) solution was mixed with LPS preparations and placed in a -20°C freezer overnight. Solutions were then washed 3 times with the sodium acetate and ethanol solution and centrifuged at 48,000 x g for 20 minutes to eliminate contaminating DNA and RNA before being lyophilized overnight. The precipitate was resuspended in PBS (Invitrogen) to 1 mg/ml, and purity was verified by Coomassie stain (Bio-Rad, Hercules, CA) and western blot. *E. coli* LPS was purchased from Difco Laboratories (Detroit, MI).

Western blot. Antibody production was screened in mice infected with sublethal doses of *F. tularensis* LVS. Mice were sacrificed on various days post-inoculation, and whole blood was immediately collected by cardiac puncture. Plasma was obtained after centrifugation of citrated whole blood for 10 minutes at 10,000 rpm and then frozen at -20°C until analysis. Sonicated whole-cell *F. tularensis* LVS lysate or purified LPS was electrophoresed on 12.5% sodium dodecyl sulfate polyacrylamide gels (SDS-PAGE) under reducing conditions. Gels were transferred to nitrocellulose for immunoblotting. Nitrocellulose was cut into multiple strips containing ~8 μg of sonicate per strip. Thawed plasma was diluted

1:100 in PBS containing 5% casein (Sigma) and incubated with strips for 1 hour. Alkaline phosphatase-conjugated goat anti-mouse IgM (Sigma) or alkaline phosphatase-conjugated sheep anti-mouse IgG (Sigma) were used as secondary antibodies, diluted 1:1000 in PBS and incubated for an additional hour. Immunoblots were developed with nitroblue tetrazolium/5-bromo-4-chloro3-indolyl-phosphate (Kirkegaard & Perry Laboratories).

ELISA. Enzyme-linked immunosorbent assay (ELISA), using sonicated whole-cell *F. tularensis* lysate or *F. tularensis* LVS purified LPS as the antigen, was used for detection of levels of IgM and IgG in plasma from infected mice on various DPI. Briefly, 96-well polystyrene plates were coated by overnight incubation with 0.375 μg/well of lysate or 0.2 μg/well of purified LPS as the antigen in high pH (9.6) carbonate buffer. Plates were blocked with 1% BSA in PBS for 1 hour at RT, followed by three washes and shaking to dry. Plasma was diluted 1:100, as above, and incubated for 1 hour at 37°C. Plasma was removed, and wells were washed before addition of secondary alkaline phosphatase-conjugated anti-mouse IgG (Sigma) diluted 1:1000 and incubation for 1 hour at 37°C. Secondary antibodies were removed, and wells were washed multiple times before development with 1 mg/ml 104 substrate (Sigma). Plates were then read with a Dynatech MR-580 Micro ELISA reader (Dynatech Laboratories, Alexandria, VA) at a wavelength of 405 nm.

Hematoxylin and eosin and immunofluorescent staining on tissue sections. Livers and spleens were aseptically removed, immediately fixed in 10% neutral buffered formalin, embedded in paraffin, sectioned and stained with hematoxylin and eosin, and examined by light microscopy. For immunofluorescence analysis of frozen sections, livers and spleens were removed from mice, processed, and analyzed by confocal microscopy, as previously described (Chapter II).

Determination of bacterial burden in organs. At various days after bacterial inoculation, mice were euthanized, and spleen, liver, lung and blood were removed aseptically. Organ to mouse ratio was determined by dividing the organ weight by the weight of mouse. To determine number of bacteria, organs were placed in sterile Whirl-paks (Nasco, Ft. Atkinson, WI) with 2-5 ml of PBS and liquefied by rolling a glass pipette over the tissues. For bacteremia detection, whole blood was collected by cardiac puncture and osmotically lysed by addition of 1 ml of sterile water for 10 minutes to account for intracellular bacteria. Serial dilutions of emulsified organs and lysed blood were made in sterile PBS, plated on Chocolate II agar and incubated at 37°C and 5% CO_2 for 48 hours before counting CFUs.

Monoclonal antibody purification. Anne Savitt of the Monoclonal Antibody Core at Stony Brook University, Stony Brook, NY, developed the monoclonal antibodies. Monoclonal antibodies against *F.*

tularensis LVS were derived from spleens of infected mice after primary clearance of bacteremia. Heat inactivated *F. tularensis* LVS was used to boost the immune response. Four days after boost, spleens were removed, and splenocytes were fused to a hybridoma Sp2/O myeloma cell line. Clones were screened by ELISA and western blot. Two IgM clones, designated as IgM-9 and IgM-142, had specific activity against *F. tularensis*. Hybridomas producing IgM-9 and IgM-142 were grown in 60% SFM4Mab (HyClone, Logan, UT) and 40% DMEM supplemented with 100 μm/ml nonessential amino acids (Invitrogen, Carlsbad, CA), 100 U/ml penicillin (Invitrogen), and 100 μg/ml streptomycin (Invitrogen) at 37°C and 5% CO_2, in tissue culture flasks for 1-2 weeks before harvest of supernatant by centrifugation at 1200 rpm for 10 minutes.

Antibody from hybridoma supernatant collections was diluted in binding buffer (20 mM sodium phospate, 0.8 M ammounium sulfate, pH 7.5) in preparation for concentration in an AKTA fast protein liquid chromatography instrument (GE Healthcare Amersham Biosciences, Piscataway, NJ) with a 1 ml HiTrap IgM affinity column (GE Healthcare Amersham Biosciences). Affinity-purified IgM was then applied to a Superdex 200 16/60 size exclusion column (GE Healthcare Amersham Biosciences). Purity and reactivity of antibodies was checked by SDS-PAGE and western blotting to *F. tularensis* sonicate and LPS.

Passive immunization. B cell deficient mice were passively immunized with 50 μg of purified IgM-142 or an irrelevant IgM (Southern Biotech, Birmingham, AL) diluted in PBS, by IP injection on the day of *F. tularensis* inoculation. Mice received a daily booster of 50 μg of IgM-142 or irrelevant IgM for 5 DPI. The daily immunization treatment was chosen to compensate for the half-life of IgM (185). Bacteremia was monitored for the first five days, as each day one IgM-142 treated mouse and one irrelevant IgM treated mouse were sacrificed, and blood was collected, diluted in PBS and plated on Chocolate II agar for CFU counts. Also, 5 mice treated with IgM-142 and 5 mice treated with an irrelevant IgM were monitored for mortality for two weeks post-*F. tularensis* inoculation.

Statistics. Two-tailed *P*-values were calculated comparing normal uninfected (NI) data to infected data by an unpaired analysis of variance using the Dunnett multiple comparison test, or by using an unpaired *t* test to determine significance with InStat software (GraphPad, San Diego, CA).

C. Results

As previously discussed, mice infected with sublethal doses of *F. tularensis* LVS develop a bacteremia that peaks from 3-6 DPI, which corresponds to the height of the infection (Figure 2.1). The mean liver to mouse weight increased (Figure 2.3), while the infected spleen to mouse ratio dramatically increased by 10 DPI to five times that of uninfected ratios (Figure 3.1). The largest cellular increases in the spleen were due

to the Gr-1$^+$ CD11b$^+$ immature myeloid cells (Figure 3.4). In order to determine the cellular response to a *F. tularensis* infection, subsets of lymphocytes and myeloid cells were analyzed by flow cytometry (note, Table 3.1 was created using specific time points from these data).

Splenic B cell populations shift during acute tularemia infection. The B cell response in tularemia shows an initial decrease of FO B cell numbers until 10 DPI (Figure 4.1A). Unlike FO B cells, MZ B cells sustained expression similarly to uninfected levels for the first 5 DPI (Figure 4.1B). Markers for plasma cells increased dramatically by 10 DPI, indicating an activated adaptive response and increased antibody secretion (Figure 4.1C).

IgM production in acute tularemia is not protective. IgM and IgG production in response to *F. tularensis* infection was detected by immunoblotting and ELISA screening. An early IgM production was seen by 5 DPI and increased until 10 DPI and was directed toward the LPS as it detected the typical ladder formation of LPS (Figure 4.2A). Although MZ B cells did not increase significantly by 5 DPI, they also did not decrease in expression similar to what was shown with FO B cells. The association of MZ B cells with the early antibody response to *F. tularensis* is in accord with the documented bacteremia (78), as these cells are the main responders to this type of blood-borne infection in a T cell independent manner. This suggests that MZ B cells may be producing the initial IgM

antibody response and therefore may be important players in bacterial clearance. An IgG response is detected by 8 DPI and is specific to individual proteins rather than to LPS (Figure 4.2B). Similar increases of IgM and IgG were also seen by ELISA screening (Figure 4.3).

This early IgM response to *F. tularensis* infection was further investigated by passive immunization. Mice inoculated with sublethal doses of *F. tularensis* LVS were allowed to clear the primary infection before receiving an immune boost of heat inactivated *F. tularensis*. B cells were harvested from these mice and fused to a myeloma cell line. Two IgM monoclonals, designated IgM-9 and IgM-142, from the hybridomas had specific reactivity to *F. tularensis* LPS, but did not recognize LPS from *E. coli* (Figure 4.4). These monoclonal antibodies did not show the typical ladder pattern of LPS by western blot as seen in Figure 4.2A, indicating that IgM-9 and IgM-142 have reactivity to the non-repeating moiety of the LPS molecule. IgM monoclonal antibodies were purified by FPLC and gel filtration in preparation for passive immunization experiments. However, passive transfer of the monoclonal antibodies did not protect mice from death or produce a decreased bacteremia (Figure 4.5). These results indicated that the IgM antibodies do not have a major role in the clearance of bacteremia.

Splenic B cells are associated with the myeloid population. To monitor direct contribution of B cells, B6.129S2-Igh-6^{tm1Cgn}/J mice were

infected with *F. tularensis* LVS and compared to WT (C57BL/6) infected mice. The livers and spleens of both WT and B6.129S2-Igh-6^{tm1Cgn}/J mice increased in weight and size (Figure 4.6) similarly to previously described C3H/HeN infections. Initially, both B6.129S2-Igh-6^{tm1Cgn}/J mice and WT mice were infected with different log doses in order to establish an LD_{50} for B6.129S2-Igh-6^{tm1Cgn}/J mice (Table 4.2). However, no major differences were observed between WT and B6.129S2-Igh-6^{tm1Cgn}/J mice, which is consistent with findings from Elkins et al. (66). B6.129S2-Igh-6^{tm1Cgn}/J mice harbor increased amounts of bacteria in the spleen, liver and lungs (66). The study herein further demonstrated an increase of bacteria in the blood of B6.129S2-Igh-6^{tm1Cgn}/J mice when compared to that of WT mice (Figure 4.7). Even though the susceptibility to the bacteria was not significantly different, B6.129S2-Igh-6^{tm1Cgn}/J mice harbored higher levels of LVS, suggesting that B cells can optimize the clearance of bacteria from the host.

Spleens and livers of WT and B6.129S2-Igh-6^{tm1Cgn}/J mice were analyzed by flow cytometry for expression of specific markers of macrophage, NK cell, T cell and DC populations during an active infection. Of particular note was the difference in myeloid cells between WT and B6.129S2-Igh-6^{tm1Cgn}/J infected mice. WT mice accumulated large numbers of Gr-1^{+} CD11b^{+} cells by 10 DPI before decreasing to normal expression by 20 DPI. B6.129S2-Igh-6^{tm1Cgn}/J mice did not accumulate Gr-

1^+ $CD11b^+$ cells as rapidly as WT mice. Accumulation of Gr-1^+ $CD11b^+$ cells in B6.129S2-Igh-6^{tmlCgn}/J mice was seen by 10 DPI at levels similar to WT mice, but by 20 DPI, B6.129S2-Igh-6^{tmlCgn}/J mice sustained elevated amounts of Gr-1^+ $CD11b^+$ cells that were significantly higher than WT mice (Figure 4.8A). The livers of B6.129S2-Igh-6^{tmlCgn}/J mice also show increased levels of Gr-1^+ $CD11b^+$ cells compared to WT mice during the first week post inoculation (data not shown). These results indicate that B cells may play a role in recruitment of MDSCs, the prominent cellular phenotype in liver granulomas (Chapter II) and in the spleen and bone marrow (Chapter III) of mice infected with *F. tularensis*. Notably delayed expression of important antigen presenting cells (DCs and macrophages) was also seen in B6.129S2-Igh-6^{tmlCgn}/J mice. Accumulation of $CD11c^+$ $CD11b^+$ cells (DCs) (Figure 4.8B) and MHC II^+ $CD11b^+$ (Figure 4.8C) and F4/80^+ $CD11b^+$ cells (Figure 4.8D) (macrophage phenotypes) was significantly lower for B6.129S2-Igh-6^{tmlCgn}/J mice in the early infection (5 DPI) and never increased to significantly higher levels at later time points when compared to WT mice. These data suggest that B cells are instrumental in enhancing the infiltration of the spleen and liver with myeloid cells (MDSCs, DCs and macrophages). The delay shown (Figure 4.8) could be due to inhibition of infiltration or to an inhibition of extramedullary proliferation.

Histology of tissue sections from WT and B6.129S2-Igh-6^{tm1Cgn}/J mice confirmed an increase of pathology in the liver with an abundance of granuloma formation in mice without B lymphocytes (Figure 4.9). Hepatic lesions were similar in size and number from 5-10 DPI (Figure 4.9A-D), but by 20 DPI, few lesions were seen in WT mice, while many lesions were found in B6.129S2-Igh-6^{tm1Cgn}/J mice (Figure 4.9E and 4.9F). Histological sections from spleens of B6.129S2-Igh-6^{tm1Cgn}/J mice also revealed increased pathology and splenocyte disruption in comparison to WT mice (data not shown). Thus, a lack of B cells in mice results in a higher bacterial burden, increased amounts of MDSCs, delayed accumulation of DCs and macrophages and increased pathology in target organs.

Disruption of the splenic architecture was observed by confocal microscopy. CD4 and CD8 T cell markers were used with the B cell marker B220 (Figure 4.10). Distribution of lymphocytes at 1 DPI is comparable to that of normal mice. T lymphocyte-rich zones (blue and green) were indicative of the white pulp of the spleen while B cells (red) were found on the periphery (Figure 4.10D and 4.10E). However, by one week post-inoculation of *F. tularensis*, the spleen dramatically increased in size and the white pulp was completely disrupted compared to the normal distribution of lymphocytes (Figure 4.107F and 4.10G).

D. Discussion

Contributions of B lymphocytes to *F. tularensis* LVS infections have not been adequately addressed. An early protective immunity from B cells has been described that is independent of antibody functions (53). B cells are not required to provide an appropriate adaptive response to develop protective immunity, but they optimize the clearance of bacteria. Mice deficient in B cells exhibited increased amounts of viable bacteria in the blood and tissues, although disease severity and mortality were no different from WT mice.

Results from this study demonstrate that B cells contribute to drastic changes in the spleen. The splenic B cell subset of FO B cells showed significant decreases from normal expression during the first 9 DPI. These decreases are in line with what is known about the behavior of splenic B cells in blood-borne infections. Extracellular blood-borne relapsing fever *Borrelia* murine infections induce loss of splenic MZ and FO B cells by egress and cellular differentiation before robust expression of IgM^+ plasmablasts (134). A similar downregulation of MZ B cell markers and a dramatic increase of plasma cell marker expression have also been noted in murine malaria infections (1). This suggests that the B cell changes in the spleen in tularemia are similar to that seen in other extracellular blood-borne infections. Markers for MZ B and FO B cells underwent downregulation as these cells likely differentiated into antibody

producing plasma cells (Figure 4.1). A robust IgM response to *F. tularensis* was detected in mice beginning at 5 DPI, which was associated with MZ B cell differentiation and the clearance of the bacteremia from the blood. In general, the function of MZ B cells appears to be two-fold. One function is to provide a first-line defense against blood-borne pathogens, and the second function is to produce antibody in a T cell-independent immune response (201). MZ B cells are far more active than FO B cells in inducing a T cell response and producing cytokines, in both in vitro and in vivo studies (11). Moreover, it has been shown that MZ B cells can interact with DCs to expand and activate the adaptive T cell response (57).

To investigate the possible benefit from an initial robust IgM response, monoclonal antibodies were made. LVS-reactive IgM was purified from hybridomas and used in passive immunization experiments. These monoclonal recognized only small molecular weight proteins of the LPS and did not detect the O-chain repeating subunits. One can expect other IgMs would recognize other antigenic proteins of *F. tularensis*, which may prove to contain protective properties. However, passive immunizations with reactive monoclonal IgM-142 alone did not lead to protection from a *F. tularensis* infection. Overall, these results indicate that MZ B cells may have an early contribution during the course of the infection that corresponds to an increase of IgM production, but at this time, it is not clear if this antibody will protect against the infection.

However, IgG antibodies to LPS are protective in LVS infections (129, 159), which indicates that somatic mutation may be necessary for ultimate protection.

Comparable to C3H/HeN mice (Figure 4.1), C57BL/6 and BALB/c mice infected with *F. tularensis* LVS also showed similar expression of MZ B cells in the spleen (data not shown). Furthermore, B6.129S2-Igh-6^{tmlCgn}/J mice were infected with *F. tularensis* LVS along with age- and sex-matched C57BL/6 WT mice to clarify the importance of B cells. B cell deficient mice were only marginally compromised in controlling the primary infection (Table 4.2), but had increased numbers of bacteria recovered from their organs (Figure 4.7) and increased pathology, specifically in the number of granulomas seen in the liver (Figure 4.9). Similar to mice with tularemia, B cell deficient mice infected with the intracellular pathogen *Mycobacterium tuberculosis,* had increased bacterial burdens in the liver with increased pathology (188). Another study has documented a connection between the accumulation of Gr-1^+ $CD11b^+$ cells and B lymphocytes. Gr-1^+ $CD11b^+$ cells accumulate upon alum injection, which induces priming of the immune system by B cells and increased productivity of antibody secretion (105).

In B cell deficient mice infected with *F. tularensis*, accumulation of splenic and hepatic Gr-1^+ $CD11b^+$ cells was delayed in the acute infection when compared to WT mice. However, by 20 DPI, Gr-1^+ $CD11b^+$ cell

numbers were decreased to uninfected levels in WT mice, but B cell deficient mice sustained Gr-1$^+$ CD11b$^+$ cell expansion at significantly higher levels. These sustained increases correlated to elevated bacterial counts in the spleen and liver of B cell deficient mice. This is suggestive that MDSCs may provide a niche where bacteria can survive, but await the appropriate cytokine signaling to differentiate into mature phagocytes or DCs that will clear the infection as discussed in Chapter III. B cell deficient mice appear to delay the appropriate immune response to combat the acute infection, as seen by decreased amounts of antigen presenting cells, suggesting that without B cells antigen presentation does not function optimally, hence allowing for more bacterial colonization and increased amounts of pathology.

In summary of Chapter IV:

- There is likely differentiation of MZ B and FO B cells into plasmablasts that leads to production of specific antibody to *F. tularensis.*
- Monoclonal IgM does not protect against *F. tularensis* infection.
- B cell deficient mice carry higher bacterial burdens for longer duration in the blood, spleen, liver and lung when compared to WT mice, corresponding with increased pathology.

- B cell deficient mice have a delayed immune response to tularemia with decreased amounts of Gr-1$^+$ CD11b$^+$ cells, DCs and macrophages in the early infection.
- Increased expression of Gr-1$^+$ CD11b$^+$ cells at 20 DPI in B cell deficient mice corresponds to increased pathology of the liver and spleen.

E. Tables and Figures

Marginal Zone B cells	Follicular B cells	Plasma cells
$CD21^{+}$ $CD23^{-}$	$CD21^{+/-}$ $CD23^{+}$	$CD138^{+}$
T cell-independent IgM>IgG Rapid response	T cell-dependent IgG>IgM Memory	Differentiated Secrete antibody

Table 4.1. Splenic B cell subsets. The spleen consists of three main subsets of B cells, Follicular B cells, Marginal Zone B cells and plasma cells. Specific markers used to detect B cell populations and defining properties of each are listed.

Dose	Wild type survival	B cell deficient survival
10^1	5/5	5/5
10^2	5/5	5/5
10^3	5/5	5/5
10^4	5/5	4/5
10^5	5/5	4/5

Table 4.2. B cell deficient mice do not greatly differ from wild type (WT) mice in survival of sublethal doses of *F. tularensis*. Both WT mice and B6.129S2-Igh-6^{tm1Cgn}/J mice were inoculated with sublethal doses of *F. tularensis* and observed for mortality for one month post-inoculation.

Figure 4.1. C3H/HeN murine B cell response to *F. tularensis* infection. Single cell suspensions were made from harvested splenocytes and stained with fluorescent labeled antibodies. IgM, CD21, CD23 and CD138 were used as cell surface markers specific for B cells. (A) Follicular B cells – IgM^{+} $CD21^{+/-}$ $CD23^{+}$. (B) Marginal zone B cells – IgM^{+} $CD21^{+}$ $CD23^{-}$. (C) IgM Plasma cells – IgM^{+} $CD138^{+}$. Normal (Nl) spleens were compared to infected spleens for statistical relevance. Each bar represents mean ± SD of 3-4 mice. * $P < 0.05$, ** $P < 0.01$.

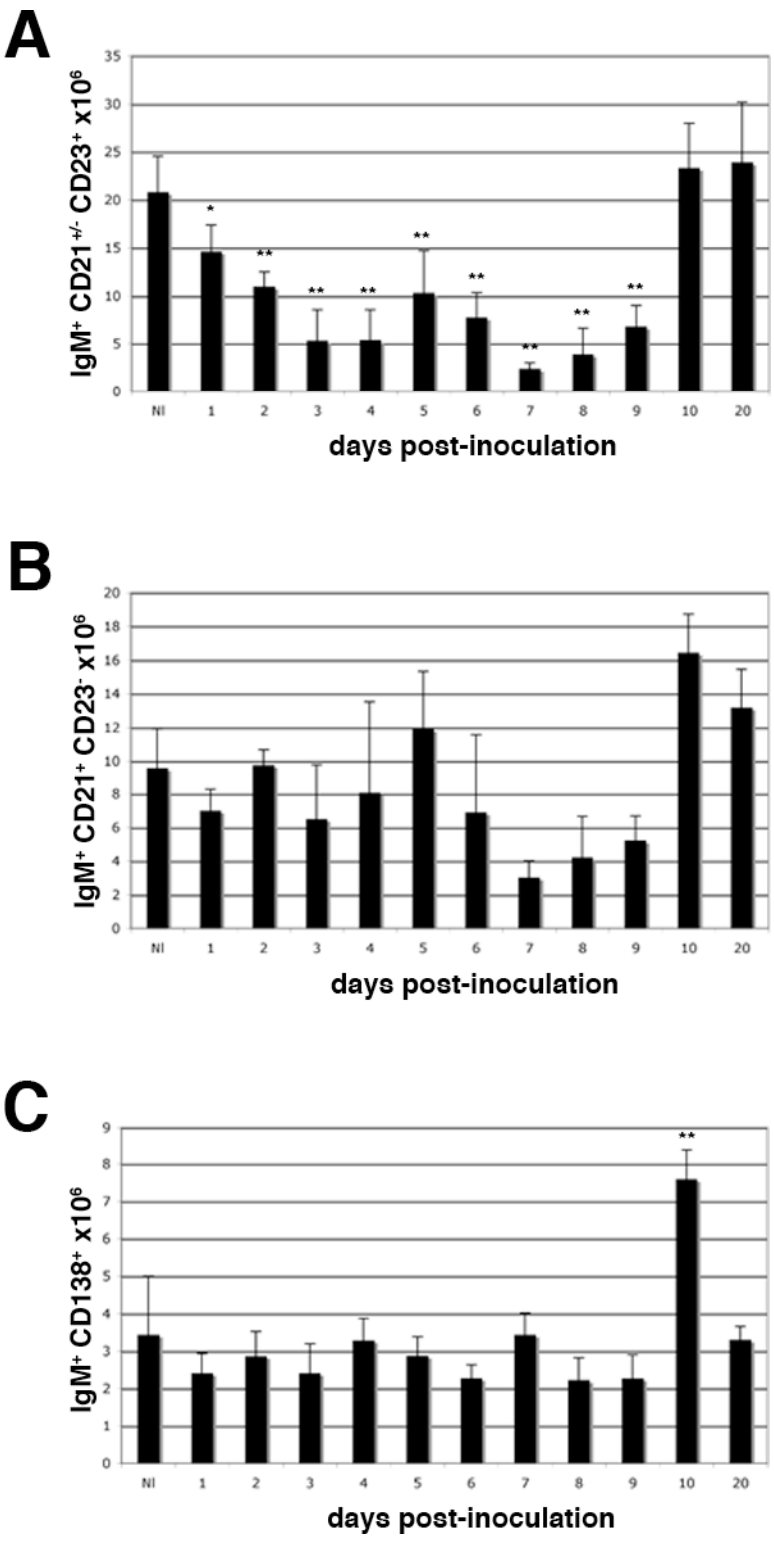
A
IgM+ CD21+/- CD23+ x10^6
35
30
25
20
15
10
5
0
*
**
**
**
**
**
**
**
**
NI 1 2 3 4 5 6 7 8 9 10 20
days post-inoculation
B
IgM+ CD21+ CD23- x10^6
20
18
16
14
12
10
8
6
4
2
0
NI 1 2 3 4 5 6 7 8 9 10 20
days post-inoculation
C
IgM+ CD138+ x10^6
9
8
7
6
5
4
3
2
1
0
**
NI 1 2 3 4 5 6 7 8 9 10 20
days post-inoculation

Figure 4.2. Development of IgM and IgG antibody response to *F. tularensis* by western blot. Serum from uninfected and infected mice was collected and analyzed for antibody production. Each strip represents an individual mouse. A normal (N) uninfected mouse is also shown. (A) IgM appears by 5 DPI and appears directed toward the LPS. (B) IgG appears by 8 DPI and is specific to individual proteins of the *F. tularensis* lysate.

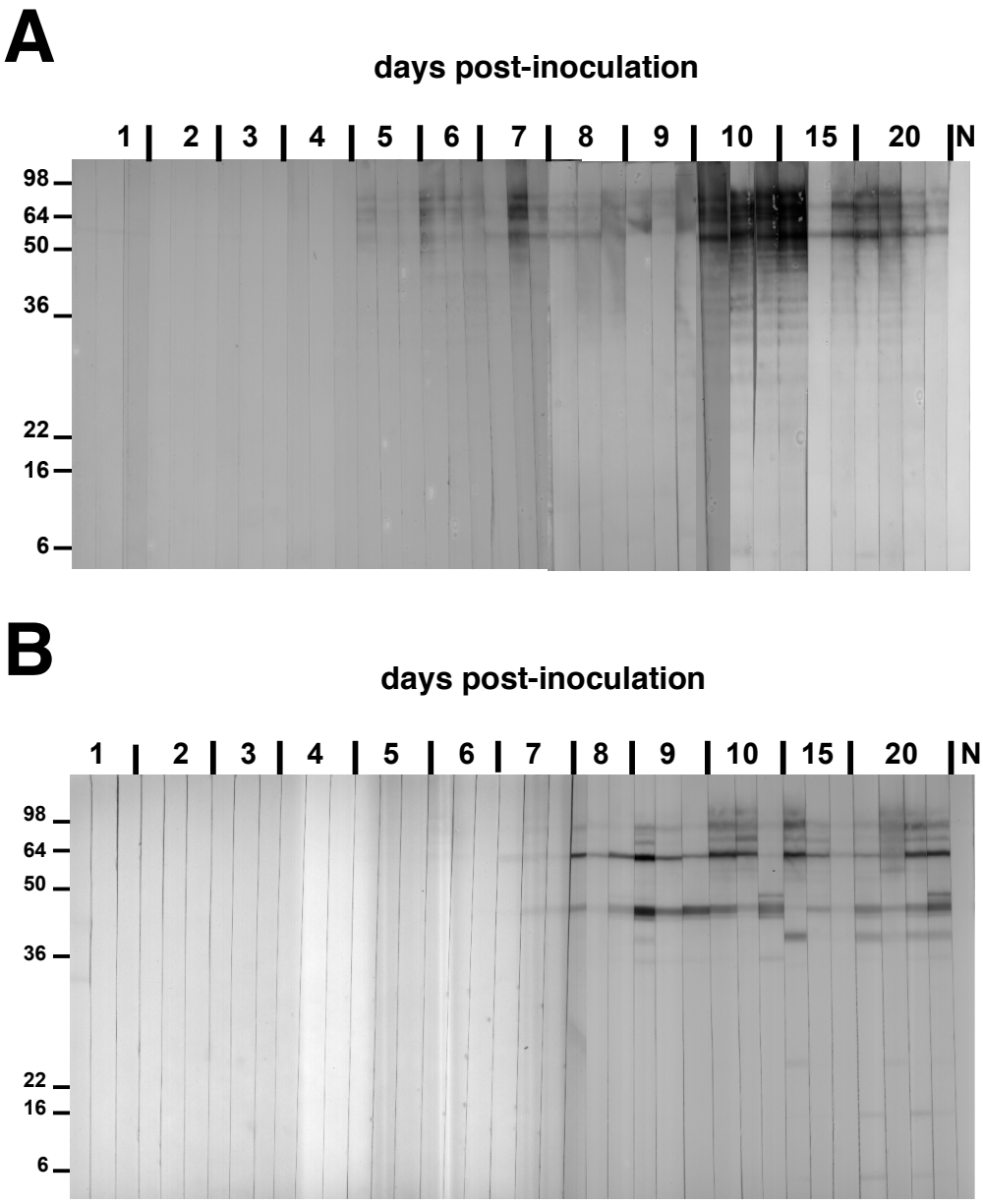
A
days post-inoculation
1
2
3
4
5
6
7
8
9
10
15
20
N
98
64
50
36
22
16
6
B
days post-inoculation
1
2
3
4
5
6
7
8
9
10
15
20
N
98
64
50
36
22
16
6

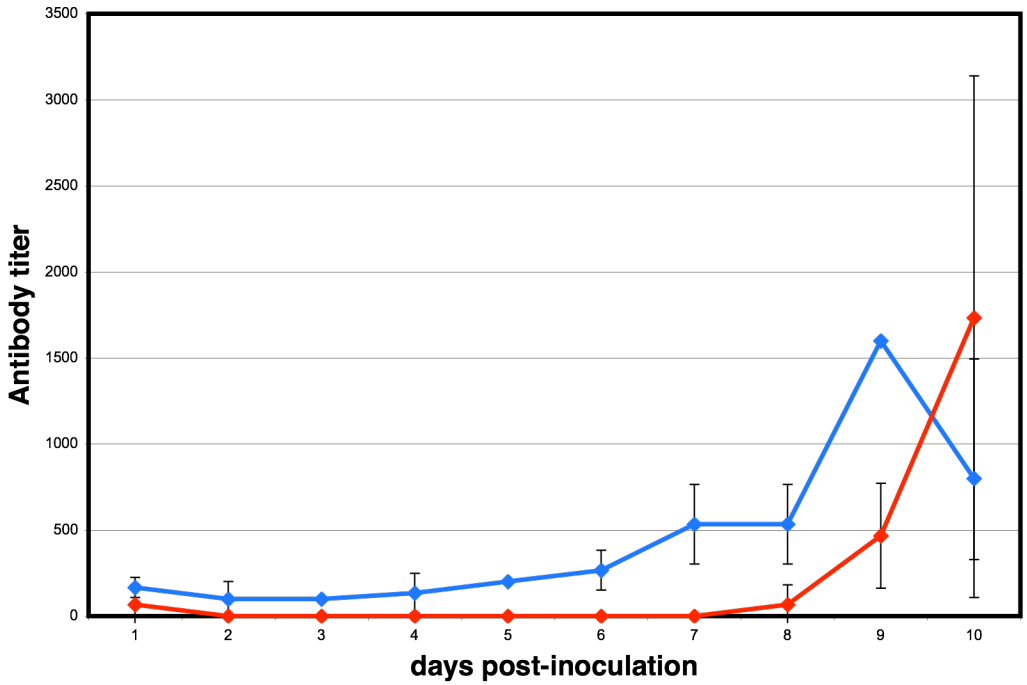

Figure 4.3: Development of IgM and IgG antibody responses to *F. tularensis* by ELISA. Antibodies to *F. tularensis* LVS lysate were detected by enzyme-linked immunosorbant assays (ELISA). Similarly to western blots, IgM (blue) was detected earlier than IgG (red) production.

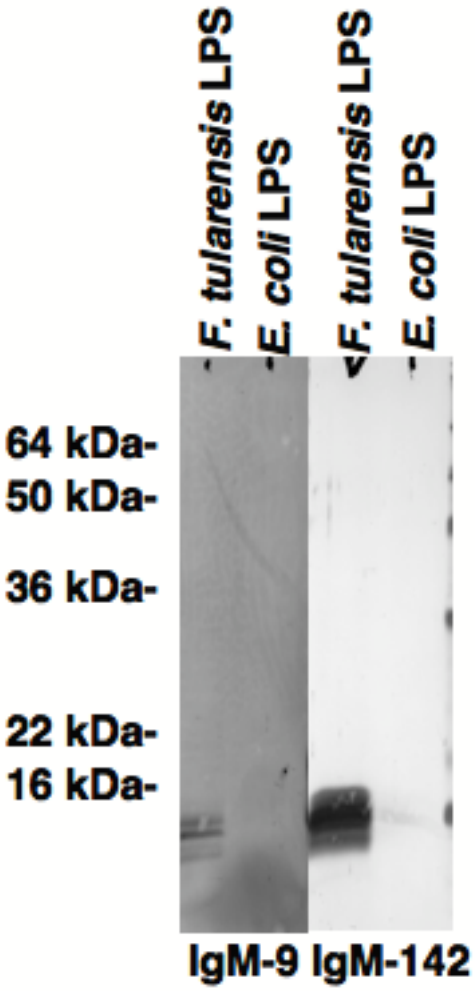

Figure 4.4. Monoclonal antibodies showing specific reactivity to *F. tularensis* LPS. Monoclonal antibodies against *F. tularensis* were derived from the spleen of an infected mouse after clearance of bacteremia. Two IgM clones had reactivity to *F. tularensis* LPS and were designated IgM-9 and IgM-142. Antibody produced by the IgM monoclonals only recognized a few proteins ~12 kDa in size of the *F. tularensis* LPS had no reactivity to *E. coli* LPS.

Figure 4.5. Passive immunization with monoclonal antibody in mice infected with *F. tularensis*. Supernatant from hybridoma cells was harvested and purified by fast protein liquid chromatography and gel filtration. At the day of infection, 50 μg of a monoclonal antibody, designated IgM-142, or an irrelevant IgM was injected intraperitoneally into mice. Mice received a daily booster of 50 μg of IgM-142 or irrelevant IgM for five days after bacterial inoculation. (A) On each of the first 5 days post-inoculation, one mouse was sacrificed that received IgM-142 (blue) and one mouse was sacrificed that received irrelevant IgM (red). Blood was collected by cardiac puncture, serially diluted, and plated on Chocolate II agar for CFU growth of *F. tularensis*. (B) Five mice from both the IgM-142 (blue) group and the irrelevant IgM (red) group were followed for two weeks post-inoculation to monitor mortality.

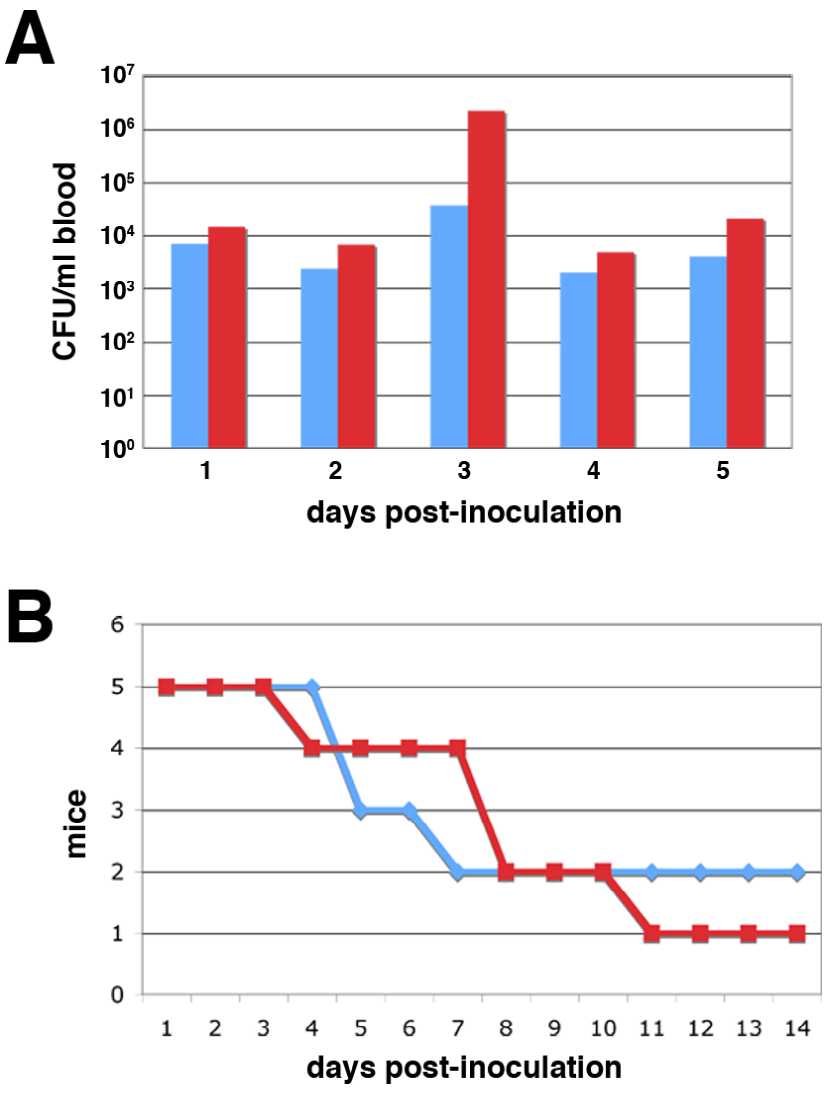
A
CFU/ml blood
10^7
10^6
10^5
10^4
10^3
10^2
10^1
10^0
1
2
3
4
5
days post-inoculation
B
mice
6
5
4
3
2
1
0
1 2 3 4 5 6 7 8 9 10 11 12 13 14
days post-inoculation

Figure 4.6. Livers and spleens of both WT and B cell deficient mice infected with *F. tularensis* greatly increase in size and weight. Blue bars – WT mice. Red bars – B cell deficient mice. (A) Mean liver index ± SD of three mice per time point during the infection. (B) Mean spleen index ± SD of three mice per time point during infection. Organ index was calculated by using the formula: (organ weight in mg/total body weight in mg) x 1000. Marked increases are due to both an increase in organ weight and a mouse weight loss during infection.

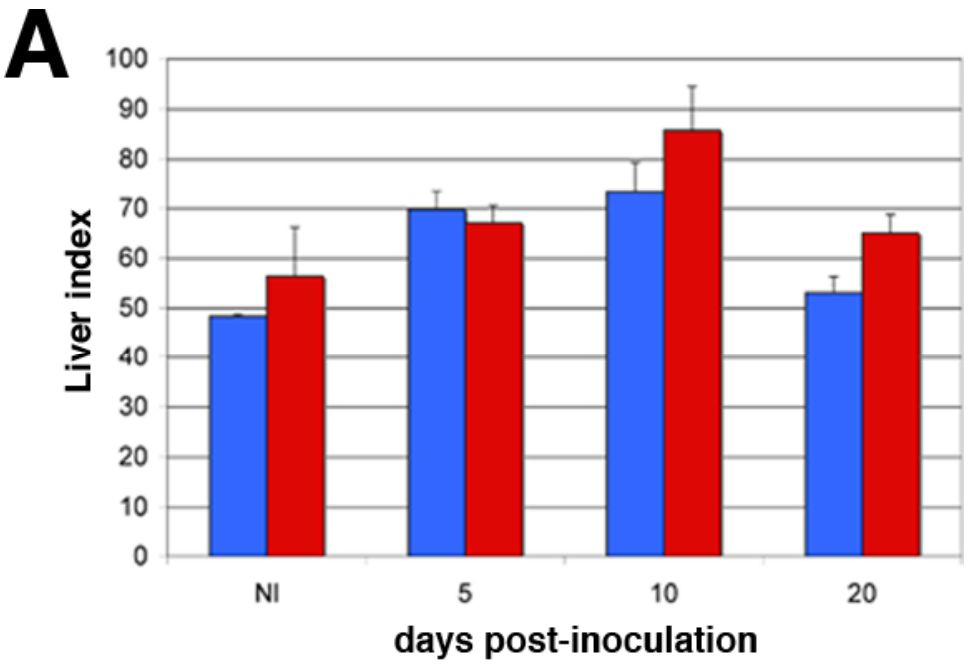
A
Liver index
100
90
80
70
60
50
40
30
20
10
0
NI
5
10
20
days post-inoculation

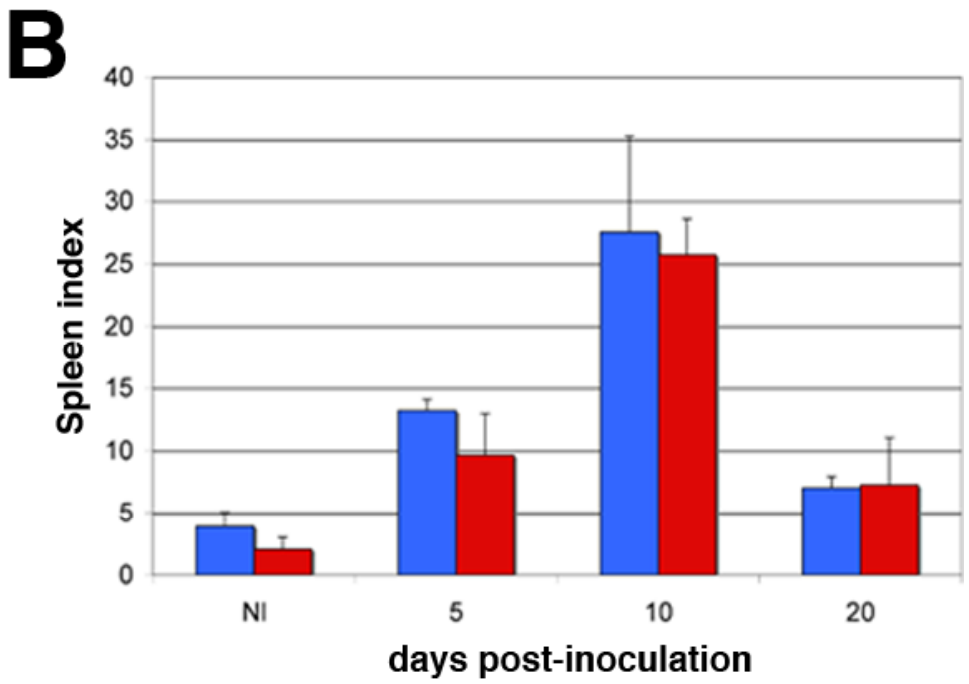
B
Spleen index
40
35
30
25
20
15
10
5
0
NI
5
10
20
days post-inoculation

Figure 4.7. Increased amount of *F. tularensis* in the blood, spleen, liver and lung of B cell deficient mice compared to WT mice. Blue lines – WT mice. Red lines – B cell deficient mice. WT and B cell deficient mice were inoculated with sublethal doses of *F. tularensis* and on various days post-inoculation organs were processed and plated on Chocolate agar for CFU assays. (A) Blood. (B) Spleen. (C) Liver. (D) Lung.

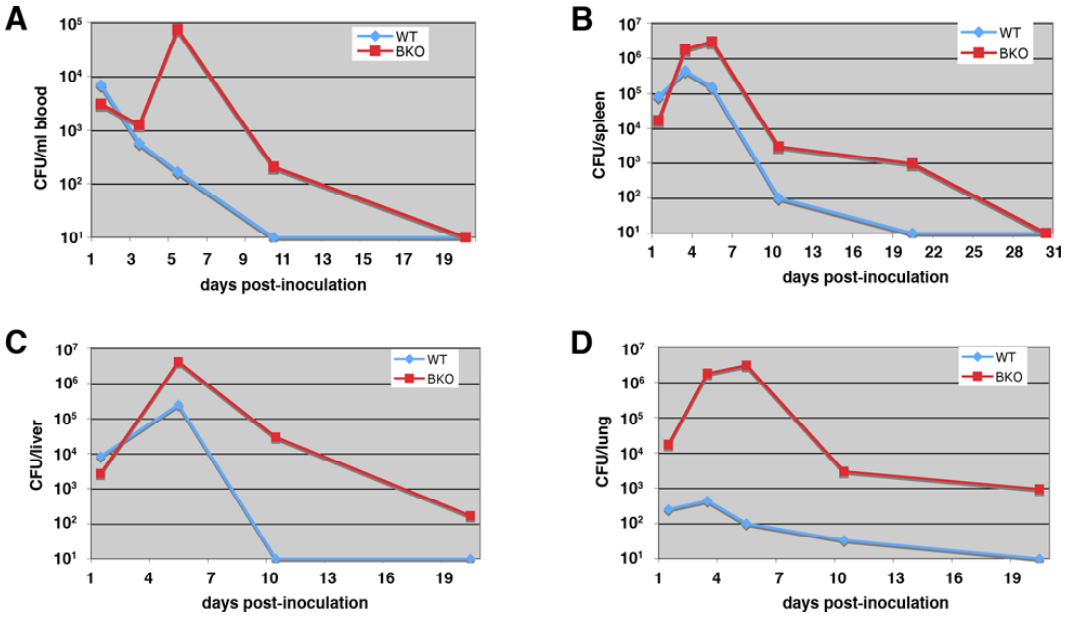
A
CFU/ml blood
WT
BKO
days post-inoculation
B
CFU/spleen
WT
BKO
days post-inoculation
C
CFU/liver
WT
BKO
days post-inoculation
D
CFU/lung
WT
BKO
days post-inoculation

Figure 4.8. Cellular differences in WT and B cell deficient mice inoculated with *F. tularensis.* Spleens were collected from both WT and B cell deficient mice during a tularemia infection. Single cell suspensions were made and cells were stained with antibodies specific for cell surface markers and analyzed by flow cytometry. Blue bars – WT mice. Red bars – B cell deficient mice. (A) Gr-1$^+$ CD11b$^+$ cells. MDSCs have prolonged expression in B cell deficient mice, which correlates to an increased amount of bacteria and heightened pathology in livers. (B) CD11c$^+$ CD11b$^+$. (C) MHC II$^+$ CD11b$^+$. (D) F4/80$^+$ CD11b$^+$. * $P < 0.05$, ** $P < 0.01$.

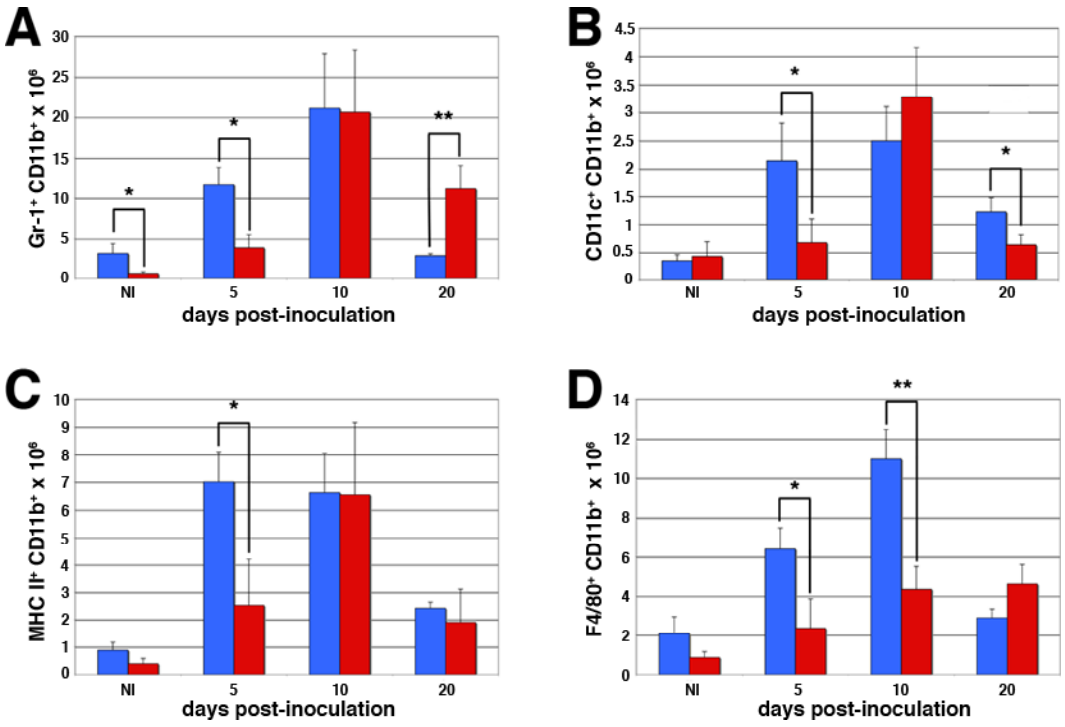
A
Gr-1+ CD11b+ x 10^6
30
25
20
15
10
5
0
*
*
**
NI
5
10
20
days post-inoculation
B
CD11c+ CD11b+ x 10^6
4.5
4
3.5
3
2.5
2
1.5
1
0.5
0
*
*
NI
5
10
20
days post-inoculation
C
MHC II+ CD11b+ x 10^6
10
9
8
7
6
5
4
3
2
1
0
*
NI
5
10
20
days post-inoculation
D
F4/80+ CD11b+ x 10^6
14
12
10
8
6
4
2
0
*
**
NI
5
10
20
days post-inoculation

Figure 4.9. Hematoxylin and eosin stained sections of livers of WT and B cell deficient mice infected with sublethal doses of *F. tularensis*. (A) WT liver and (B) B cell deficient liver infected five days earlier showing granulomatous lesions. (C) WT liver and (D) B cell deficient liver at ten days post-inoculation, showing more granulomatous lesions. Low power view of 20 DPI liver sections of (E) WT and (F) B cell deficient mice. B cell deficient mice prolong the duration of granuloma formation, and many granulomas can be seen in comparison to WT mice (arrows), which have recovered from the infection. Bars, 50 μm (A-D) and 100 μm (E-F).

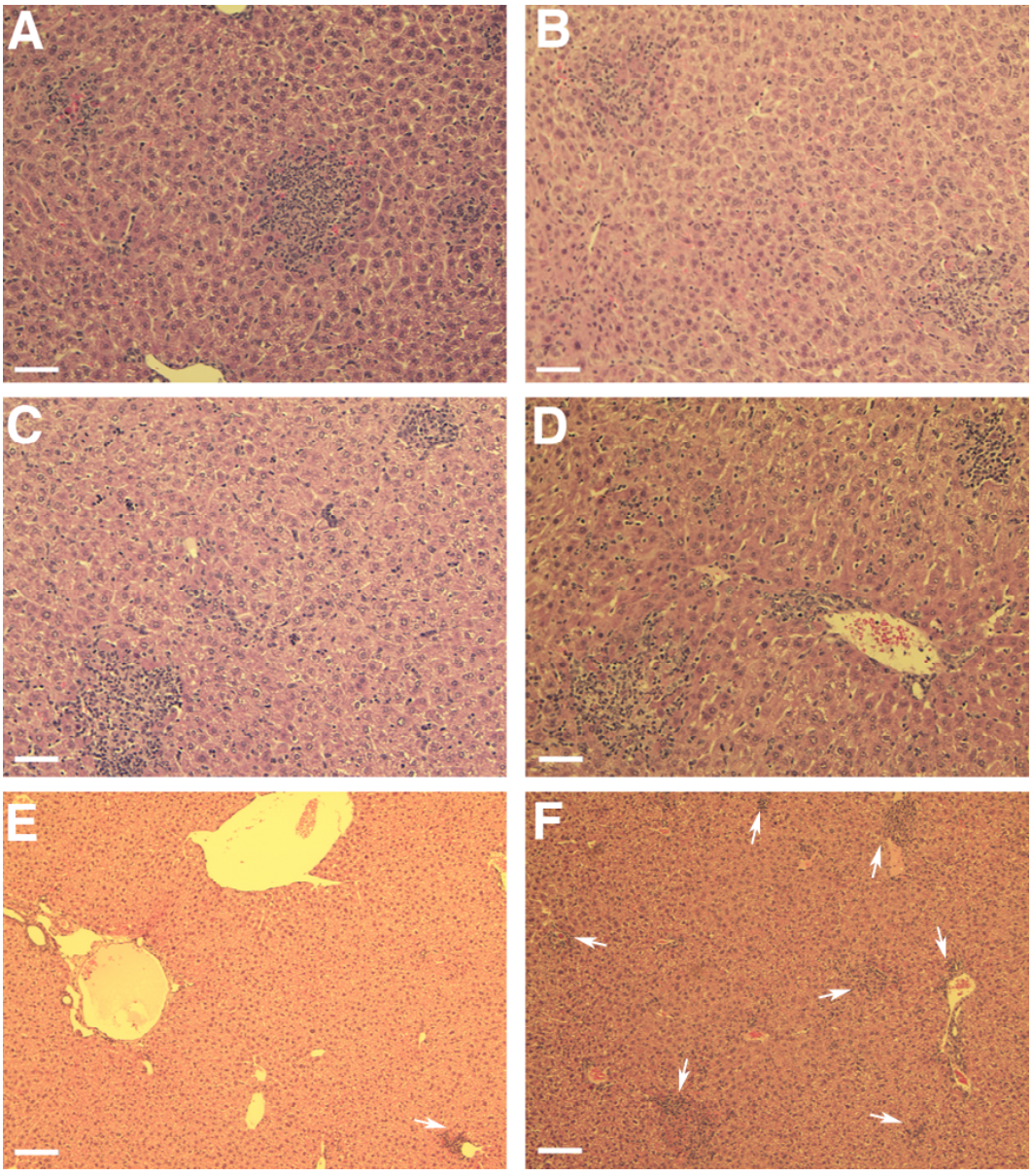
A
B
C
D
E
F

Figure 4.10. Immunofluorescence markers of B and T lymphocytes in the spleens of mice infected with sublethal doses viewed by confocal microscopy. Frozen tissue sections were stained with fluorescent antibodies directed toward B cells (B220) and T cells (CD4 and CD8). Drastic changes of splenic architecture were seen by lymphocyte distribution. Panels A-D are from day 1 post-inoculation showing individual stains of (A) $CD4^+$ cells (green), (B) $B220^+$ cells (red) and (C) $CD8^+$ cells (blue). (D) Merged image of panels A-C of spleen inoculated with *F. tularensis*. The white pulp is T cell rich (green and blue) outlined by B cells (red). Panels E-F are merged images of CD4 (green), B220 (red) and CD8 (blue). (E) Low power view of normal uninfected spleen showing similar distribution of lymphocytes as compared to D. (F) Beginning of splenic disruption by 5 DPI. (G) Total disruption of splenic architecture by 7 DPI, the white pulp and red pulp are unrecognizable. Bars, 75 μm (A-D) and 150 μm (E-G).

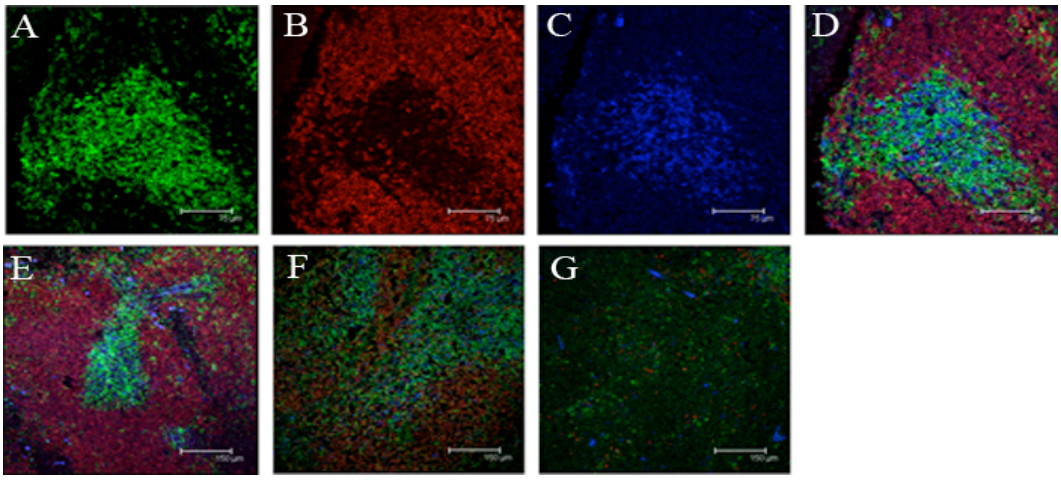
A
B
C
D
E
F
G

Chapter V

Concluding Remarks

In conclusion, this dissertation has revealed an encompassing hepatic and splenic cellular response to murine infection with *F. tularensis* LVS. A previously undescribed population of Gr-1$^+$ CD11b$^+$ cells (MDSCs) in *F. tularensis* infection dominates the cellular diversity and rapidly accumulates in the liver, spleen and bone marrow of infected mice. Gr-1$^+$ CD11b$^+$ cells have been strongly associated with immune suppression in diverse pathological conditions. In tularemia, MDSCs appear to have a dual role involving suppressive behavior and an important role in allowing the appropriate adaptive immune responses to occur. This dissertation has defined the importance of Gr-1$^+$ CD11b$^+$ cells in tularemia, and these cells may be key in promoting immunity, understanding virulence and in developing potential vaccines.

The most common pathology, and possibly the most damaging, associated with *F. tularensis* is the granulomatous lesions of the liver. Liver failure is a likely contributor to death. Tularemia-induced hepatitis has been demonstrated in this dissertation by immunohistology and enzymatic profiles. Studies of the hepatic response to tularemia provided evidence for a rapid accumulation of MDSCs in the granulomatous lesions in the acute infection. The cellular composition of these lesions had not been previously characterized in tularemia, and the lesions could be

divided into three subpopulations, MDSCs (Gr-1$^+$ CD11b$^+$), macrophages (MHC II$^+$ CD11b$^+$) and to a lesser degree DCs (CD11c$^+$ CD11b$^+$). At the same time during the infection, the hepatic population of B and T lymphocytes did not expand. We interpreted this as a possible suppression of the immune system, possibly due to the highly abundant and concurrent accumulation of MDSCs. Because of the fact that MDSCs have been associated with immune suppression, this cell phenotype was further analyzed in other organs during a *F. tularensis* infection.

Similar to the liver, the spleen and bone marrow showed a rapid and large accumulation of Gr-1$^+$ CD11b$^+$ cells during a *F. tularensis* infection. The spleen drastically changes in gross and cellular morphology during the acute course of infection. Splenomegaly occurs during infection, and the most prominent cellular population responsible for this increase expressed Gr-1 and CD11b cell markers. Further cellular characterization of MDSCs revealed an immature population, as they lack expression of mature phagocyte markers F4/80 and MHC class II. The overwhelming presence of MDSCs in the murine host is indicative of a prominent role in regulating the bacterial infection.

For our experiments, splenic Gr-1$^+$ CD11b$^+$ cells were purified by magnetic and fluorescent separation for ex vivo culture and for in vivo adoptive transfer in experimental tularemia infection. When cultured with *F. tularensis*, MDSCs ingested bacteria but did not support their growth.

Another possibility is that infection with the bacteria could result in the death of the MDSCs, and this could result in a decrease of viable cells that could become infected, thus decreasing the total numbers of bacteria. Gr-1^+ $CD11b^+$ cells were found to be a heterogeneous population of ring-shaped and mononuclear-like immature myeloid cells. In ex vivo culture MDSCs differentiated into antigen presenting cells when stimulated with GM-CSF. This differentiation of the MDSCs is suggestive of the same differentiation pathway in the bone marrow where antigen presentation markers are associated with mature cells. If this is the case in vivo, differentiation into antigen presenting cells needs to be viewed as advantageous to the immune system.

Research in this dissertation was initially based on the premise, based on data from other pathologic conditions for an immunosuppressive role of Gr-1^+ $CD11b^+$ cells in tularemia. In support of this hypothesis, data pointed to a delayed T lymphocyte response that was concurrent with accumulation of MDSCs in the livers of infected mice. However, evidence as shown above suggests a possible role in host defense or at least a mixed role in defense and immunosuppression. This behavior may be due to the heterogeneous nature of the MDSCs.

Obvious immune suppression was not detected in mice that received MDSCs intravenously before infection with *F. tularensis*. While we used only one passive immunization scheme, we followed traditional

methods from other studies. Published studies with MDSCs have transferred between 1-5 x 10^6 cells (55, 61), just as we did in our own study. Nonetheless, it is also possible that other passive immunization schemes could lead to different results. These results indicated that Gr-1^+ $CD11b^+$ cells may not suppress the host immune response, but rather may aid in controlling the infection and providing an initial barrier to bacterial dissemination.

Ring-shaped and mononuclear-like MDSCs can be separated by expression of the lymphocyte antigens Ly6C and Ly6G, and have been documented to have opposing roles in the immune response (55, 58). Separation of Gr-1^+ $CD11b^+$ cells by Ly6 expression could further define the cellular population responsible for the large accumulation of MDSCs in *F. tularensis* infected mice. Furthermore, cell sorting could be performed for both Ly6C and Ly6G subpopulations, which could be grown and monitored in primary culture for differentiation and then prepared for adoptive transfer into mice infected with *F. tularensis*. We have considered that the different functions of the MDSCs observed in this dissertation may be related to the predominance of one or the other subpopulations based on morphology and Ly6 markers.

The role of B cells in MDSC accumulation was also investigated by infecting B cell deficient mice with *F. tularensis*. B cell deficient mice harbor higher amounts of bacteria and have increased pathology in the

liver and spleen, when compared to immunocompetent mice (66). This dissertation has showed that B cells may have a role in providing initial immunity in tularemia, as B cell deficient mice have decreased numbers of DCs and macrophages in the early infection. These cell phenotypes are critical to mount appropriate host defense actions and clear the infection to allow the adaptive immune system to become activated. Moreover, there is a delayed expansion of MDSCs in B cell deficient mice that is subsequently sustained at significantly higher levels when compared to immunocompetent mice. During this time of sustained accumulation of MDSCs, there is increased pathology in both the livers and spleens of B cell deficient mice infected with *F. tularensis*. Without B cells, MDSCs appear to maintain their immature phenotype and lack the appropriate responses to become activated. This result suggests that B cells are required to facilitate MDSC differentiation into mature antigen presenting cells, which can expedite bacterial clearance from the host.

Revealing prominent cellular populations and their role in regulating murine *F. tularensis* infections has opened the door to many new questions. As cytokines are central players in cellular regulation in innate immunity, it would be interesting to profile the cytokine response in infected mice. Similar to what has been documented in this dissertation for tularemia, there is an accumulation of Gr-1$^+$ CD11b$^+$ cells in mice undergoing bacterial sepsis (55). However, these cells suppress T

lymphocyte activity with an anti-inflammatory cytokine response in bacterial sepsis. These results could be compared and contrasted to what is observed in tularemia by monitoring both proinflammatory and anti-inflammatory cytokines.

To further investigate the role B cells have in tularemia and in accumulation of MDSCs, more experimentation with B cell deficient mice could be performed. As discussed above, B cell deficient mice are able to control a primary infection with *F. tularensis*. However, upon secondary infection, B cell deficient mice are unable to control bacterial colonization and succumb to the infection (66). Gr-1$^+$ CD11b$^+$ cell accumulation, or lack of accumulation, in a secondary infection may further define an interplay between MDSCs and B cells. If MDSCs are found in abundance in these mice, this may indicate a stronger preference for immunosuppression or a lack of differentiation into mature phenotypes. If MDSCs do not accumulate in B cell deficient mice undergoing a secondary infection, this may further indicate that there is a regulatory role for B cells in the accumulation of MDSCs.

Another immunodeficient animal model, IFN-γ deficient mice, could be used to investigate the course of an *F. tularensis* infection. IFN-γ is required to clear an acute infection and has a central role in the innate immune response (67). Mice deficient in IFN-γ production lack granuloma formation in their livers when infected with *F. tularensis* (17, 38). As noted

earlier, granulomatous lesions of infected mice are filled with Gr-1$^+$ CD11b$^+$ cells. It would be interesting to monitor the accumulation and contribution of MDSCs in mice deficient in IFN-γ production. As granuloma formation is reduced in mice without IFN-γ production, one can hypothesize that MDSCs may be recruited to the liver but not arranged in a granuloma, thus potentially linking IFN-γ production to an accumulation of MDSCs and granuloma formation in the liver. Alternatively, MDSC accumulation may not occur in mice deficient in IFN-γ, which would suggest a requirement for IFN-γ secretion for expansion of MDSC population.

Another possible direction would be to directly monitor IFN-γ production in vitro from combined incubation of T cells, MDSCs and bacteria. Basal levels of IFN-γ production from T cells could be measured and then compared to IFN-γ levels with the addition of MDSCs and *F. tularensis*. These experiments could demonstrate an immunosuppressive response by detecting decreasing amounts of IFN-γ production. These assays could also be compared to IFN-γ production from T cells incubated with proinflammatory cells such as macrophages and DCs.

Ultimately, Gr-1$^+$ CD11b$^+$ cells may provide potential vaccine targets in preventing tularemia. The systemic accumulation of MDSCs in mice suggests a regulatory role that is important to control bacterial infection. If subsets of MDSCs are important for T cell suppression,

depleting antibodies against these subpopulations could be used to decrease the level of immunosuppression in the host. Alternatively, if subsets of MDSCs are found to boost host defense mechanisms, these cells, or the factors that are responsible for their induction, could be introduced to increase immunity to *F. tularensis*. Also, for development of an effective vaccine, it would be important to describe MDSC accumulation in mice infected with highly virulent Type A strains of *F. tularensis* such as Schu4. These experiments could further define Gr-1$^+$ CD11b$^+$ cell function in an infectious model and provide greater understanding of pathogenic mechanisms of one of the most virulent bacteria known to man, *Francisella tularensis*.

References

1. **Achtman, A. H., M. Khan, I. C. MacLennan, and J. Langhorne.** 2003. *Plasmodium chabaudi chabaudi* infection in mice induces strong B cell responses and striking but temporary changes in splenic cell distribution. J Immunol **171:**317-24.

2. **al-Ramadi, B. K., M. A. Brodkin, D. M. Mosser, and T. K. Eisenstein.** 1991. Immunosuppression induced by attenuated *Salmonella*. Evidence for mediation by macrophage precursors. J Immunol **146:**2737-46.

3. **Allen, W. P.** 1962. Immunity against tularemia: passive protection of mice by transfer of immune tissues. J Exp Med **115:**411-20.

4. **Almand, B., J. I. Clark, E. Nikitina, J. van Beynen, N. R. English, S. C. Knight, D. P. Carbone, and D. I. Gabrilovich.** 2001. Increased production of immature myeloid cells in cancer patients: a mechanism of immunosuppression in cancer. J Immunol **166:**678-89.

5. **Anda, P., J. Segura del Pozo, J. M. Diaz García, R. Escudero, F. J. Garcí Peña, M. C. López Velasco, R. E. Sellek, M. R. Jiménez Chillarón, L. P. Sánchez Serrano, and J. F. Martínez Navarro.** 2001. Waterborne outbreak of tularemia associated with crayfish fishing. Emerg Infect Dis **7:**575-82.

6. **Anthony, L. D., R. D. Burke, and F. E. Nano.** 1991. Growth of *Francisella* spp. in rodent macrophages. Infect Immun **59:**3291-6.

7. **Anthony, L. S., E. Ghadirian, F. P. Nestel, and P. A. Kongshavn.** 1989. The requirement for gamma interferon in resistance of mice to experimental tularemia. Microb Pathog **7:**421-8.

8. **Anthony, L. S., and P. A. Kongshavn.** 1987. Experimental murine tularemia caused by *Francisella tularensis*, live vaccine strain: a model of acquired cellular resistance. Microb Pathog **2:**3-14.

9. **Anthony, L. S., P. J. Morrissey, and F. E. Nano.** 1992. Growth inhibition of *Francisella tularensis* live vaccine strain by IFN-gamma-activated macrophages is mediated by reactive nitrogen intermediates derived from L-arginine metabolism. J Immunol **148:**1829-34.

10. **Asgharpour, A., C. Gilchrist, D. Baba, S. Hamano, and E. Houpt.** 2005. Resistance to intestinal *Entamoeba histolytica* infection is conferred by innate immunity and Gr-1+ cells. Infect Immun **73:**4522-9.

11. **Attanavanich, K., and J. F. Kearney.** 2004. Marginal zone, but not follicular B cells, are potent activators of naive CD4 T cells. J Immunol **172:**803-11.

12. **Barker, J. R., and K. E. Klose.** 2007. Molecular and genetic basis of pathogenesis in Francisella tularensis. Ann N Y Acad Sci **1105:**138-59.

13. **Barsig, J., and S. H. Kaufmann.** 1997. The mechanism of cell death in *Listeria monocytogenes*-infected murine macrophages is distinct from apoptosis. Infect Immun **65:**4075-81.

14. **Baskerville, A., and P. Hambleton.** 1976. Pathogenesis and pathology of respiratory tularaemia in the rabbit. Br J Exp Pathol **57:**339-47.

15. **Ben Nasr, A., J. Haithcoat, J. E. Masterson, J. S. Gunn, T. Eaves-Pyles, and G. R. Klimpel.** 2006. Critical role for serum opsonins and complement receptors CR3 (CD11b/CD18) and CR4 (CD11c/CD18) in phagocytosis of *Francisella tularensis* by human dendritic cells (DC): uptake of *Francisella* leads to activation of immature DC and intracellular survival of the bacteria. J Leukoc Biol **80:**774-86.

16. **Bergmann, C. C., C. Ramakrishna, M. Kornacki, and S. A. Stohlman.** 2001. Impaired T cell immunity in B cell-deficient mice following viral central nervous system infection. J Immunol **167:**1575-83.

17. **Bokhari, S. M., K. J. Kim, D. M. Pinson, J. Slusser, H. W. Yeh, and M. J. Parmely.** 2008. NK cells and gamma interferon coordinate the formation and function of hepatic granulomas in mice infected with the *Francisella tularensis* live vaccine strain. Infect Immun **76:**1379-89.

18. **Bolger, C. E., C. A. Forestal, J. K. Italo, J. L. Benach, and M. B. Furie.** 2005. The live vaccine strain of *Francisella tularensis* replicates in human and murine macrophages but induces only the human cells to secrete proinflammatory cytokines. J Leukoc Biol **77:**893-7.

19. **Bosio, C. M., H. Bielefeldt-Ohmann, and J. T. Belisle.** 2007. Active suppression of the pulmonary immune response by *Francisella tularensis* Schu4. J Immunol **178:**4538-47.

20. **Bosio, C. M., and S. W. Dow.** 2005. *Francisella tularensis* induces aberrant activation of pulmonary dendritic cells. J Immunol **175:**6792-801.

21. **Bosio, C. M., and K. L. Elkins.** 2001. Susceptibility to secondary *Francisella tularensis* live vaccine strain infection in B-cell-deficient mice is associated with neutrophilia but not with defects in specific T-cell-mediated immunity. Infect Immun **69:**194-203.

22. **Boyce, J. M.** 1975. Recent trends in the epidemiology of tularemia in the United States. J Infect Dis **131:**197-9.

23. **Breel, M., M. Van der Ende, T. Sminia, and G. Kraal.** 1988. Subpopulations of lymphoid and non-lymphoid cells in bronchus-associated lymphoid tissue (BALT) of the mouse. Immunology **63:**657-62.

24. **Brengman, M. L., D. Wang, K. B. Wilkins, N. Sakamoto, T. Arai, E. P. Ceppa, A. S. Klein, and G. B. Bulkley.** 2003. Hepatic killing but not clearance of systemically circulating bacteria is dependent upon peripheral leukocytes via Mac-1 (CD11b/CD18). Shock **19:**263-7.

25. **Brissette-Storkus, C. S., S. M. Reynolds, A. J. Lepisto, and R. L. Hendricks.** 2002. Identification of a novel macrophage population in the normal mouse corneal stroma. Invest Ophthalmol Vis Sci **43:**2264-71.

26. **Bronte, V., E. Apolloni, A. Cabrelle, R. Ronca, P. Serafini, P. Zamboni, N. P. Restifo, and P. Zanovello.** 2000. Identification of a CD11b(+)/Gr-1(+)/CD31(+) myeloid progenitor capable of activating or suppressing CD8(+) T cells. Blood **96:**3838-46.

27. **Bronte, V., P. Serafini, E. Apolloni, and P. Zanovello.** 2001. Tumor-induced immune dysfunctions caused by myeloid suppressor cells. J Immunother **24:**431-46.

28. **Bronte, V., M. Wang, W. W. Overwijk, D. R. Surman, F. Pericle, S. A. Rosenberg, and N. P. Restifo.** 1998. Apoptotic death of CD8+ T lymphocytes after immunization: induction of a suppressive population of Mac-1+/Gr-1+ cells. J Immunol **161:**5313-20.

29. **Bronte, V., and P. Zanovello.** 2005. Regulation of immune responses by L-arginine metabolism. Nat Rev Immunol **5:**641-54.

30. **Buddingh, G. J., and F. C. J. Womack.** 1941. Observations on the infection of chick embryos with *Bacterium tularense, Brucella*, and *Pasteurella pestis*. J Exp Med **74:**213-222.

31. **Bunt, S. K., L. Yang, P. Sinha, V. K. Clements, J. Leips, and S. Ostrand-Rosenberg.** 2007. Reduced inflammation in the tumor microenvironment delays the accumulation of myeloid-derived suppressor cells and limits tumor progression. Cancer Res **67:**10019-26.

32. **Casadevall, A.** 2002. Passive antibody administration (immediate immunity) as a specific defense against biological weapons. Emerg Infect Dis **8:**833-41.

33. **Castillo-Mendez, S. I., C. A. Zago, L. R. Sardinha, A. P. Freitas do Rosario, J. M. Alvarez, and M. R. D'Imperio Lima.** 2007. Characterization of the spleen B-cell compartment at the early and

late blood-stage *Plasmodium chabaudi* malaria. Scand J Immunol **66:**309-19.

34. **CDC.** 2002. Tularemia--United States, 1990-2000. MMWR Morb Mortal Wkly Rep **51:**181-4.

35. **Chakraborty, S., M. Monfett, T. M. Maier, J. L. Benach, D. W. Frank, and D. G. Thanassi.** 2008. Type IV pili in *Francisella tularensis*: roles of pilF and pilT in fiber assembly, host cell adherence, and virulence. Infect Immun **76:**2852-61.

36. **Chen, W., R. Kuolee, J. W. Austin, H. Shen, Y. Che, and J. W. Conlan.** 2005. Low dose aerosol infection of mice with virulent type A *Francisella tularensis* induces severe thymus atrophy and CD4+CD8+ thymocyte depletion. Microb Pathog **39:**189-96.

37. **Chen, W., R. Kuolee, H. Shen, M. Busa, and J. W. Conlan.** 2005. Toll-like receptor 4 (TLR4) plays a relatively minor role in murine defense against primary intradermal infection with *Francisella tularensis* LVS. Immunol Lett **97:**151-4.

38. **Chen, W., R. KuoLee, H. Shen, and J. W. Conlan.** 2004. Susceptibility of immunodeficient mice to aerosol and systemic infection with virulent strains of *Francisella tularensis*. Microb Pathog **36:**311-8.

39. **Chen, W., H. Shen, A. Webb, R. KuoLee, and J. W. Conlan.** 2003. Tularemia in BALB/c and C57BL/6 mice vaccinated with *Francisella tularensis* LVS and challenged intradermally, or by aerosol with virulent isolates of the pathogen: protection varies depending on pathogen virulence, route of exposure, and host genetic background. Vaccine **21:**3690-700.

40. **Cole, L. E., K. L. Elkins, S. M. Michalek, N. Qureshi, L. J. Eaton, P. Rallabhandi, N. Cuesta, and S. N. Vogel.** 2006. Immunologic consequences of *Francisella tularensis* live vaccine strain infection: role of the innate immune response in infection and immunity. J Immunol **176:**6888-99.

41. **Collazo, C. M., A. Sher, A. I. Meierovics, and K. L. Elkins.** 2006. Myeloid differentiation factor-88 (MyD88) is essential for control of primary in vivo *Francisella tularensis* LVS infection, but not for control of intra-macrophage bacterial replication. Microbes Infect **8:**779-90.

42. **Conlan, J. W., W. Chen, H. Shen, A. Webb, and R. KuoLee.** 2003. Experimental tularemia in mice challenged by aerosol or intradermally with virulent strains of *Francisella tularensis*: bacteriologic and histopathologic studies. Microb Pathog **34:**239-48.

43. **Conlan, J. W., R. KuoLee, H. Shen, and A. Webb.** 2002. Different host defences are required to protect mice from primary systemic vs pulmonary infection with the facultative intracellular bacterial pathogen, *Francisella tularensis* LVS. Microb Pathog **32:**127-34.

44. **Conlan, J. W., and R. J. North.** 1992. Early pathogenesis of infection in the liver with the facultative intracellular bacteria Listeria monocytogenes, Francisella tularensis, and Salmonella typhimurium involves lysis of infected hepatocytes by leukocytes. Infect Immun **60:**5164-71.

45. **Conlan, J. W., H. Shen, R. Kuolee, X. Zhao, and W. Chen.** 2005. Aerosol-, but not intradermal-immunization with the live vaccine strain of *Francisella tularensis* protects mice against subsequent aerosol challenge with a highly virulent type A strain of the pathogen by an alphabeta T cell- and interferon gamma- dependent mechanism. Vaccine **23:**2477-85.

46. **Conlan, J. W., H. Shen, A. Webb, and M. B. Perry.** 2002. Mice vaccinated with the O-antigen of *Francisella tularensis* LVS lipopolysaccharide conjugated to bovine serum albumin develop varying degrees of protective immunity against systemic or aerosol challenge with virulent type A and type B strains of the pathogen. Vaccine **20:**3465-71.

47. **Conlan, J. W., A. Sjostedt, and R. J. North.** 1994. CD4+ and CD8+ T-cell-dependent and -independent host defense mechanisms can operate to control and resolve primary and

secondary *Francisella tularensis* LVS infection in mice. Infect Immun **62:**5603-7.

48. **Conlan, J. W., E. Vinogradov, M. A. Monteiro, and M. B. Perry.** 2003. Mice intradermally-inoculated with the intact lipopolysaccharide, but not the lipid A or O-chain, from *Francisella tularensis* LVS rapidly acquire varying degrees of enhanced resistance against systemic or aerogenic challenge with virulent strains of the pathogen. Microb Pathog **34:**39-45.

49. **Councilman, W. T., and R.P. Strong.** 1921. Plague-like infections in rodents. Trans. Assoc. Am. Phys **5**.

50. **Cowley, S. C., and K. L. Elkins.** 2003. Multiple T cell subsets control *Francisella tularensis* LVS intracellular growth without stimulation through macrophage interferon gamma receptors. J Exp Med **198:**379-89.

51. **Cowley, S. C., E. Hamilton, J. A. Frelinger, J. Su, J. Forman, and K. L. Elkins.** 2005. CD4-CD8- T cells control intracellular bacterial infections both in vitro and in vivo. J Exp Med **202:**309-19.

52. **Cowley, S. C., J. D. Sedgwick, and K. L. Elkins.** 2007. Differential requirements by CD4+ and CD8+ T cells for soluble and membrane TNF in control of *Francisella tularensis* live vaccine strain intramacrophage growth. J Immunol **179:**7709-19.

53. **Culkin, S. J., T. Rhinehart-Jones, and K. L. Elkins.** 1997. A novel role for B cells in early protective immunity to an intracellular pathogen, *Francisella tularensis* strain LVS. J Immunol **158:**3277-84.

54. **Daley, J. M., A. A. Thomay, M. D. Connolly, J. S. Reichner, and J. E. Albina.** 2008. Use of Ly6G-specific monoclonal antibody to deplete neutrophils in mice. J Leukoc Biol **83:**64-70.

55. **Delano, M. J., P. O. Scumpia, J. S. Weinstein, D. Coco, S. Nagaraj, K. M. Kelly-Scumpia, K. A. O'Malley, J. L. Wynn, S. Antonenko, S. Z. Al-Quran, R. Swan, C. S. Chung, M. A.**

Atkinson, R. Ramphal, D. I. Gabrilovich, W. H. Reeves, A. Ayala, J. Phillips, D. Laface, P. G. Heyworth, M. Clare-Salzler, and L. L. Moldawer. 2007. MyD88-dependent expansion of an immature GR-1(+)CD11b(+) population induces T cell suppression and Th2 polarization in sepsis. J Exp Med **204:**1463-74.

56. **Dennis, D. T., T. V. Inglesby, D. A. Henderson, J. G. Bartlett, M. S. Ascher, E. Eitzen, A. D. Fine, A. M. Friedlander, J. Hauer, M. Layton, S. R. Lillibridge, J. E. McDade, M. T. Osterholm, T. O'Toole, G. Parker, T. M. Perl, P. K. Russell, and K. Tonat.** 2001. Tularemia as a biological weapon: medical and public health management. JAMA **285:**2763-73.

57. **Diaz-de-Durana, Y., G. T. Mantchev, R. J. Bram, and A. Franco.** 2006. TACI-BLyS signaling via B-cell-dendritic cell cooperation is required for naive CD8+ T-cell priming in vivo. Blood **107:**594-601.

58. **Dietlin, T. A., F. M. Hofman, B. T. Lund, W. Gilmore, S. A. Stohlman, and R. C. van der Veen.** 2007. Mycobacteria-induced Gr-1+ subsets from distinct myeloid lineages have opposite effects on T cell expansion. J Leukoc Biol **81:**1205-12.

59. **Dreisbach, V. C., S. Cowley, and K. L. Elkins.** 2000. Purified lipopolysaccharide from *Francisella tularensis* live vaccine strain (LVS) induces protective immunity against LVS infection that requires B cells and gamma interferon. Infect Immun **68:**1988-96.

60. **Duckett, N. S., S. Olmos, D. M. Durrant, and D. W. Metzger.** 2005. Intranasal interleukin-12 treatment for protection against respiratory infection with the *Francisella tularensis* live vaccine strain. Infect Immun **73:**2306-11.

61. **Dunay, I. R., R. A. Damatta, B. Fux, R. Presti, S. Greco, M. Colonna, and L. D. Sibley.** 2008. Gr1(+) Inflammatory Monocytes Are Required for Mucosal Resistance to the Pathogen *Toxoplasma gondii*. Immunity **29:**306-17.

62. **Edelson, B. T., P. Cossart, and E. R. Unanue.** 1999. Cutting edge: paradigm revisited: antibody provides resistance to *Listeria* infection. J Immunol **163:**4087-90.

63. **Egan, C. E., W. Sukhumavasi, A. L. Bierly, and E. Y. Denkers.** 2008. Understanding the multiple functions of Gr-1(+) cell subpopulations during microbial infection. Immunol Res **40:**35-48.

64. **Eigelsbach, H. T., and C. M. Downs.** 1961. Prophylactic effectiveness of live and killed tularemia vaccines. I. Production of vaccine and evaluation in the white mouse and guinea pig. J Immunol **87:**415-25.

65. **El-Zammar, O. A., and A. L. Katzenstein.** 2007. Pathological diagnosis of granulomatous lung disease: a review. Histopathology **50:**289-310.

66. **Elkins, K. L., C. M. Bosio, and T. R. Rhinehart-Jones.** 1999. Importance of B cells, but not specific antibodies, in primary and secondary protective immunity to the intracellular bacterium *Francisella tularensis* live vaccine strain. Infect Immun **67:**6002-7.

67. **Elkins, K. L., S. C. Cowley, and C. M. Bosio.** 2003. Innate and adaptive immune responses to an intracellular bacterium, *Francisella tularensis* live vaccine strain. Microbes Infect **5:**135-42.

68. **Elkins, K. L., S. C. Cowley, and C. M. Bosio.** 2007. Innate and adaptive immunity to *Francisella*. Ann N Y Acad Sci **1105:**284-324.

69. **Elkins, K. L., D. A. Leiby, R. K. Winegar, C. A. Nacy, and A. H. Fortier.** 1992. Rapid generation of specific protective immunity to *Francisella tularensis*. Infect Immun **60:**4571-7.

70. **Elkins, K. L., T. Rhinehart-Jones, C. A. Nacy, R. K. Winegar, and A. H. Fortier.** 1993. T-cell-independent resistance to infection and generation of immunity to *Francisella tularensis*. Infect Immun **61:**823-9.

71. **Elkins, K. L., T. R. Rhinehart-Jones, S. J. Culkin, D. Yee, and R. K. Winegar.** 1996. Minimal requirements for murine resistance to infection with *Francisella tularensis* LVS. Infect Immun **64:**3288-93.

72. **Ellis, J., P. C. Oyston, M. Green, and R. W. Titball.** 2002. Tularemia. Clin Microbiol Rev **15:**631-46.

73. **Evans, M. E., D. W. Gregory, W. Schaffner, and Z. A. McGee.** 1985. Tularemia: a 30-year experience with 88 cases. Medicine (Baltimore) **64:**251-69.

74. **Ezekowitz, R. A., J. Austyn, P. D. Stahl, and S. Gordon.** 1981. Surface properties of bacillus Calmette-Guerin-activated mouse macrophages. Reduced expression of mannose-specific endocytosis, Fc receptors, and antigen F4/80 accompanies induction of Ia. J Exp Med **154:**60-76.

75. **Ezernitchi, A. V., I. Vaknin, L. Cohen-Daniel, O. Levy, E. Manaster, A. Halabi, E. Pikarsky, L. Shapira, and M. Baniyash.** 2006. TCR zeta down-regulation under chronic inflammation is mediated by myeloid suppressor cells differentially distributed between various lymphatic organs. J Immunol **177:**4763-72.

76. **Fleming, T. J., M. L. Fleming, and T. R. Malek.** 1993. Selective expression of Ly-6G on myeloid lineage cells in mouse bone marrow. RB6-8C5 mAb to granulocyte-differentiation antigen (Gr-1) detects members of the Ly-6 family. J Immunol **151:**2399-408.

77. **Forestal, C. A., J. L. Benach, C. Carbonara, J. K. Italo, T. J. Lisinski, and M. B. Furie.** 2003. *Francisella tularensis* selectively induces proinflammatory changes in endothelial cells. J Immunol **171:**2563-70.

78. **Forestal, C. A., M. Malik, S. V. Catlett, A. G. Savitt, J. L. Benach, T. J. Sellati, and M. B. Furie.** 2007. *Francisella tularensis* has a significant extracellular phase in infected mice. J Infect Dis **196:**134-7.

79. **Fortier, A. H., S. J. Green, T. Polsinelli, T. R. Jones, R. M. Crawford, D. A. Leiby, K. L. Elkins, M. S. Meltzer, and C. A. Nacy.** 1994. Life and death of an intracellular pathogen: *Francisella tularensis* and the macrophage. Immunol Ser **60:**349-61.

80. **Fortier, A. H., D. A. Leiby, R. B. Narayanan, E. Asafoadjei, R. M. Crawford, C. A. Nacy, and M. S. Meltzer.** 1995. Growth of *Francisella tularensis* LVS in macrophages: the acidic intracellular compartment provides essential iron required for growth. Infect Immun **63:**1478-83.

81. **Fortier, A. H., T. Polsinelli, S. J. Green, and C. A. Nacy.** 1992. Activation of macrophages for destruction of *Francisella tularensis*: identification of cytokines, effector cells, and effector molecules. Infect Immun **60:**817-25.

82. **Fortier, A. H., M. V. Slayter, R. Ziemba, M. S. Meltzer, and C. A. Nacy.** 1991. Live vaccine strain of *Francisella tularensis*: infection and immunity in mice. Infect Immun **59:**2922-8.

83. **Fricke, I., N. Mirza, J. Dupont, C. Lockhart, A. Jackson, J. H. Lee, J. A. Sosman, and D. I. Gabrilovich.** 2007. Vascular endothelial growth factor-trap overcomes defects in dendritic cell differentiation but does not improve antigen-specific immune responses. Clin Cancer Res **13:**4840-8.

84. **Fuller, C. L., J. L. Flynn, and T. A. Reinhart.** 2003. In situ study of abundant expression of proinflammatory chemokines and cytokines in pulmonary granulomas that develop in cynomolgus macaques experimentally infected with *Mycobacterium tuberculosis*. Infect Immun **71:**7023-34.

85. **Fulop, M., P. Mastroeni, M. Green, and R. W. Titball.** 2001. Role of antibody to lipopolysaccharide in protection against low- and high-virulence strains of *Francisella tularensis*. Vaccine **19:**4465-72.

86. **Gabrilovich, D. I., M. P. Velders, E. M. Sotomayor, and W. M. Kast.** 2001. Mechanism of immune dysfunction in cancer mediated by immature Gr-1+ myeloid cells. J Immunol **166:**5398-406.

87. **Geissmann, F., C. Auffray, R. Palframan, C. Wirrig, A. Ciocca, L. Campisi, E. Narni-Mancinelli, and G. Lauvau.** 2008. Blood monocytes: distinct subsets, how they relate to dendritic cells, and

their possible roles in the regulation of T-cell responses. Immunol Cell Biol **86:**398-408.

88. **Geissmann, F., S. Jung, and D. R. Littman.** 2003. Blood monocytes consist of two principal subsets with distinct migratory properties. Immunity **19:**71-82.

89. **Gil, H., J. L. Benach, and D. G. Thanassi.** 2004. Presence of pili on the surface of *Francisella tularensis*. Infect Immun **72:**3042-7.

90. **Gil, H., G. J. Platz, C. A. Forestal, M. Monfett, C. S. Bakshi, T. J. Sellati, M. B. Furie, J. L. Benach, and D. G. Thanassi.** 2006. Deletion of TolC orthologs in *Francisella tularensis* identifies roles in multidrug resistance and virulence. Proc Natl Acad Sci U S A **103:**12897-902.

91. **Goethert, H. K., I. Shani, and S. R. Telford, 3rd.** 2004. Genotypic diversity of *Francisella tularensis* infecting Dermacentor variabilis ticks on Martha's Vineyard, Massachusetts. J Clin Microbiol **42:**4968-73.

92. **Goldsby, R. A., T. J. Kindt, B. A. Osborne, and J. Kuby.** 2003. Immunolgy, Fifth ed, vol. 1. W. H. Freeman and Company, New York City.

93. **Golovliov, I., G. Sandstrom, M. Ericsson, A. Sjostedt, and A. Tarnvik.** 1995. Cytokine expression in the liver during the early phase of murine tularemia. Infect Immun **63:**534-8.

94. **Goni, O., P. Alcaide, and M. Fresno.** 2002. Immunosuppression during acute *Trypanosoma cruzi* infection: involvement of Ly6G (Gr1(+))CD11b(+)immature myeloid suppressor cells. Int Immunol **14:**1125-34.

95. **Goni, O., P. Alcaide, and M. Fresno.** 2002. Immunosuppression during acute *Trypanosoma cruzi* infection: involvement of Ly6G (Gr1(+))CD11b(+) immature myeloid suppressor cells. Int Immunol **14:**1125-34.

96. **Griffin, K. F., P. C. Oyston, and R. W. Titball.** 2007. *Francisella tularensis* vaccines. FEMS Immunol Med Microbiol **49:**315-23.

97. **Hall, J. D., R. R. Craven, J. R. Fuller, R. J. Pickles, and T. H. Kawula.** 2007. *Francisella tularensis* replicates within alveolar type II epithelial cells in vitro and in vivo following inhalation. Infect Immun **75:**1034-9.

98. **Heninger, E., L. H. Hogan, J. Karman, S. Macvilay, B. Hill, J. P. Woods, and M. Sandor.** 2006. Characterization of the *Histoplasma capsulatum*-induced granuloma. J Immunol **177:**3303-13.

99. **Hong, K. J., J. R. Wickstrum, H. W. Yeh, and M. J. Parmely.** 2007. Toll-like receptor 2 controls the gamma interferon response to *Francisella tularensis* by mouse liver lymphocytes. Infect Immun **75:**5338-45.

100. **Hrstka, R., J. Stulík, and B. Vojtěšek.** 2005. The role of MAPK signal pathways during *Francisella tularensis* LVS infection-induced apoptosis in murine macrophages. Microbes Infect **7:**619-25.

101. **Hume, D. A., I. L. Ross, S. R. Himes, R. T. Sasmono, C. A. Wells, and T. Ravasi.** 2002. The mononuclear phagocyte system revisited. J Leukoc Biol **72:**621-7.

102. **Inaba, K., M. Inaba, M. Deguchi, K. Hagi, R. Yasumizu, S. Ikehara, S. Muramatsu, and R. M. Steinman.** 1993. Granulocytes, macrophages, and dendritic cells arise from a common major histocompatibility complex class II-negative progenitor in mouse bone marrow. Proc Natl Acad Sci U S A **90:**3038-42.

103. **Ishiguro, T., M. Naito, T. Yamamoto, G. Hasegawa, F. Gejyo, M. Mitsuyama, H. Suzuki, and T. Kodama.** 2001. Role of macrophage scavenger receptors in response to *Listeria monocytogenes* infection in mice. Am J Pathol **158:**179-88.

104. **Jakubzick, C., H. Wen, A. Matsukawa, M. Keller, S. L. Kunkel, and C. M. Hogaboam.** 2004. Role of CCR4 ligands, CCL17 and

CCL22, during *Schistosoma mansoni* egg-induced pulmonary granuloma formation in mice. Am J Pathol **165:**1211-21.

105. **Jordan, M. B., D. M. Mills, J. Kappler, P. Marrack, and J. C. Cambier.** 2004. Promotion of B cell immune responses via an alum-induced myeloid cell population. Science **304:**1808-10.

106. **Katz, J., P. Zhang, M. Martin, S. N. Vogel, and S. M. Michalek.** 2006. Toll-like receptor 2 is required for inflammatory responses to *Francisella tularensis* LVS. Infect Immun **74:**2809-16.

107. **Kawai, T., and S. Akira.** 2006. TLR signaling. Cell Death Differ **13:**816-25.

108. **Kitamura, D., J. Roes, R. Kuhn, and K. Rajewsky.** 1991. A B cell-deficient mouse by targeted disruption of the membrane exon of the immunoglobulin mu chain gene. Nature **350:**423-6.

109. **Kobayashi, M., T. Yoshida, D. Takeuchi, V. C. Jones, K. Shigematsu, D. N. Herndon, and F. Suzuki.** 2008. Gr-1(+)CD11b(+) cells as an accelerator of sepsis stemming from *Pseudomonas aeruginosa* wound infection in thermally injured mice. J Leukoc Biol **83:**1354-62.

110. **Krocova, Z., A. Hartlova, D. Souckova, L. Zivna, M. Kroca, E. Rudolf, A. Macela, and J. Stulik.** 2008. Interaction of B cells with intracellular pathogen *Francisella tularensis*. Microb Pathog **45:**79-85.

111. **Kusmartsev, S., and D. I. Gabrilovich.** 2002. Immature myeloid cells and cancer-associated immune suppression. Cancer Immunol Immunother **51:**293-8.

112. **Kusmartsev, S., and D. I. Gabrilovich.** 2003. Inhibition of myeloid cell differentiation in cancer: the role of reactive oxygen species. J Leukoc Biol **74:**186-96.

113. **Kusmartsev, S., Y. Nefedova, D. Yoder, and D. I. Gabrilovich.** 2004. Antigen-specific inhibition of CD8+ T cell response by immature myeloid cells in cancer is mediated by reactive oxygen species. J Immunol **172:**989-99.

114. **Kusmartsev, S. A., Y. Li, and S. H. Chen.** 2000. Gr-1+ myeloid cells derived from tumor-bearing mice inhibit primary T cell activation induced through CD3/CD28 costimulation. J Immunol **165:**779-85.

115. **Lai, L., N. Alaverdi, L. Maltais, and H. C. Morse, 3rd.** 1998. Mouse cell surface antigens: nomenclature and immunophenotyping. J Immunol **160:**3861-8.

116. **Lai, X. H., I. Golovliov, and A. Sjostedt.** 2001. *Francisella tularensis* induces cytopathogenicity and apoptosis in murine macrophages via a mechanism that requires intracellular bacterial multiplication. Infect Immun **69:**4691-4.

117. **Lai, X. H., I. Golovliov, and A. Sjöstedt.** 2004. Expression of IglC is necessary for intracellular growth and induction of apoptosis in murine macrophages by *Francisella tularensis*. Microb Pathog **37:**225-30.

118. **Lai, X. H., I. Golovliov, and A. Sjöstedt.** 2001. *Francisella tularensis* induces cytopathogenicity and apoptosis in murine macrophages via a mechanism that requires intracellular bacterial multiplication. Infect Immun **69:**4691-4.

119. **Lai, X. H., and A. Sjöstedt.** 2003. Delineation of the molecular mechanisms of *Francisella tularensis*-induced apoptosis in murine macrophages. Infect Immun **71:**4642-6.

120. **Lamps, L. W., J. M. Havens, A. Sjostedt, D. L. Page, and M. A. Scott.** 2004. Histologic and molecular diagnosis of tularemia: a potential bioterrorism agent endemic to North America. Mod Pathol **17:**489-95.

121. **Lamps, L. W., J. M. Havens, A. Sjöstedt, D. L. Page, and M. A. Scott.** 2004. Histologic and molecular diagnosis of tularemia: a potential bioterrorism agent endemic to North America. Mod Pathol **17:**489-95.

122. **Lee, B. Y., M. A. Horwitz, and D. L. Clemens.** 2006. Identification, recombinant expression, immunolocalization in macrophages, and T-cell responsiveness of the major extracellular proteins of *Francisella tularensis*. Infect Immun **74:**4002-13.

123. **Leiby, D. A., A. H. Fortier, R. M. Crawford, R. D. Schreiber, and C. A. Nacy.** 1992. In vivo modulation of the murine immune response to *Francisella tularensis* LVS by administration of anticytokine antibodies. Infect Immun **60:**84-9.

124. **Li, H., S. Nookala, X. R. Bina, J. E. Bina, and F. Re.** 2006. Innate immune response to *Francisella tularensis* is mediated by TLR2 and caspase-1 activation. J Leukoc Biol **80:**766-73.

125. **Liu, Y. J.** 2001. Dendritic cell subsets and lineages, and their functions in innate and adaptive immunity. Cell **106:**259-62.

126. **Long, G. W., J. J. Oprandy, R. B. Narayanan, A. H. Fortier, K. R. Porter, and C. A. Nacy.** 1993. Detection of *Francisella tularensis* in blood by polymerase chain reaction. J Clin Microbiol **31:**152-4.

127. **Lopes-Carvalho, T., and J. F. Kearney.** 2004. Development and selection of marginal zone B cells. Immunol Rev **197:**192-205.

128. **Lopez, M. C., N. S. Duckett, S. D. Baron, and D. W. Metzger.** 2004. Early activation of NK cells after lung infection with the intracellular bacterium, *Francisella tularensis* LVS. Cell Immunol **232:**75-85.

129. **Lu, Z., M. I. Roche, J. H. Hui, B. Unal, P. L. Felgner, S. Gulati, G. Madico, and J. Sharon.** 2007. Generation and characterization of hybridoma antibodies for immunotherapy of tularemia. Immunol Lett **112:**92-103.

130. **Lyons, A. B.** 2000. Analysing cell division in vivo and in vitro using flow cytometric measurement of CFSE dye dilution. J Immunol Methods **243:**147-54.

131. **Lyons, A. B., J. Hasbold, and P. D. Hodgkin.** 2001. Flow cytometric analysis of cell division history using dilution of carboxyfluorescein diacetate succinimidyl ester, a stably integrated fluorescent probe. Methods Cell Biol **63:**375-98.

132. **Makarenkova, V. P., V. Bansal, B. M. Matta, L. A. Perez, and J. B. Ochoa.** 2006. CD11b+/Gr-1+ myeloid suppressor cells cause T cell dysfunction after traumatic stress. J Immunol **176:**2085-94.

133. **Malik, M., C. S. Bakshi, B. Sahay, A. Shah, S. A. Lotz, and T. J. Sellati.** 2006. Toll-like receptor 2 is required for control of pulmonary infection with *Francisella tularensis*. Infect Immun **74:**3657-62.

134. **Malkiel, S., C. J. Kuhlow, P. Mena, and J. L. Benach.** 2008. The loss and gain of marginal zone and peritoneal B cells is different in response to relapsing fever and Lyme Disease *Borrelia*. In Press.

135. **Mariathasan, S., D. S. Weiss, V. M. Dixit, and D. M. Monack.** 2005. Innate immunity against *Francisella tularensis* is dependent on the ASC/caspase-1 axis. J Exp Med **202:**1043-9.

136. **Marshall, M. A., D. Jankovic, V. E. Maher, A. Sher, and J. A. Berzofsky.** 2001. Mice infected with *Schistosoma mansoni* develop a novel non-T-lymphocyte suppressor population which inhibits virus-specific CTL induction via a soluble factor. Microbes Infect **3:**1051-61.

137. **Martin, F., and J. F. Kearney.** 2001. B1 cells: similarities and differences with other B cell subsets. Curr Opin Immunol **13:**195-201.

138. **Martin, F., and J. F. Kearney.** 2002. Marginal-zone B cells. Nat Rev Immunol **2:**323-35.

139. **Martin, F., A. M. Oliver, and J. F. Kearney.** 2001. Marginal zone and B1 B cells unite in the early response against T-independent blood-borne particulate antigens. Immunity **14:**617-29.

140. **Mastroeni, P., C. Simmons, R. Fowler, C. E. Hormaeche, and G. Dougan.** 2000. Igh-6(-/-) (B-cell-deficient) mice fail to mount solid acquired resistance to oral challenge with virulent *Salmonella enterica* serovar typhimurium and show impaired Th1 T-cell responses to *Salmonella* antigens. Infect Immun **68:**46-53.

141. **McCaffrey, R. L., and L. A. Allen.** 2006. *Francisella tularensis* LVS evades killing by human neutrophils via inhibition of the respiratory burst and phagosome escape. J Leukoc Biol **80:**1224-30.

142. **McCoy, G. W., and C. W. Chapin.** 1912. Further observations on a plague-like disease of rodents with a preliminary note on the causative agent, *Bacterium tularense*. J Infect Dis **10:**61-72.

143. **Mencacci, A., C. Montagnoli, A. Bacci, E. Cenci, L. Pitzurra, A. Spreca, M. Kopf, A. H. Sharpe, and L. Romani.** 2002. CD80+Gr-1+ myeloid cells inhibit development of antifungal Th1 immunity in mice with candidiasis. J Immunol **169:**3180-90.

144. **Mildner, A., M. Djukic, D. Garbe, A. Wellmer, W. A. Kuziel, M. Mack, R. Nau, and M. Prinz.** 2008. Ly-6G+CCR2- myeloid cells rather than Ly-6ChighCCR2+ monocytes are required for the control of bacterial infection in the central nervous system. J Immunol **181:**2713-22.

145. **Mittrucker, H. W., B. Raupach, A. Kohler, and S. H. Kaufmann.** 2000. Cutting edge: role of B lymphocytes in protective immunity against *Salmonella typhimurium* infection. J Immunol **164:**1648-52.

146. **Nano, F. E., N. Zhang, S. C. Cowley, K. E. Klose, K. K. Cheung, M. J. Roberts, J. S. Ludu, G. W. Letendre, A. I. Meierovics, G. Stephens, and K. L. Elkins.** 2004. A *Francisella tularensis* pathogenicity island required for intramacrophage growth. J Bacteriol **186:**6430-6.

147. **Nausch, N., I. E. Galani, E. Schlecker, and A. Cerwenka.** 2008. Mononuclear Myeloid-Derived "Suppressor" Cells express RAE-1 and activate NK cells. Blood.

148. **Otsuji, M., Y. Kimura, T. Aoe, Y. Okamoto, and T. Saito.** 1996. Oxidative stress by tumor-derived macrophages suppresses the expression of CD3 zeta chain of T-cell receptor complex and antigen-specific T-cell responses. Proc Natl Acad Sci U S A **93:**13119-24.

149. **Oyston, P. C., A. Sjostedt, and R. W. Titball.** 2004. Tularaemia: bioterrorism defence renews interest in *Francisella tularensis*. Nat Rev Microbiol **2:**967-78.

150. **Parsa, K. V., J. P. Butchar, M. V. Rajaram, T. J. Cremer, J. S. Gunn, L. S. Schlesinger, and S. Tridandapani.** 2008. *Francisella* gains a survival advantage within mononuclear phagocytes by suppressing the host IFNgamma response. Mol Immunol **45:**3428-37.

151. **Petersen, J. M., and M. E. Schriefer.** 2005. Tularemia: emergence/re-emergence. Vet Res **36:**455-67.

152. **Polsinelli, T., M. S. Meltzer, and A. H. Fortier.** 1994. Nitric oxide-independent killing of *Francisella tularensis* by IFN-gamma-stimulated murine alveolar macrophages. J Immunol **153:**1238-45.

153. **Rajewsky, K.** 1996. Clonal selection and learning in the antibody system. Nature **381:**751-8.

154. **Rasmussen, J. W., J. Cello, H. Gil, C. A. Forestal, M. B. Furie, D. G. Thanassi, and J. L. Benach.** 2006. Mac-1+ cells are the predominant subset in the early hepatic lesions of mice infected with *Francisella tularensis*. Infect Immun **74:**6590-8.

155. **Rhinehart-Jones, T. R., A. H. Fortier, and K. L. Elkins.** 1994. Transfer of immunity against lethal murine *Francisella infection* by specific antibody depends on host gamma interferon and T cells. Infect Immun **62:**3129-37.

156. **Rogers, H. W., M. P. Callery, B. Deck, and E. R. Unanue.** 1996. *Listeria monocytogenes* induces apoptosis of infected hepatocytes. J Immunol **156:**679-84.

157. **Sandstrom, G., S. Lofgren, and A. Tarnvik.** 1988. A capsule-deficient mutant of *Francisella tularensis* LVS exhibits enhanced sensitivity to killing by serum but diminished sensitivity to killing by polymorphonuclear leukocytes. Infect Immun **56:**1194-202.

158. **Sandstrom, G., A. Sjostedt, T. Johansson, K. Kuoppa, and J. C. Williams.** 1992. Immunogenicity and toxicity of lipopolysaccharide from *Francisella tularensis* LVS. FEMS Microbiol Immunol **5:**201-10.

159. **Savitt, A. G.** 2008. Unpublished observations.

160. **Sebastian, S., S. T. Dillon, J. G. Lynch, L. T. Blalock, E. Balon, K. T. Lee, L. E. Comstock, J. W. Conlan, E. J. Rubin, A. O. Tzianabos, and D. L. Kasper.** 2007. A defined O-antigen polysaccharide mutant of *Francisella tularensis* live vaccine strain has attenuated virulence while retaining its protective capacity. Infect Immun **75:**2591-602.

161. **Serafini, P., I. Borrello, and V. Bronte.** 2006. Myeloid suppressor cells in cancer: recruitment, phenotype, properties, and mechanisms of immune suppression. Semin Cancer Biol **16:**53-65.

162. **Serafini, P., C. De Santo, I. Marigo, S. Cingarlini, L. Dolcetti, G. Gallina, P. Zanovello, and V. Bronte.** 2004. Derangement of immune responses by myeloid suppressor cells. Cancer Immunol Immunother **53:**64-72.

163. **Shapiro, D. S., and D. R. Schwartz.** 2002. Exposure of laboratory workers to *Francisella tularensis* despite a bioterrorism procedure. J Clin Microbiol **40:**2278-81.

164. **Sica, A., and V. Bronte.** 2007. Altered macrophage differentiation and immune dysfunction in tumor development. J Clin Invest **117:**1155-66.

165. **Sinha, P., V. K. Clements, A. M. Fulton, and S. Ostrand-Rosenberg.** 2007. Prostaglandin E2 promotes tumor progression by inducing myeloid-derived suppressor cells. Cancer Res **67:**4507-13.

166. **Sinha, P., C. Okoro, D. Foell, H. H. Freeze, S. Ostrand-Rosenberg, and G. Srikrishna.** 2008. Proinflammatory s100 proteins regulate the accumulation of myeloid-derived suppressor cells. J Immunol **181:**4666-75.

167. **Sjostedt, A.** 2005. Intracellular survival mechanisms of *Francisella tularensis*, a stealth pathogen. Microbes Infect.

168. **Sjostedt, A., J. W. Conlan, and R. J. North.** 1994. Neutrophils are critical for host defense against primary infection with the facultative intracellular bacterium *Francisella tularensis* in mice and participate in defense against reinfection. Infect Immun **62:**2779-83.

169. **Sjöstedt, A., J. W. Conlan, and R. J. North.** 1994. Neutrophils are critical for host defense against primary infection with the facultative intracellular bacterium *Francisella tularensis* in mice and participate in defense against reinfection. Infect Immun **62:**2779-83.

170. **Sjostedt, A., M. Eriksson, G. Sandstrom, and A. Tarnvik.** 1992. Various membrane proteins of *Francisella tularensis* induce interferon-gamma production in both CD4+ and CD8+ T cells of primed humans. Immunology **76:**584-92.

171. **Sjostedt, A., R. J. North, and J. W. Conlan.** 1996. The requirement of tumour necrosis factor-alpha and interferon-gamma for the expression of protective immunity to secondary murine tularaemia depends on the size of the challenge inoculum. Microbiology **142 (Pt 6):**1369-74.

172. **Song, A., X. Tang, K. M. Harms, and M. Croft.** 2005. OX40 and Bcl-xL promote the persistence of CD8 T cells to recall tumor-associated antigen. J Immunol **175:**3534-41.

173. **Song, X., Y. Krelin, T. Dvorkin, O. Bjorkdahl, S. Segal, C. A. Dinarello, E. Voronov, and R. N. Apte.** 2005. CD11b+/Gr-1+ immature myeloid cells mediate suppression of T cells in mice bearing tumors of IL-1beta-secreting cells. J Immunol **175:**8200-8.

174. **Stenmark, S., H. Lindgren, A. Tarnvik, and A. Sjostedt.** 2003. Specific antibodies contribute to the host protection against strains of *Francisella tularensis* subspecies *holarctica*. Microb Pathog **35:**73-80.

175. **Stenmark, S., and A. Sjostedt.** 2004. Transfer of specific antibodies results in increased expression of TNF-alpha and IL12 and recruitment of neutrophils to the site of a cutaneous *Francisella tularensis* infection. J Med Microbiol **53:**501-4.

176. **Sutinen, S., and H. Syrjala.** 1986. Histopathology of human lymph node tularemia caused by *Francisella tularensis* var *palaearctica*. Arch Pathol Lab Med **110:**42-6.

177. **Tacke, F., and G. J. Randolph.** 2006. Migratory fate and differentiation of blood monocyte subsets. Immunobiology **211:**609-18.

178. **Takeda, K., T. Kaisho, and S. Akira.** 2003. Toll-like receptors. Annu Rev Immunol **21:**335-76.

179. **Tarnvik, A.** 1989. Nature of protective immunity to *Francisella tularensis*. Rev Infect Dis **11:**440-51.

180. **Tarnvik, A., and L. Berglund.** 2003. Tularaemia. Eur Respir J **21:**361-73.

181. **Telepnev, M., I. Golovliov, T. Grundstrom, A. Tarnvik, and A. Sjostedt.** 2003. *Francisella tularensis* inhibits Toll-like receptor-mediated activation of intracellular signalling and secretion of TNF-alpha and IL-1 from murine macrophages. Cell Microbiol **5:**41-51.

182. **Thorpe, B. D., and S. Marcus.** 1965. Phagocytosis and Intracellular Fate of *Pasteurella Tularensis*. 3. In Vivo Studies with Passively Transferred Cells and Sera. J Immunol **94:**578-85.

183. **Unanue, E. R.** 1997. Inter-relationship among macrophages, natural killer cells and neutrophils in early stages of *Listeria* resistance. Curr Opin Immunol **9:**35-43.

184. **Viau, M., and M. Zouali.** 2005. B-lymphocytes, innate immunity, and autoimmunity. Clin Immunol **114:**17-26.

185. **Vieira, P., and K. Rajewsky.** 1988. The half-lives of serum immunoglobulins in adult mice. Eur J Immunol **18:**313-6.

186. **Vinogradov, E., M. B. Perry, and J. W. Conlan.** 2002. Structural analysis of *Francisella tularensis* lipopolysaccharide. Eur J Biochem **269:**6112-8.

187. **Voisin, M. B., D. Buzoni-Gatel, D. Bout, and F. Velge-Roussel.** 2004. Both expansion of regulatory GR1+ CD11b+ myeloid cells and anergy of T lymphocytes participate in hyporesponsiveness of the lung-associated immune system during acute toxoplasmosis. Infect Immun **72:**5487-92.

188. **Vordermeier, H. M., N. Venkataprasad, D. P. Harris, and J. Ivanyi.** 1996. Increase of tuberculous infection in the organs of B cell-deficient mice. Clin Exp Immunol **106:**312-6.

189. **West, A. P., A. A. Koblansky, and S. Ghosh.** 2006. Recognition and signaling by toll-like receptors. Annu Rev Cell Dev Biol **22:**409-37.

190. **White, J. D., J. R. Rooney, P. A. Prickett, E. B. Derrenbacher, C. W. Beard, and W. R. Griffith.** 1964. Pathogenesis Of Experimental Respiratory Tularemia In Monkeys. J Infect Dis **114:**277-83.

191. **Wickstrum, J. R., K. J. Hong, S. Bokhari, N. Reed, N. McWilliams, R. T. Horvat, and M. J. Parmely.** 2007. Coactivating

signals for the hepatic lymphocyte gamma interferon response to *Francisella tularensis*. Infect Immun **75:**1335-42.

192. **Winslow, G. M., E. Yager, K. Shilo, E. Volk, A. Reilly, and F. K. Chu.** 2000. Antibody-mediated elimination of the obligate intracellular bacterial pathogen *Ehrlichia chaffeensis* during active infection. Infect Immun **68:**2187-95.

193. **Witmer, M. D., and R. M. Steinman.** 1984. The anatomy of peripheral lymphoid organs with emphasis on accessory cells: light-microscopic immunocytochemical studies of mouse spleen, lymph node, and Peyer's patch. Am J Anat **170:**465-81.

194. **Woolard, M. D., L. L. Hensley, T. H. Kawula, and J. A. Frelinger.** 2008. Respiratory *Francisella tularensis* live vaccine strain infection induces Th17 cells and prostaglandin E2, which inhibits generation of gamma interferon-positive T cells. Infect Immun **76:**2651-9.

195. **Woolard, M. D., J. E. Wilson, L. L. Hensley, L. A. Jania, T. H. Kawula, J. R. Drake, and J. A. Frelinger.** 2007. *Francisella tularensis*-infected macrophages release prostaglandin E2 that blocks T cell proliferation and promotes a Th2-like response. J Immunol **178:**2065-74.

196. **Xu, H., A. Manivannan, R. Dawson, I. J. Crane, M. Mack, P. Sharp, and J. Liversidge.** 2005. Differentiation to the CCR2+ inflammatory phenotype in vivo is a constitutive, time-limited property of blood monocytes and is independent of local inflammatory mediators. J Immunol **175:**6915-23.

197. **Yamamoto, Y., H. Ishigaki, H. Ishida, Y. Itoh, Y. Noda, and K. Ogasawara.** 2008. Analysis of splenic Gr-1int immature myeloid cells in tumor-bearing mice. Microbiol Immunol **52:**47-53.

198. **Yang, X., and R. C. Brunham.** 1998. Gene knockout B cell-deficient mice demonstrate that B cells play an important role in the initiation of T cell responses to *Chlamydia trachomatis* (mouse pneumonitis) lung infection. J Immunol **161:**1439-46.

199. **Yee, D., T. R. Rhinehart-Jones, and K. L. Elkins.** 1996. Loss of either CD4+ or CD8+ T cells does not affect the magnitude of protective immunity to an intracellular pathogen, *Francisella tularensis* strain LVS. J Immunol **157:**5042-8.

200. **Youn, J. I., S. Nagaraj, M. Collazo, and D. I. Gabrilovich.** 2008. Subsets of myeloid-derived suppressor cells in tumor-bearing mice. J Immunol **181:**5791-802.

201. **Zandvoort, A., and W. Timens.** 2002. The dual function of the splenic marginal zone: essential for initiation of anti-TI-2 responses but also vital in the general first-line defense against blood-borne antigens. Clin Exp Immunol **130:**4-11.

202. **Zheng, H., M. B. Furie.** 2006. Unpublished observations.

203. **Zheng, S. J., P. Wang, G. Tsabary, and Y. H. Chen.** 2004. Critical roles of TRAIL in hepatic cell death and hepatic inflammation. J Clin Invest **113:**58-64.

204. **Zhu, B., Y. Bando, S. Xiao, K. Yang, A. C. Anderson, V. K. Kuchroo, and S. J. Khoury.** 2007. CD11b+Ly-6C(hi) suppressive monocytes in experimental autoimmune encephalomyelitis. J Immunol **179:**5228-37.